

# Design of a Flexure Mount for Optics in Dynamic and Cryogenic Environments

Lloyd Wayne Pollard

(NASA-CR-177495) DESIGN OF A FLEXURE MOUNT  
FOR OPTICS IN DYNAMIC AND CRYOGENIC  
ENVIRONMENTS (Arizona Univ.) 135 pCSCL 14B

N89-26025

Unclas  
G3/14 0217933

CONTRACT NCC2-426  
February 1989



National Aeronautics and  
Space Administration

# **Design of a Flexure Mount for Optics in Dynamic and Cryogenic Environments**

Lloyd Wayne Pollard  
The University of Arizona  
Tucson, Arizona

Prepared for  
Ames Research Center  
CONTRACT NCC2-426  
February 1989



National Aeronautics and  
Space Administration

Ames Research Center  
Moffett Field, California 94035

## ACKNOWLEDGEMENTS

The author wishes to express his gratitude to the staff and faculty of the Departments of Engineering Mechanics and Optical Sciences for the opportunity to pursue advanced studies at the University of Arizona. In particular, a special thanks goes to Dr. Ralph Richard for his concentrated guidance and instruction during the past two years and for his constant availability for counsel during the last twenty years.

Funding for this design research was provided by NASA Ames Research Center through the NASA Cooperative Agreement NCC2-426 with the University of Arizona. The author wishes to thank Ramsey Melugin, the technical monitor of the NASA Ames Technical Staff, for his many contributions to this design effort and for allowing this very interesting project to be my thesis topic.

The author wishes to acknowledge Myung Cho, my friend and office partner for the last two years, for his never ending patience during the many hurdles we endured together in learning NASTRAN. And finally, a special thank you to Dorothy, my wife, for allowing me to do this in the first place.

PRECEDING PAGE BLANK NOT FILMED

## TABLE OF CONTENTS

	Page
LIST OF ILLUSTRATIONS .....	vii
LIST OF TABLES .....	ix
ABSTRACT .....	1
1. INTRODUCTION .....	2
2. REQUIREMENTS RESULTING FROM CRYOGENIC COOLDOWN .....	12
3. DYNAMIC ANALYSIS WITH A SINGLE DEGREE OF FREEDOM MODEL .....	16
Develop gimbal torsional stiffness of cruciforms, $K_{rh}$ .....	26
Develop gimbal torsional stiffness in flexure blades, $K_{rs}$ .....	28
Develop flexure assembly lateral stiffnesses, hard and soft .....	30
Develop horizontal blade stiffnesses .....	33
Develop gimbal blade stiffnesses .....	35
Develop frame stiffness .....	47
Develop stability model .....	40
Finalize SDOF program .....	41
A numerical example .....	43
Isolated modes of the flexure blades .....	49
4. DYNAMIC ANALYSIS WITH A THREE DEGREE OF FREEDOM MODEL ..	52
Develop the three DOF stiffness matrix .....	52
Develop the eigenvalues .....	55
Develop the relationship between $K_t$ and $K_v$ .....	55
A numerical example .....	57
5. DYNAMIC ANALYSIS WITH A NASTRAN FINITE ELEMENT MODEL ..	61
Solution Type 3 — Normal Modes Analysis .....	61
Solution Type 63 — Superelement Normal Modes Analysis .....	76
Solution Type 30 — Modal Frequency Response Analysis .....	81
6. A COST COMPARISON OF THE SIRTf DYNAMIC ANALYSIS .....	84
Cost of analysis with the FORTRAN model .....	85
Cost of analysis with the NASTRAN SOL 3 model .....	85
Cost of analysis with the NASTRAN SOL 63 model .....	86
Cost of analysis with the NASTRAN SOL 30 model .....	87
Cost summary of analyses .....	88
7. SUMMARY AND CONCLUSIONS .....	90
8. REFERENCES .....	95

**TABLE OF CONTENTS**  
(continued)

	Page
9. APPENDIX I Listing of FORTRAN program for SDOF parametric study .	96
10. APPENDIX II Listing of NASTRAN input file for SOL 3. ....	103
11. APPENDIX III Listing of NASTRAN input file for SOL 63 ....	108
12. APPENDIX IV Listing of NASTRAN input file for SOL 30 ....	113
13. APPENDIX V Listing of NASTRAN input file for SOL 5, Buckling. ....	122

## LIST OF ILLUSTRATIONS

Figure		Page
1.1	Three Point Support Spring Model with Parallel Spring Guide .....	3
1.2	Parallel Spring Guide with Gimbal .....	5
1.3	Two Single Bladed Flexure Assembly .....	6
1.4	Final SDOF Design .....	8
1.5	Final Design Submitted to NASA .....	9
2.1	Flow Diagram for FRINGE - NASTRAN Analysis .....	15
3.1	Lateral SDOF Justification .....	17
3.2	Reactions at Support 1 .....	18
3.3	Reactions at Support 2 .....	18
3.4	Reactions at Support 3 .....	18
3.5	SDOF Model .....	20
3.6	Design PSDF Supplied by NASA Ames .....	22
3.7	Gimbal Configuration - Torsion .....	27
3.8	Flexure Configuration - Torsion .....	29
3.9	Vertical Post Configuration - Bending and Shear .....	32
3.10	Flexure Blades Configuration .....	34
3.11	Gimbal Blades Configuration - Axial, Shear and Bending .....	36
3.12	Frame Configuration .....	39
3.13	Free Body of Torsion Model .....	48
3.14	Isolated Modes of Flexure Blades Model .....	49

# LIST OF ILLUSTRATIONS (continued)

Figure		Page
4.1	Free Body Diagram of Three Degree of Freedom Model.....	54
4.2	Relationship Between $K_v$ and $K_t$ .....	56
4.3	Vertical Stiffness of Single Flexure Assembly.....	58
5.1	NASTRAN Finite Element Model .....	62
5.2	NASTRAN Plot of Mode Shape 1 - 69 Hz .....	63
5.3	NASTRAN Plot of Mode Shape 2 - 69 Hz .....	64
5.4	NASTRAN Plot of Mode Shape 3 - 73 Hz .....	66
5.5	NASTRAN Plot of Mode Shape 4 - 81 Hz .....	67
5.6	NASTRAN Plot of Mode Shape 5 - 81 Hz .....	68
5.7	NASTRAN Plot of Mode Shape 6 - 81 Hz .....	69
5.8	NASTRAN Plot of Mode Shape 7 - 81 Hz .....	70
5.9	NASTRAN Plot of Mode Shape 8 - 81 Hz .....	71
5.10	NASTRAN Plot of Mode Shape 9 - 81 Hz .....	72
5.11	NASTRAN Plot of Mode Shape 10 - 129 Hz.....	73
5.12	NASTRAN Plot of Mode Shape 11 - 129 Hz.....	74
5.13	NASTRAN Plot of Mode Shape 12 - 175 Hz.....	75
5.14	Modal Response Combinations .....	79
5.15	Histogram of SIRTF Natural Frequencies .....	80
5.16	Typical Deflection PSD Plot From SOL 30.....	82
5.17	Typical Internal Load PSD Plot From SOL 30 .....	83

## LIST OF TABLES

Table		Page
2.1	Summary of FRINGE Analysis . . . . .	13
4.1	Element Loads for Vertical Stiffness . . . . .	59
5.1	First Twelve Natural Frequencies of SIRTf . . . . .	76
6.1	Cost Comparison of the SIRTf Dynamic Analysis . . . . .	89
7.1	Numerical Summary of Dynamic Analysis . . . . .	94



## ABSTRACT

The design of a flexure mount for a mirror operating in a cryogenic environment is presented. This structure represents a design effort recently submitted to NASA Ames for the support of the primary mirror of the Space Infrared Telescope Facility (SIRTF). The support structure must passively accommodate the differential thermal contraction between the glass mirror and the aluminum structure of the telescope during cryogenic cooldown. Further, it must support the one meter diameter, 116 kilogram (258 pound) primary mirror during a severe launch to orbit without exceeding the micro-yield of the material anywhere in the flexure mount. Procedures used to establish the maximum allowable radial stiffness of the flexural mount, based on the finite element program NASTRAN and the optical program FRINGE, are discussed. Early design concepts were evaluated using a parametric design program, and the development of that program is presented. Dynamic loading analyses performed with NASTRAN are discussed. Methods of combining modal responses resulting from a displacement response spectrum analysis are discussed, and a combination scheme called MRSS, Modified Root of Sum of Squares, is presented. Modal combination schemes using MRSS, SRSS, and ABS are compared to the results of a Modal Frequency Response analysis performed with NASTRAN.

## CHAPTER 1

### INTRODUCTION

The design of the flexure mount for the primary mirror of the Space Infrared Telescope Facility (SIRTF) is presented, and the methods used to develop that design for NASA Ames are discussed. For the optics of SIRTF to remain unaffected by the temperature excursions that the facility will experience in the space environment, the optical system is cryogenically cooled with liquid helium prior to launch. This cooling maintains the optics at a uniform temperature for operation but it also causes a differential thermal contraction between the fused silica glass mirror<sup>1,2</sup> and the aluminum structure of the telescope due to the differences in coefficients of thermal expansion. This contraction imposes the primary design requirement on the support structure, which connects the mirror to its aluminum base plate. The NASA Ames design criteria required that the support structure absorb the thermal contraction, passively, while maintaining acceptable deflections on the mirror's optical surface and without causing a permanent set in the support structure which would effect the mirror's optical alignment. Hence, the support structure must contain a flexure mount.

A support structure that is compliant in the radial direction of the mirror satisfies the above requirements. The launch load design criteria, on the other hand, impose the requirement on the support structure that the three sigma working stress during launch remains less than the micro-yield of the material. The support structure that has the strength to satisfy that requirement is also necessarily structurally stiff.

Earlier work<sup>3</sup> for NASA at the University of Arizona developed a three point titanium parallel spring guide<sup>4</sup> for the flexure configuration. Shown in Figure 1.1 is a spring model of that configuration which demonstrates the orientation of the flexure stiffnesses as well as the orientation of the vertical parallel spring guide at each of the

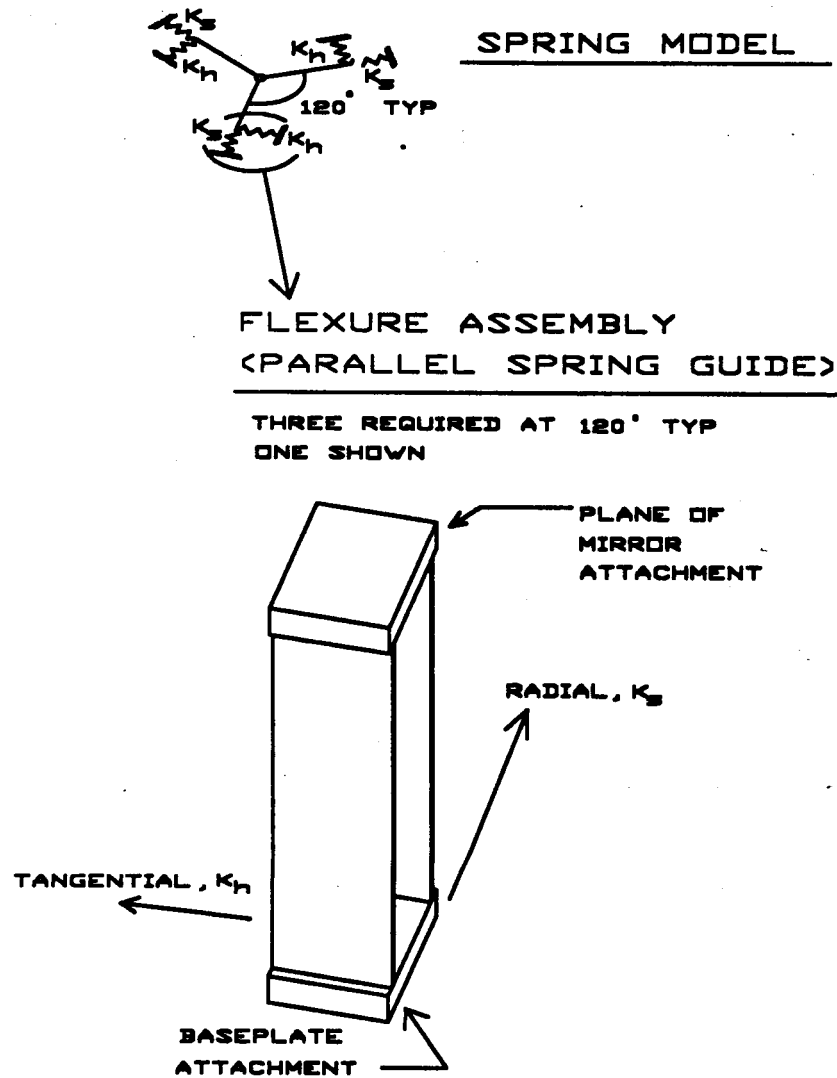


Figure 1.1 Three Point Support - Spring Model with Parallel Spring Guide

three support points. A statics analysis, as will be shown in Chapter 3, demonstrates that the net system stiffness of such a configuration is a function of the sum of the two orthogonal stiffnesses of each flexure assembly,  $K_s$  and  $K_h$ , and the net system stiffness is independent of the assembly orientation. Therefore, the radial stiffness can be made compliant for cryogenic cooldown and the tangential stiffness can be made large for the launch loads. Titanium was selected as the flexure material primarily because of its predictability under high working stress at cryogenic temperatures.

Manufacturing tolerances on parallelism between the baseplate and the mirror's socket impose the requirement that each flexure assembly accommodate a fixed angular displacement in any orientation at its base during assembly. The resulting moment on the mirror must not cause excessive deflections on the mirror's optical surface. The baseline configuration shown in Figure 1.1 could not meet that requirement and was therefore changed to the gimbal configuration shown in Figure 1.2. Each gimbal structure has four cruciforms which allow the gimbal to be torsionally compliant about orthogonal axes. When mounted between each parallel spring-guide assembly and the baseplate, as shown in Figure 1.2, the gimbal structures accommodate the manufacturing tolerances. Further design iterations, however, determined that no satisfactory design space was available for the configuration shown in Figure 1.2. Both the radial compliance and the tangential stiffness are functions of the blade dimensions of the vertical parallel spring guide. Its radial compliance is a function of  $bt^3$ , and its tangential stiffness is a function of  $b^3t$ , where  $b$  is the width of the blades and  $t$  is the thickness. This coupling makes it impossible to construct a flexure with blades that are both strong enough tangentially to sustain the loading during launch and soft enough radially to meet the cryogenic cooldown requirements.

During a design review at NASA Ames, the configuration shown in Figure 1.3 evolved. With this design concept, manufacturing tolerances are accommodated

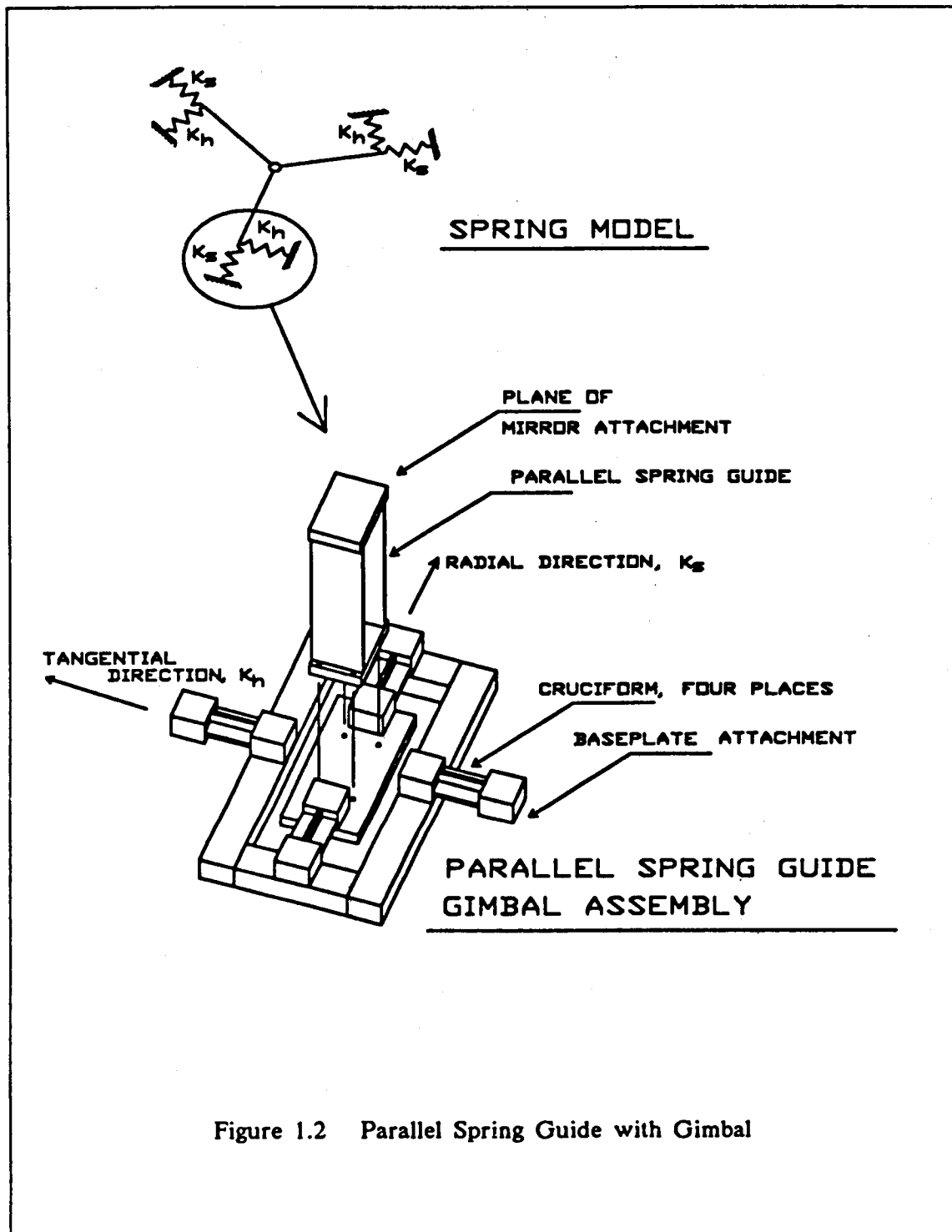
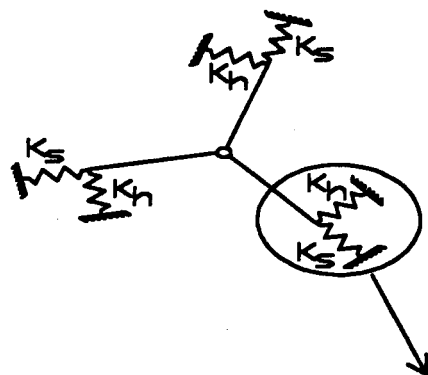


Figure 1.2 Parallel Spring Guide with Gimbal



# SPRING MODEL

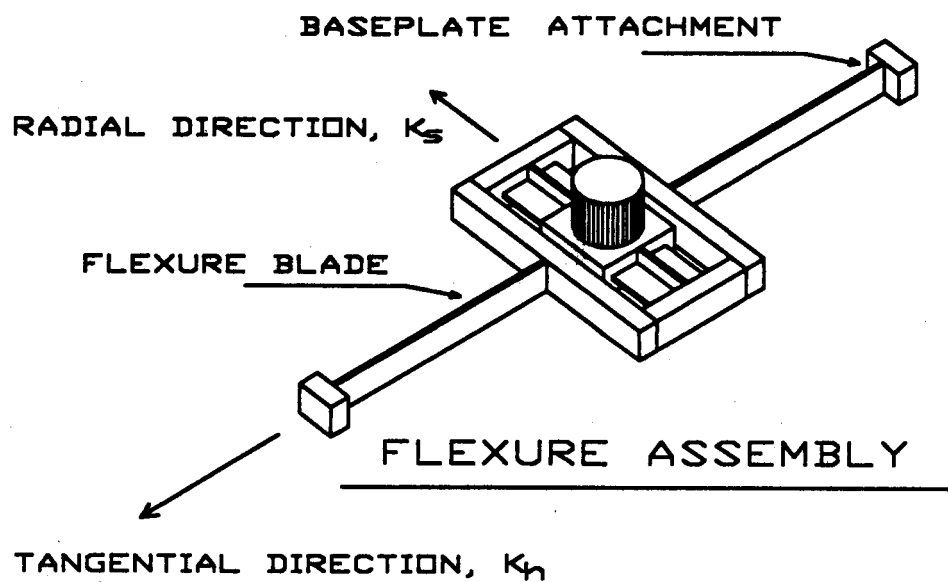


Figure 1.3 Two Single Bladed Flexure Assembly

tangentially with the torsionally soft cruciforms and radially with the torsionally soft flexure blades. Radial softness has been maintained with the flexure except now, rather than a double bladed flexure mounted vertically, there are two single blades mounted horizontally. The design equations for the system remained essentially the same as before except that the tangentially stiff horizontal blades of the cruciform have beneficially been decoupled from the radially soft flexure blades. A vertical rigid post now attaches the mirror to the flexure assembly.

As design iterations continued on the configuration shown in Figure 1.3, blade lengths on the horizontal flexure grew in order to maintain the necessary radial compliance for cryogenic cooldown. The differential thermal contraction between the titanium flexures and the aluminum baseplate then became the design concern as that differential contraction caused the horizontal titanium blades to be in compression. Consequently, the final design length of the blades that satisfied all other requirements for SIRTF was elastically unstable due to Euler buckling. Folding the blades back on themselves, as shown in Figure 1.4, solved the buckling problem by shortening the effective length over which the differential contraction of the aluminum and titanium occurred. The configuration shown in Figure 1.4 is the final design configuration of each flexure assembly based upon the SDOF model that is discussed in Chapter 3. For comparison, the final design configuration that has been submitted to NASA Ames for the SIRTF program based upon the final dynamic analysis performed on NASTRAN and discussed in Chapter 5 is shown in Figure 1.5.

The capability exists in the NASTRAN finite element program to apply the loading described by a power spectral density function (PSDF) onto a structural model simultaneously in all three orthogonal directions as specified by SIRTF's design criteria. Because the center of mass of the mirror is above the plane of the flexure assemblies, lateral motion of the mirror is always coupled with a rotational motion.

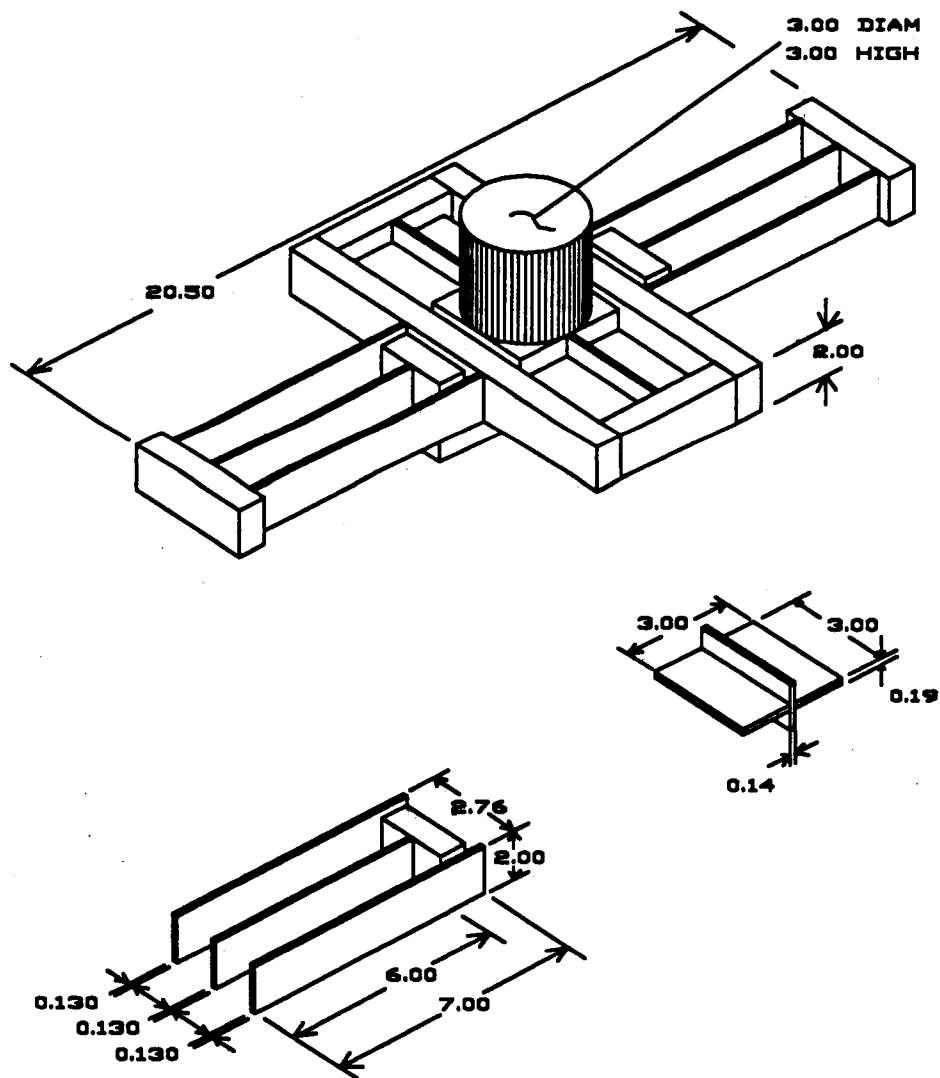


Figure 1.4 Final SDOF Design



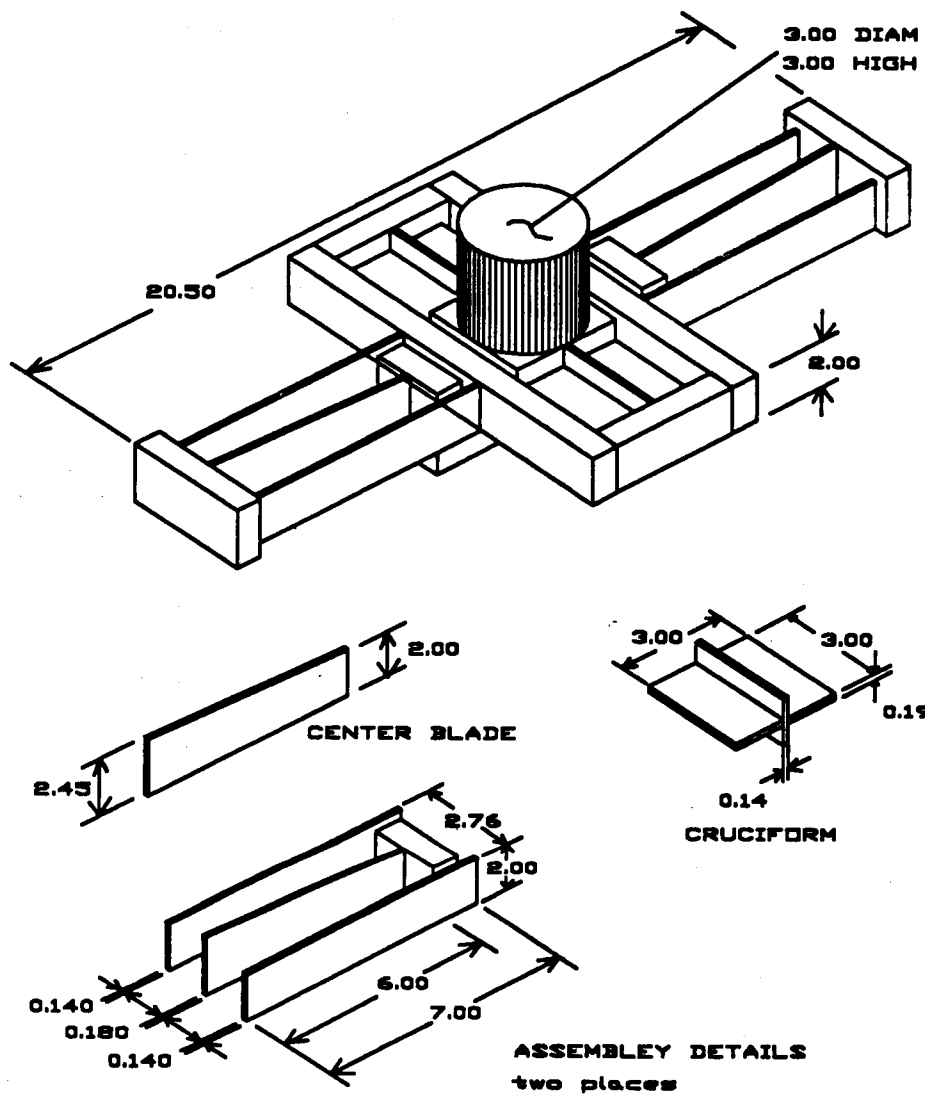


Figure 1.5 Final Design Submitted to NASA

That coupling causes a higher bending moment to occur in the blades of the flexure than the SDOF model predicted. An early assumption in the SDOF model was that the vertical stiffness along the optical axis was essentially rigid in comparison to the lateral stiffness. That assumption was valid for the configurations shown in Figures 1.1 and 1.2. As the configuration evolved through those shown in Figures 1.3 and 1.4 into that shown in Figure 1.5, the vertical stiffness of the assembly decreased thereby making the vertical rigidity assumption inaccurate and allowing coupling to occur. Even with that inaccurate assumption, however, the SDOF model was the tool used to provide the detail design shown in Figure 1.4, which required very few iterations to finalize with the NASTRAN analysis. As seen in Figures 1.4 and 1.5 the cruciform configuration that was determined from the SDOF model remained unchanged throughout the NASTRAN dynamic analysis. The flexure blades, on the other hand, had to be strengthened by increasing both their thickness and depth. The center blade, which carries twice the axial load as the outer blades, was finally tapered as a trade-off between it being as soft as possible in the radial direction while being as strong as necessary in the vertical direction. The three DOF model discussed in Chapter 4 was used to specifically demonstrate the effects of the coupling between the rotational and lateral translation modes and to confirm the coupling frequencies and mode shapes predicted by the NASTRAN analysis.

This design study has used three of the solution types provided by NASTRAN for performing dynamic analysis. The first, Solution 3 (SOL 3), referred to in NASTRAN as Normal Modes Analysis, provides the capability to determine a structure's eigenvalues and mode shapes with little more effort or cost than performing a static analysis. Because SOL 3 is inexpensive to use, it was used for evaluating the various dynamic models which had more complicated input files. The second solution type used in this study is Solution 63 (SOL 63), referred to in NASTRAN as

Superelement Normal Modes analysis. SOL 63 provides the capability to perform a complete dynamic analysis based on the user defined response spectrum. The SIRTf displacement response spectrum was generated from the power spectral density function (PSDF) from the SIRTf design criteria. Many eigenvalues calculated for the SIRTf system are equal or clustered while others are well spaced. Consequently, the method of combining modal maxima effects is discussed. The third solution type is Solution 30 (SOL 30), referred to in NASTRAN as Modal Frequency Response analysis. SOL 30 provides the capability to perform a dynamic analysis that directly accepts the user defined PSDF as input, performs a frequency response analysis, and integrates the resulting power spectral density curves of the response quantities to provide the RMS displacements and loads. Assumptions of this random vibration analysis are that the system is linear and that the excitation is statistically stationary and ergodic with a Gaussian probability distribution. Procedures used in the NASTRAN types of analysis are discussed in Chapter 5, costs are compared in Chapter 6, and the results are compared in Chapter 7.

The NASA Cooperative Agreement under which this work was performed at the University of Arizona required support system designs for two mirror sizes. The 0.5 meter diameter mirror which weighs 35 pounds is to be the testing prototype of the 1.0 meter diameter mirror which weighs 258 pounds. Both support systems were to be similar in design configuration with differences only in the member sizes. Although the work described in this thesis actually resulted in two flexure assembly designs, only the support system for the 1.0 meter mirror is specifically discussed.

## CHAPTER 2

### REQUIREMENTS RESULTING FROM CRYOGENIC COOLDOWN

Design loads required of the SIRTf support system are primarily determined by launch and cryogenic cooldown environments. During launch, SIRTf is at cryogenic temperature but it is not in an optical operation mode. System strength therefore becomes the major design concern. In orbit, SIRTf is both at cryogenic temperature and in an optical operation mode. System compliance then becomes the major design concern. The dynamic analyses performed during this design study that consider the launch load environment are presented in Chapters 3 through 5. The material presented in the present chapter will outline the procedure used to develop the required compliance of each flexure assembly in the radial direction of the mirror during optical operation at cryogenic temperature. The design loads that the support structure is allowed to transmit to the glass mirror are based on the maximum aberrations that those loads are allowed to cause on the mirror's optical surface. Once those loads are determined and the relative radial thermal contraction between the glass mirror and the aluminum baseplate during cryogenic cooldown has been calculated, the radial compliance required of the support system is directly established.

Procedures to determine the effects of mechanical and thermal loads on the performance of optical elements have been developed at the University of Arizona. These include the use of finite element programs and the optical analysis program FRINGE. Program FRINGE is used to quantitatively determine the characteristics of optical surfaces from either test data or analysis. Earlier research<sup>3</sup> on this NASA project at the University of Arizona had modified the FRINGE program to accept as its input, the output from the structural analysis finite element program SAP IV. Current work by the author and others has further modified FRINGE such that it can

also except as input, the output from the structural analysis program NASTRAN.

The results of the FRINGE and NASTRAN analysis for SIRTf are summarized in Table 2.1. Unit loads were applied to a NASTRAN finite element model of the mirror at the support attachment points. Structural deformations of the optical surface, which are output from the finite element program NASTRAN, then become the input to program FRINGE. The output from program FRINGE gives the

<p>Influence coefficient from FRINGE and NASTRAN</p> $\text{RMS}_{\text{influence}} = 1.338 \times 10^{-8} \frac{\text{in}}{\text{in-lb}}$
<p>Allowable RMS surface displacement from error budget</p> $\text{RMS}_{\text{allowable}} = 2.0 \times 10^{-6} \text{ in}$
<p>Allowable bending moment</p> $M_{\text{allowable}} = \frac{\text{RMS}_{\text{allowable}}}{\text{RMS}_{\text{influence}}} = 149.4 \text{ in-lb}$
<p>Table 2.1 Summary of FRINGE Analysis</p>

optical distortions on the surface of the mirror. Also output from FRINGE is the RMS surface displacement over the optical surface. Based on the NASA error budget which defined the allowable aberrations in terms of the RMS displacement over the optical surface, the unit load effects were scaled to match the allowable deflections, and the allowable working loads were thereby established. Results of the SIRTf mirror analysis with FRINGE and NASTRAN indicate that lateral shear forces in the plane of the center of mass of the mirror cause negligible aberrations on the surface of the mirror compared to those caused by the bending moment which accompanies the

shear. The effects of the assembly shear loads can therefore be essentially ignored by considering the moment at the plane of the center of mass of the mirror.

When compared to the coefficient of thermal expansion of the aluminum baseplate, the coefficient of thermal expansion of the glass mirror is negligible. The difference in radial contraction,  $\delta_{\text{cryo}}$ , between the two materials is:

$$\delta_{\text{cryo}} = [(R \alpha \Delta T)_{\text{aluminum}} - (R \alpha \Delta T)_{\text{glass}}] \dots\dots (2.1)$$

$$\delta_{\text{cryo}} = R \Delta T [\alpha_{\text{aluminum}} - \alpha_{\text{glass}}]$$

$$\alpha_{\text{glass}} \ll \alpha_{\text{aluminum}}$$

Therefore:

$$\delta_{\text{cryo}} \cong R \Delta T \alpha_{\text{aluminum}} \dots\dots\dots (2.2)$$

Where:

R = Radial distance from center of  
baseplate to center post on the  
flexure assembly  
= 13.0 inches

$\Delta T$  = Temperature change from ambient  
=  $-491^{\circ}\text{F}$

$\alpha$  = Average coefficient of thermal expansion  
=  $9.691 \times 10^{-6} \frac{\text{in}}{\text{in } ^{\circ}\text{F}}$  for aluminum

$$\delta_{\text{cryo}} = 0.0619 \text{ inch} \dots\dots\dots (2.3)$$

The above constraints dictate the required radial compliance of the support structure. In summary, the radial thermal contraction of 0.0619 inch at each flexure assembly is allowed to produce a maximum moment of 149.4 in-lb in the plane of the mirror's center of mass. Compliance of the flexure assembly is the only design variable available. The procedure described above is outlined in the flow diagram shown in Figure 2.1. Structural compliance of the support system in the radial direction determined by this procedure has been incorporated into all configurations considered in the dynamic analysis that follows.

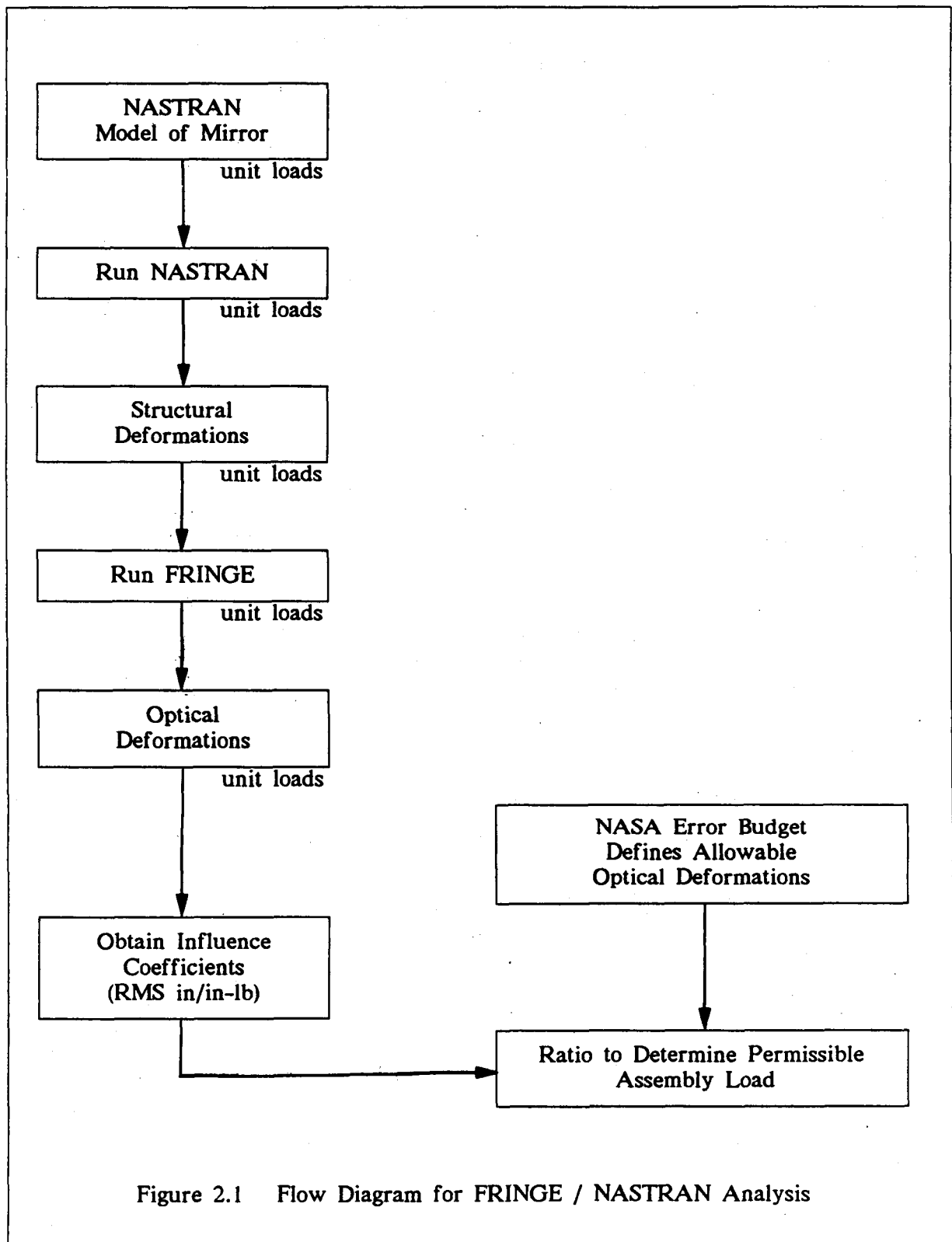


Figure 2.1 Flow Diagram for FRINGE / NASTRAN Analysis

## CHAPTER 3

### DYNAMIC ANALYSIS WITH A SINGLE DEGREE OF FREEDOM MODEL

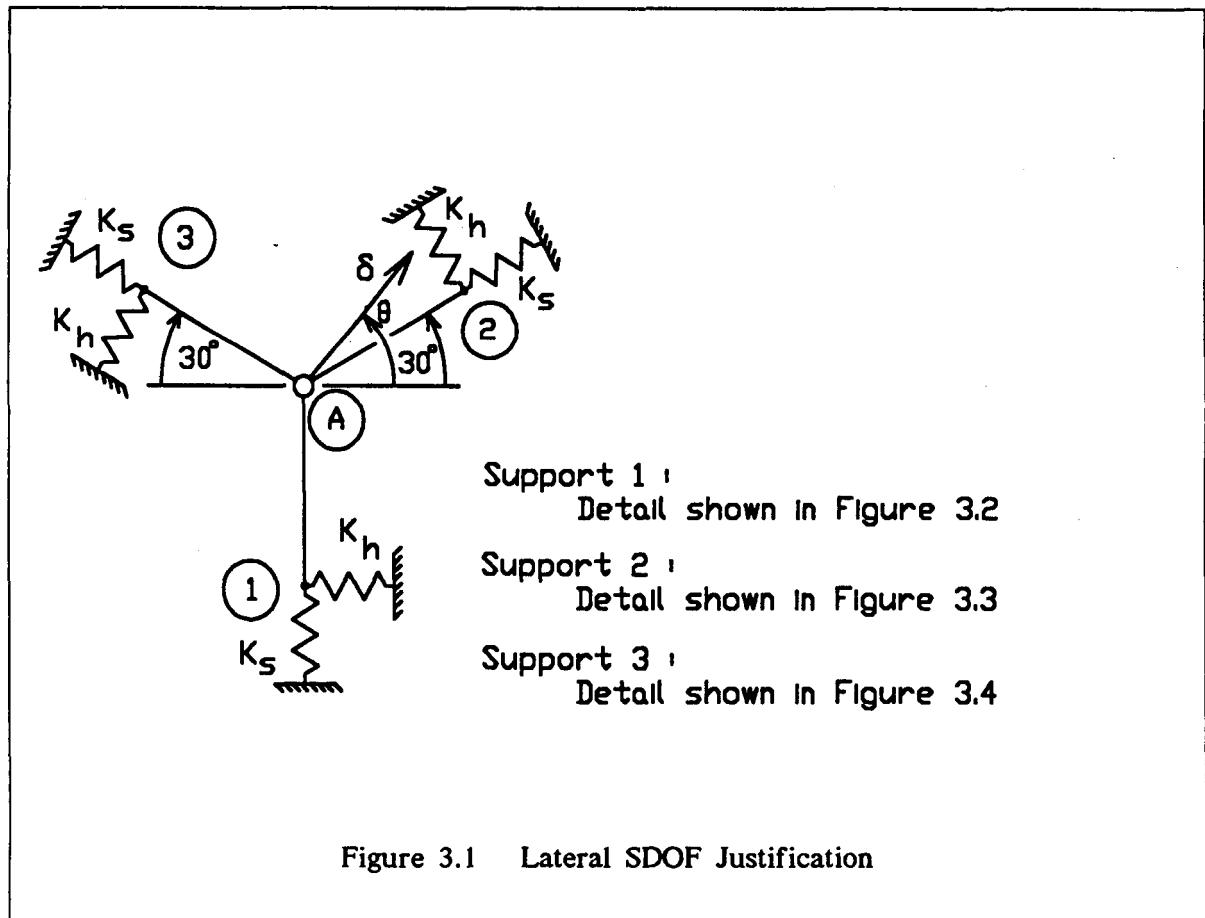
An early assumption in this design study was that the system stiffness along the optical axis, or vertical direction, was much greater than the stiffness in the lateral direction normal to the optical axis. This high stiffness was assumed to decouple the rotational mode of the mirror about a horizontal axis from the lateral displacement mode, even though it was known that the center of mass of the mirror would be approximately three inches above the plane of the support system. The SDOF model was therefore constructed assuming that the center of mass of the mirror was contained in the plane of the flexures. This assumption was valid for the vertically oriented parallel spring guide designs shown in Figures 1.1 and 1.2. As the design evolved into the concepts shown in Figures 1.4 and 1.5, the values of the vertical natural frequency and the lateral natural frequency began to converge which indicated that the mode shapes would probably couple. In fact, the dynamic analyses performed by hand on a three degree of freedom model and the dynamic analysis performed on NASTRAN using a complete finite element model of the final flexure configuration predict that the lateral mode never does occur entirely by itself, as it is always coupled with a rotational mode. Even so, the SDOF model proved to be a valuable and inexpensive design tool to use in performing the parametric design studies, as it allowed constant insight into which parameters controlled the design. Design configurations were periodically checked with NASTRAN to maintain an awareness of the accuracy of the SDOF model as configurations evolved.

Justification for the lateral SDOF model is presented by demonstrating first that any imposed lateral deflection at the center of mass of the system is always sustained by a force which is colinear with the imposed deflection. It will be shown



that no moment is required to maintain that colinearity. Then it will be demonstrated that the stiffness relationship between the lateral deflection and the applied lateral load is independent of the angular orientation of the applied load. These conditions result in a system which can be structurally represented as a SDOF system.

A deflection,  $\delta$ , is imposed at an arbitrary angle,  $\theta$ , on the center of the spring system as shown in Figure 3.1. The displacement will be maintained by the required force,  $F$ , and moment,  $M$ . Further, members A1, A2, and A3 are to be considered as rigid elements which are rigidly attached at point A. The following statements of equilibrium will demonstrate that the force,  $F$ , is colinear with the deflection,  $\delta$ ; that the moment,  $M$ , is exactly equal to zero; and that the stiffness,  $K$ , is independent of the direction,  $\theta$ , of the imposed deflection.



At 1 :

$$F_{1h} = K_h \delta \cos \theta$$

$$F_{1s} = K_s \delta \sin \theta$$

$$F_{1x} = -F_{1h}$$

$$F_{1y} = -F_{1s}$$

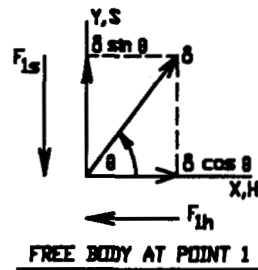


Figure 3.2 Reactions at Support 1

At 2 :

$$F_{2h} = K_h \delta \sin \theta - 3\theta$$

$$F_{2s} = K_s \delta \cos \theta - 3\theta$$

$$F_{2x} = F_{2h} \sin 3\theta - F_{2s} \cos 3\theta$$

$$F_{2y} = F_{2h} \cos 3\theta - F_{2s} \sin 3\theta$$

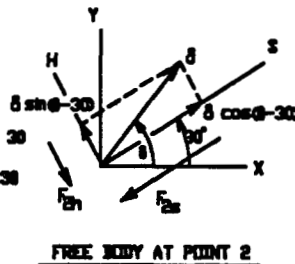


Figure 3.3 Reactions at Support 2

At 3 :

$$F_{3h} = K_h \delta \cos(60-\theta)$$

$$F_{3s} = K_s \delta \sin(60-\theta)$$

$$F_{3x} = -F_{3h} \sin 3\theta - F_{3s} \cos 3\theta$$

$$F_{3y} = -F_{3h} \cos 3\theta - F_{3s} \sin 3\theta$$

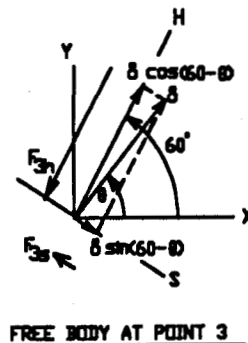


Figure 3.4 Reactions at Support 3

Equilibrium in the X-Direction

$$\begin{aligned}
 \Sigma F_X &= F_{XR} + F_{1X} + F_{2X} + F_{3X} = 0 \\
 &= F_{XR} - K_H \delta \cos\theta \\
 &\quad + (K_H \delta \sin(\theta-30)) \sin(30) - (K_S \delta \cos(\theta-30)) \cos(30) \\
 &\quad - (K_H \delta \cos(60-\theta)) \sin(30) - (K_S \delta \sin(60-\theta)) \cos(30) \\
 F_{XR} &= 1.5 (K_H + K_S) \delta \cos\theta
 \end{aligned}$$

NOTE:

$\delta \cos\theta$  = the horizontal component of the imposed displacement,  $\delta$   
and

$F_{XR}$  = the horizontal component of the applied force,  $F$

Equilibrium in the Y-Direction

$$\begin{aligned}
 \Sigma F_Y &= F_{YR} + F_{1Y} + F_{2Y} + F_{3Y} = 0 \\
 &= F_{YR} - K_S \delta \sin\theta \\
 &\quad - (K_H \delta \sin(\theta-30)) \cos(30) - (K_S \delta \cos(\theta-30)) \sin(30) \\
 &\quad - (K_H \delta \cos(60-\theta)) \cos(30) + (K_S \delta \sin(60-\theta)) \sin(30) \\
 F_{YR} &= 1.5 (K_H + K_S) \delta \sin\theta
 \end{aligned}$$

NOTE:

$\delta \sin\theta$  = the vertical component of the imposed displacement,  $\delta$   
and

$F_{YR}$  = the vertical component of the applied force,  $F$

Applied Force,  $F$ , is the vector sum of its two components

$$\begin{aligned}
 F &= \sqrt{(F_{XR})^2 + (F_{YR})^2} \\
 &= 1.5 (K_H + K_S) \delta \sqrt{(\cos\theta)^2 + (\sin\theta)^2}
 \end{aligned}$$

$$F = 1.5 (K_H + K_S) \delta$$

And:

$$K_{\text{system}} = 1.5 (K_H + K_S), \text{ independent of } \theta$$

NOTE:

$F$  has been shown to be colinear with  $\delta$ , and the system stiffness,  $K_{\text{system}}$ , has been shown to be independent of  $\theta$

### Moment Equilibrium

$$\Sigma M_{\text{center of system}} = -M + R [ F_{1H} + F_{2H} + F_{3H} ] = 0$$

$$M = R [ -K_H \delta \cos(\theta) - K_H \delta \sin(\theta-30) + K_H \delta \cos(60-\theta) ]$$

$$M = R \delta K_H [ -\cos(\theta) + \cos(\theta) ]$$

$$M = 0$$

NOTE:

Applied moment required to hold F colinear with  $\delta$  is exactly zero.

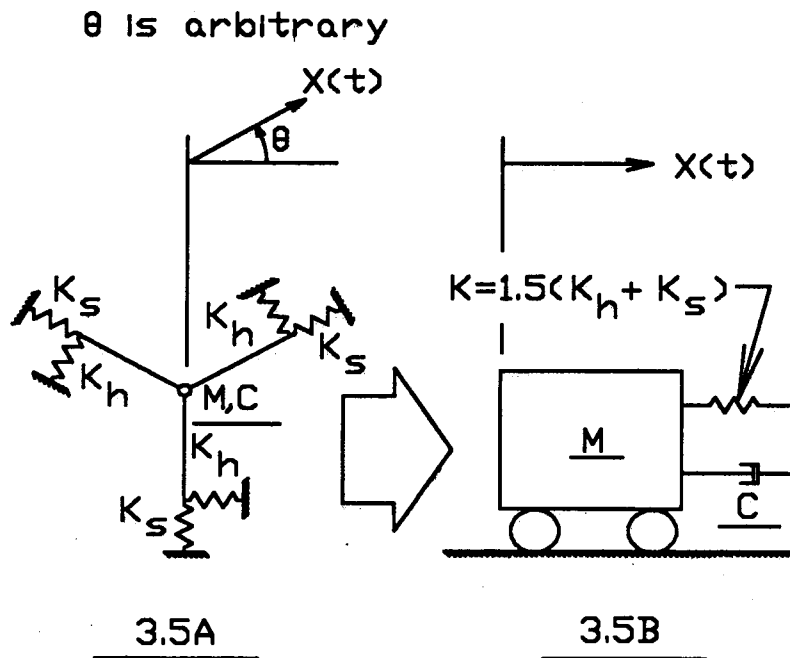


Figure 3.5 SDOF Model

Shown in Figure 3.5A is the spring-mass system for the three flexure support system that became the model for the SDOF analysis. The deformation of that system is always colinear with the applied load as already demonstrated. That allows the SDOF damped-spring-mass system shown in Figure 3.5B to be considered. The maximum allowable radial spring constants,  $K_s$ , are determined directly from the cryogenic cooldown requirements. Launch criteria was provided by NASA Ames in the form of the power spectral density function (PSDF) shown in Figure 3.6. For a SDOF system with a low critical damping ratio which is excited by the white noise PSDF as shown in Figure 3.6, the displacement response spectrum<sup>5</sup> is described by Equation 3.1.

$$\delta_{RMS} = \sqrt{\frac{PSD(f)}{(4\pi f)^3 \zeta}} \dots\dots\dots (3.1)$$

Where:

$\delta_{RMS}$  = Root Mean Square displacement

$PSD(f)$  = Value of the PSDF shown in Figure 3.6  
at frequency equal to  $f$

$f$  = natural frequency of SDOF system

$\zeta$  = critical damping ratio

Early studies of the vertical parallel spring guide, which has been shown in Figure 1.1, resulted in a simple programming algorithm for the parametric design program. The steps were as follows:

1. Perform loop over range of expected flexure lengths,  $L$ . Therefore:

$L$  = Known from current value in DO loop

2. Perform loop on range of natural frequencies,  $f$ , from 20 Hz to 300 Hz.

Therefore:

$f$  = Known from current value in DO loop

3. Determine the value of the PSDF at the current natural frequency,  $f$ , and assume a critical damping ratio,  $\zeta$ , for the system. Therefore:

$$\text{PSD} = \begin{cases} .02 \times (386.4)^2 & ; \text{ if } f \leq 250 \text{ hz} \\ \text{or} \\ .02 \times (386.4)^2 \times \left[ \frac{f}{250} \right]^{-1.993} & ; \text{ if } f > 250 \text{ hz} \end{cases} \dots\dots (3.2)$$

if  $f \leq 250 \text{ hz}$ , PSDF has slope of 0

if  $f > 250 \text{ hz}$ , PSDF has slope of  $-6 \frac{\text{dB}}{\text{octave}}$

$\zeta$  = Known:

Variable parameter in earlier studies,

later determined to be 0.004 from tests at NASA Ames

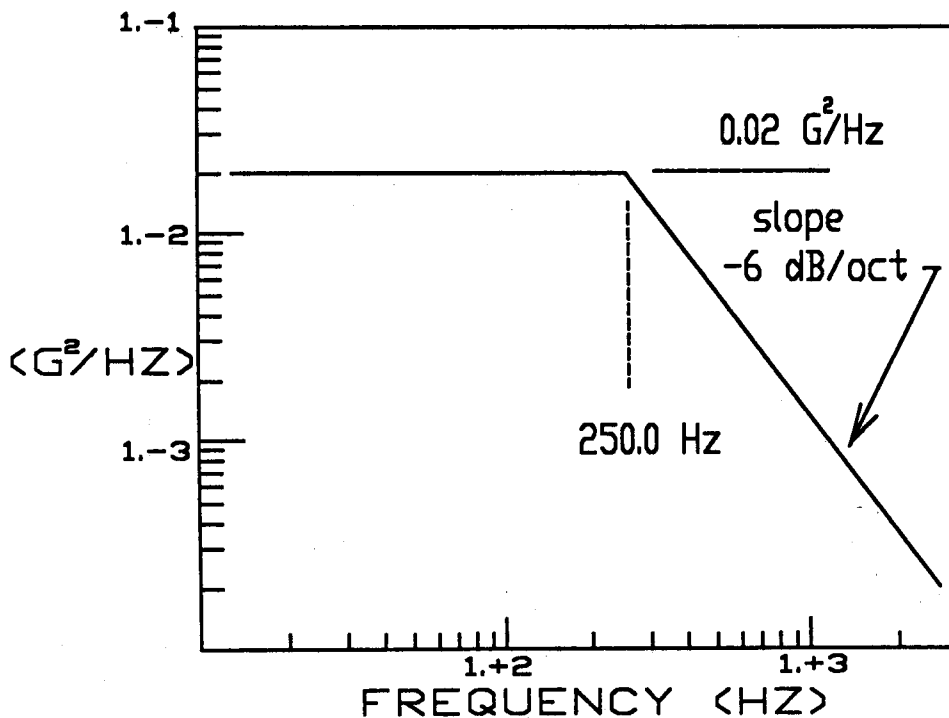


Figure 3.6 Design PSDF Supplied by NASA Ames

4. Determine the RMS lateral displacement of the system from Equation 3.1 and multiply by three to obtain the three sigma ( $3\sigma$ ) system displacement. Loading is assumed to be acting in each of the three mutually orthogonal axes simultaneously. It is further assumed that the two in-plane forcing functions are in phase. This introduces a factor of  $\sqrt{2}$  onto the  $3\sigma$  lateral displacement obtained above. Because that displacement is in an arbitrary direction, it must exactly be the maximum lateral deflection of a support assembly in its stiff direction. Therefore:

$$\delta_{3\sigma} = \text{Known from procedure stated above}$$

5. From the natural frequency,  $f$ , of the current DO loop and the known mass of the mirror,  $M$ ; the spring constant,  $K$ , of the system can be derived. Ignoring  $K_{\text{soft}}$  in the soft direction with respect to  $K_{\text{hard}}$  in the hard direction, the moment of inertia,  $I$ , of a single blade in the flexure assembly in its hard direction can be determined.

$$f = \left[ \frac{1}{2\pi} \right] \sqrt{\frac{K}{M}} \dots\dots\dots (3.3)$$

Where:

$K$  = SDOF Spring Constant

$M$  = SDOF Mass

$$K = 1.5 ( K_{\text{soft}} + K_{\text{hard}} ) \dots\dots\dots (3.4)$$

Where:

$K_{\text{soft}}$  = Single Flexure Assembly's  
Radial Stiffness

$K_{\text{hard}}$  = Single Flexure Assembly's  
Tangential Stiffness

$K_{\text{soft}} \ll K_{\text{hard}}$

Therefore:

$$K \cong 1.5 (K_{\text{hard}})$$

For the two flexure blades:

$$K = 2 \times 12 \times \frac{E I}{L^3}$$

And therefore:

$$I = \left[ \frac{M (2\pi f)^2}{1.5 \times 24 E} \right]$$

6. Knowing the length,  $L$ ; moment of inertia,  $I$ ; and the end deflection,  $\delta$ ; flexure blade moments,  $M$ , and shears,  $V$ , can be determined.

$$V = \left[ 12 \frac{E I}{L^3} \right] \delta$$

$$M = \left[ 6 \frac{E I}{L^2} \right] \delta$$

7. From the moment of inertia,  $I$ ; bending moment,  $M$ ; and allowable working stress,  $\sigma$ ; the blade width,  $B$ , can be determined.

$$\sigma = \frac{M \left[ \frac{B}{2} \right]}{I}$$

$$B = \frac{2 I \sigma}{M}$$

8. From the blade moment of inertia,  $I$ ; and width,  $B$ ; the blade thickness,  $t$ , can be determined.

$$I = \frac{t B^3}{12}$$

$$t = \frac{12 I}{B^3}$$

9. The blade dimensions at this point have been established and are based on the flexure's strength. In order to be an acceptable design, that same blade configuration must now be soft enough in the radial direction that the allowable bending moment being applied to the mirror is not exceeded. As shown in Chapter 2, the radial deflection imposed on the flexure assembly,  $\delta_{\text{cryo}}$ , during



cryogenic cooldown is due solely to the shrinkage of the aluminum baseplate because the coefficient of thermal expansion of the glass is substantially less than that of aluminum. Based on  $\delta_{\text{cryo}}$ , the bending moment applied at the plane of the center of mass of the mirror can be calculated and compared with the allowable moment determined from the FRINGE and NASTRAN analysis.

$$\begin{aligned}\delta_{\text{cryo}} &= R \alpha_{\text{aluminum}} \Delta T \\ &= 0.0619 \text{ inch from Equation 2.3}\end{aligned}$$

$$\text{Moment at mirror} = 2 V (L + \chi)$$

$\chi$  = distance from lower end of vertical  
flexure to plane of mirror's  
center of mass

$$\text{Moment at mirror} = \left[ \frac{24 E I}{L^3} \right] (L + \chi) \delta_{\text{cryo}}$$

$$\text{Moment}_{\text{allowable}} = 149.4 \text{ in-lb, from Table 2.1}$$

Accept design if:

$$[ \text{Moment at mirror} ] \leq [ \text{Moment}_{\text{allowable}} ]$$

10. Print results and continue the loops.

Blade configurations for the stiff direction that evolved from this study had depths nearly equal to their lengths. Consequently, shear deformations were of the same order of magnitude as the flexural deformations and could not be ignored. Stiffness calculations that included shear deformations could not easily be included in the simple algorithm presented above so a more direct approach was taken. The iteration loops covered a specific family of flexure and gimbal configurations. For each configuration, system stiffness, system natural frequency, mirror deflection, and internal load distribution were calculated for both the lateral mode of vibration and for the vertical mode of vibration. The development of the stiffness equation became the major difference between this new program and the one described above. In the remainder of this

chapter the details that were used in the development of that stiffness equation for the new program will be discussed.

*Develop gimbal torsional stiffness of cruciforms,  $K_{rh}$*

(  $K_{rh}$  = Variable GKRH in FORTRAN program in Appendix I )

From Figure 3.7

$$M = K_{rh} \theta \quad M_1 = K_1 \theta_1 \quad M_2 = K_2 \theta_2$$

Where:

$M$  = Gimbal moment

$\theta$  = Gimbal rotation

$M_i$  = Moment in blade  $i$        $i=1$ ; vertical

$\theta_i$  = Rotation in blade  $i$        $i=2$ ; horizontal

$$K_i = \frac{G B_i t_i^3}{3 L_i}$$

$G$  = Shear modulus

$B_i, t_i, L_i$  are gimbal blade dimensions

$$\theta = \theta_1 = \theta_2$$

$$M = 2 M_1 + 2 M_2$$

$$M = 2 K_1 \theta_1 + 2 K_2 \theta_2$$

$$M = ( 2 K_1 + 2 K_2 ) \theta$$

$$K_{rh} = 2 K_1 + 2 K_2$$

$$K_{rh} = \left[ \frac{2 G B_1 t_1^3}{3 L_1} \right] + \left[ \frac{2 G B_2 t_2^3}{3 L_2} \right] \dots\dots\dots ( 3.5 )$$

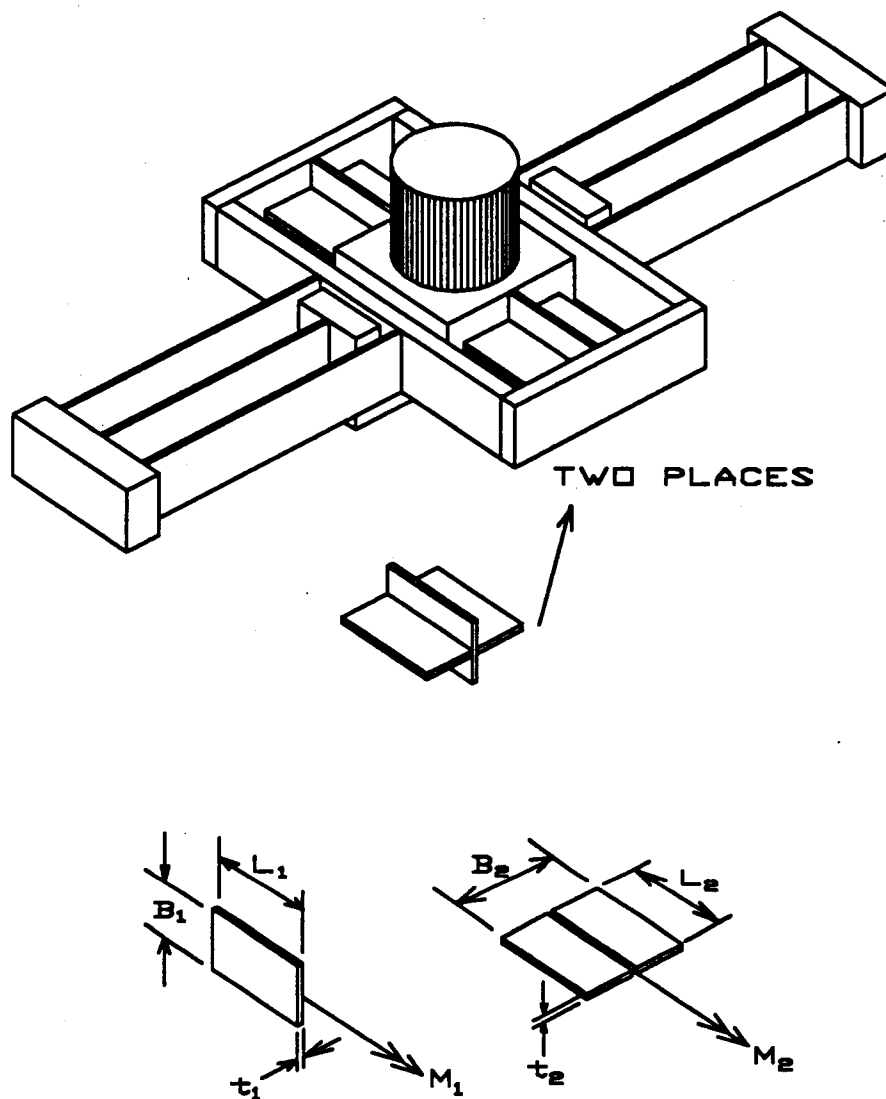


Figure 3.7 Gimbal Configuration - Torsion

Develop gimbal torsional stiffness in flexure blades,  $K_{rs}$

(  $K_{rs}$  = Variable GKRS in FORTRAN program in Appendix I )

From Figure 3.8

$$M = K_{rs} \theta \quad M_1 = K_1 \theta_1 \quad M_2 = K_2 \theta_2$$

Where:

$M$  = Flexure assembly moment

$\theta$  = Flexure assembly rotation

$$K_i = \frac{G B_i t_i^3}{3 L_i} \quad ; \quad \text{inner; } i=1 \quad \text{outer; } i=2$$

$G$  = Shear modulus

$M_i$  = Moment in blade  $i$

$\theta_i$  = Rotation in blade  $i$

$B_i, t_i, L_i$  are gimbal blade dimensions

$$\theta = \theta_1 + \theta_2 \quad ; \quad \theta_1 = \frac{M}{2 K_1} \quad ; \quad \theta_2 = \frac{M}{4 K_2}$$

$$\theta = \frac{M}{2 K_1} + \frac{M}{4 K_2}$$

$$\theta = \left[ \frac{1}{2 K_1} + \frac{1}{4 K_2} \right] M$$

$$M = \left[ \frac{1}{\left[ \frac{1}{2 K_1} + \frac{1}{4 K_2} \right]} \right] \theta$$

$$K_{rs} = \frac{8 K_1 K_2}{2 K_1 + 4 K_2}$$

$$K_{rs} = \frac{4 G B_1 t_1^3 B_2 t_2^3}{3 B_1 t_1^3 L_2 + 6 B_2 t_2^3 L_1} \dots \dots \dots ( 3.6 )$$

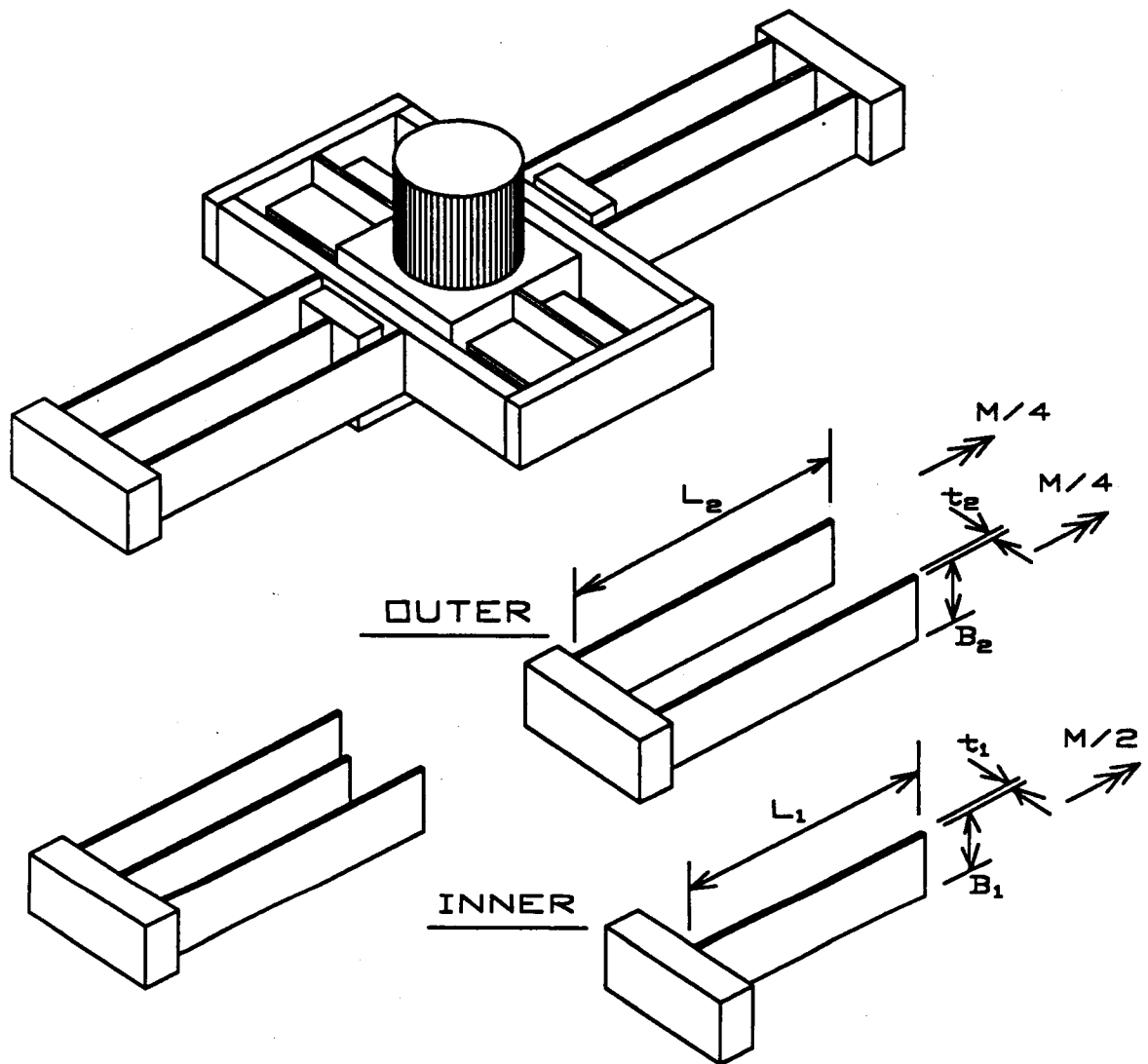


Figure 3.8 Flexure Blade Configuration - - Torsion

*Develop flexure assembly lateral stiffnesses, hard and soft*

( Variables SKSSS (soft) and SKSSH (hard) in FORTRAN program in Appendix I )

$$\frac{1}{SKSSS} = \left[ \frac{1}{K_{\text{post}}} \right]_{\text{soft}} + \left[ \frac{1}{K_{\text{blades}}} \right]_{\text{soft}} + \left[ \frac{1}{K(\text{gimbal})} \right]_{\text{axial}} + \left[ \frac{1}{K_{\text{frame}}} \right]_{\text{axial}} \quad ( 3.7 )$$

$$\frac{1}{SKSSH} = \left[ \frac{1}{K_{\text{post}}} \right]_{\text{hard}} + \left[ \frac{1}{K_{\text{blades}}} \right]_{\text{axial}} + \left[ \frac{1}{K(\text{gimbal})} \right]_{\text{hard}} + \left[ \frac{1}{K_{\text{frame}}} \right]_{\text{soft}} \quad ( 3.8 )$$

Each term in Equations 3.7 and 3.8 will now be determined based on a general set of dimensions for the post, the cruciform blades, and the flexure blades. In the final design configuration, the vertical post is a cylindrical bar with equal section properties in the hard and soft directions. Because the torsional stiffnesses,  $K_{rh}$  and  $K_{rs}$ , are in general different, the effective post stiffnesses will in general be a function of the loading direction. In the final design configuration, however, both  $K_{rh}$  and  $K_{rs}$  are small enough to be ignored. As seen by  $K_r$  in Equation 3.10, when either  $K_{rh}$  or  $K_{rs}$  is small compared to  $\frac{4EI}{L}$ , the post can be considered to be pinned on that axis.

Considering both shear and bending in the system stiffness:

$$\left[ \frac{1}{K_{\text{post}}} \right] = \left[ \frac{1}{K_{\text{post}}} \right]_{\text{flexure}} + \left[ \frac{1}{K_{\text{post}}} \right]_{\text{shear}} \dots\dots\dots ( 3.9 )$$

From Figure 3.9:

$$M_{ab} = \left[ \frac{E I}{L} \right] \left[ 4\theta_a + 2\theta_b - \frac{6\delta_a}{L} \right]$$

$$M_{ba} = \left[ \frac{E I}{L} \right] \left[ 4\theta_b + 2\theta_a - \frac{6\delta_a}{L} \right]$$

$$\theta_a = 0$$

$$M_{ba} = -K_r \theta_b$$

$$M_{ab} + M_{ba} + F L = 0$$

$$F = [K_{\text{post}}]_{\text{flexure}} \delta_a$$

Solving the above set of equations yields:

$$[K_{\text{post}}]_{\text{flexure}} = \frac{\left[ \frac{12 E I}{L^3} \right] \left[ \frac{L K_r}{4 E I} + \frac{1}{4} \right]}{\left[ \frac{L K_r}{4 E I} + 1 \right]} \dots \dots \dots ( 3.10 )$$

NOTE: As  $K_r$  increases,  $K_{\text{post}}$  approaches  $\frac{12EI}{L^3}$  which is  $K$  for the lateral translation of a fixed-fixed beam

As  $K_r$  decreases,  $K_{\text{post}}$  approaches  $\frac{3EI}{L^3}$  which is  $K$  for the lateral translation of a fixed-pinned beam

$$\delta_s = \frac{F L}{G A}$$

$$[K_{\text{post}}]_{\text{shear}} = \frac{G A}{L} \dots \dots \dots ( 3.11 )$$

Substituting Equation 3.10 and 3.11 into Equation 3.9 yields:

$$\left[ \frac{1}{K_{\text{post}}} \right] = \frac{\left[ \frac{L K_r}{4 E I} + 1 \right]}{\left[ \frac{12 E I}{L^3} \right] \left[ \frac{L K_r}{4 E I} + \frac{1}{4} \right]} + \frac{L}{G A} \dots\dots\dots (3.12)$$

Where :  $K_r = K_{rs}$  or  $K_{rh}$  , depending on direction

Because  $K_{rs}$  and  $K_{rh} \ll \left[ \frac{4 E I}{L} \right]$  :

$$\left[ \frac{1}{K_{\text{post}}} \right]_{\text{soft}} - \left[ \frac{1}{K_{\text{post}}} \right]_{\text{hard}} = \left[ \frac{1}{K_{\text{post}}} \right] \cong \left[ \frac{L^3}{3 E I} + \frac{L}{G A} \right] \dots\dots\dots (3.13)$$

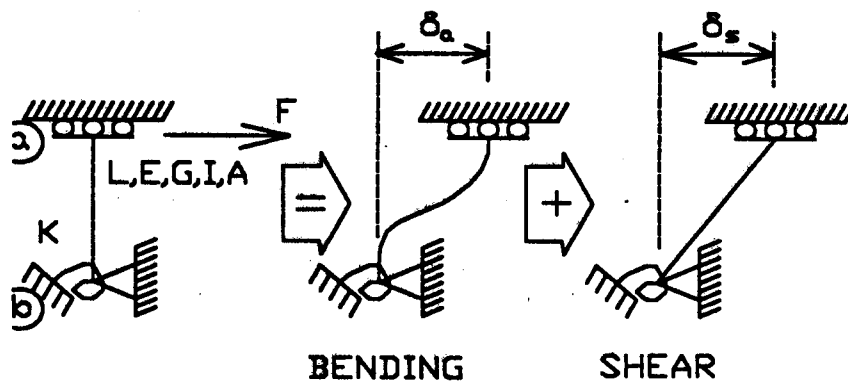


Figure 3.9 Vertical Post Configuration - - Bending and Shear



*Develop horizontal blade stiffnesses*

From Figure 3.10:

Bending Stiffness:

$$\delta = \delta_{\text{outer}} + \delta_{\text{inner}}$$

$$\frac{F}{4} = \left[ \frac{12 E I_{\text{outer}}}{L_{\text{outer}}^3} \right] \delta_{\text{outer}}$$

$$\delta_{\text{outer}} = \left[ \frac{L_{\text{outer}}^3}{48 E I_{\text{outer}}} \right] F$$

$$\frac{F}{2} = \left[ \frac{12 E I_{\text{inner}}}{L_{\text{inner}}^3} \right] \delta_{\text{inner}}$$

$$\delta_{\text{inner}} = \left[ \frac{L_{\text{inner}}^3}{24 E I_{\text{inner}}} \right] F$$

$$\delta = \left[ \frac{L_{\text{outer}}^3}{48 E I_{\text{outer}}} + \frac{L_{\text{inner}}^3}{24 E I_{\text{inner}}} \right] F$$

$$\left[ \frac{1}{K_{\text{blades}}} \right]_{\text{soft}} = \left[ \frac{L_{\text{outer}}^3 I_{\text{inner}} + 2 L_{\text{inner}}^3 I_{\text{outer}}}{48 E I_{\text{inner}} I_{\text{outer}}} \right] \dots\dots\dots ( 3.14 )$$

Axial Stiffness:

$$\delta = \delta_{\text{inner}} + \delta_{\text{outer}}$$

$$\delta_{\text{inner}} = \frac{F L_{\text{inner}}}{4 A_{\text{inner}} E}$$

$$\delta_{\text{outer}} = \frac{F L_{\text{outer}}}{2 A_{\text{outer}} E}$$

$$\delta = \left[ \frac{L_{\text{inner}}}{4 A_{\text{inner}} E} + \frac{L_{\text{outer}}}{2 A_{\text{outer}} E} \right]$$

$$\left[ \frac{1}{K_{\text{blades}}} \right]_{\text{axial}} = \left[ \frac{L_{\text{inner}} A_{\text{outer}} + 2 L_{\text{outer}} A_{\text{inner}}}{4 E A_{\text{inner}} A_{\text{outer}}} \right] \dots \dots \dots (3.15)$$

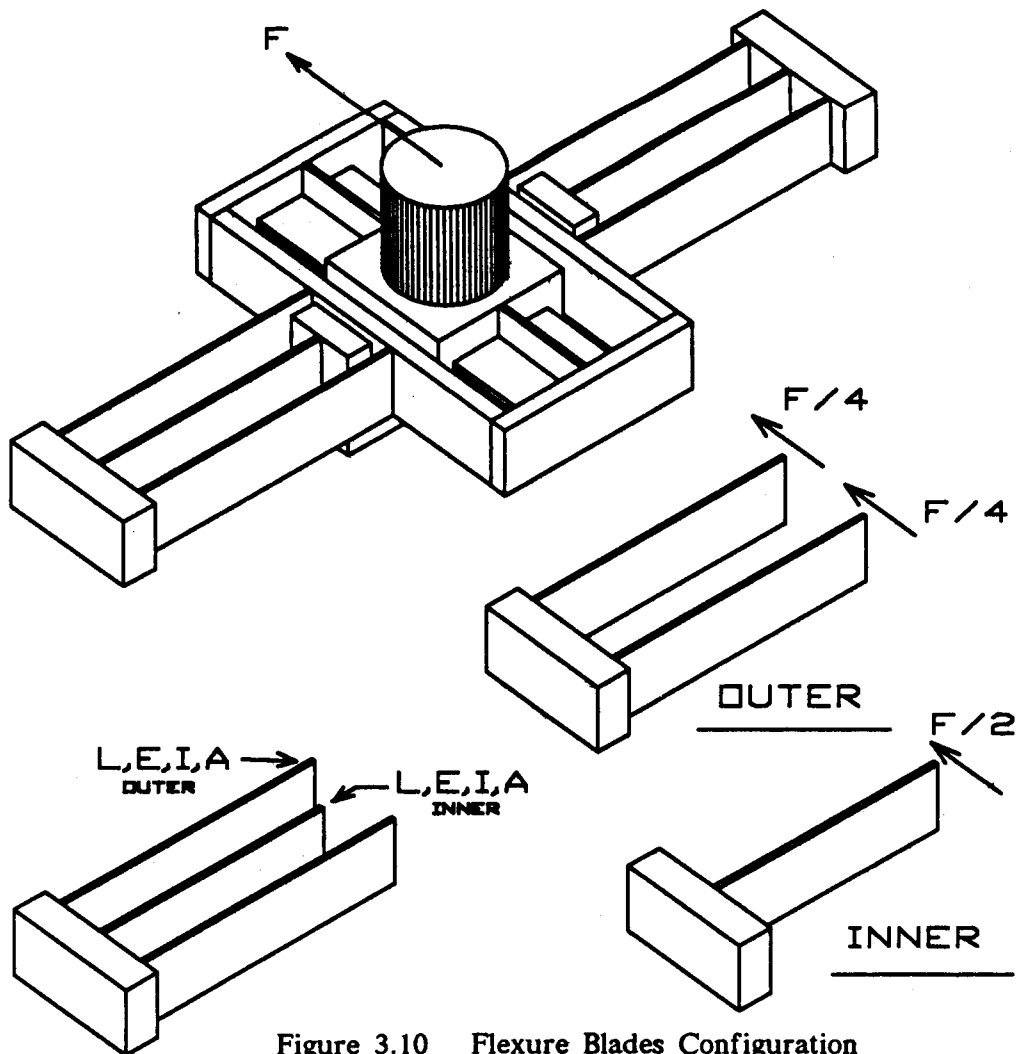


Figure 3.10 Flexure Blades Configuration

*Develop gimbal blade stiffnesses*

From Figure 3.11

Axial Stiffness:

$$\delta = \delta_{\text{vertical}} + \delta_{\text{horizontal}}$$

$$\delta_{\text{vertical}} = \frac{F_{\text{vertical}} L}{2 A_{\text{vertical}} E}$$

$$\delta_{\text{horizontal}} = \frac{F_{\text{horizontal}} L}{2 A_{\text{horizontal}} E}$$

$$F = F_{\text{vertical}} + F_{\text{horizontal}}$$

$$F = \left[ \frac{2 A_{\text{vertical}} E}{L} + \frac{2 A_{\text{horizontal}} E}{L} \right] \delta$$

$$F = 2 \frac{E}{L} (A_{\text{vertical}} + A_{\text{horizontal}}) \delta$$

$$\left[ \frac{1}{K_{\text{gimbal}}} \right]_{\text{axial}} = \frac{L}{2 E (A_{\text{vertical}} + A_{\text{horizontal}})} \dots \dots \dots (3.16)$$

Lateral Stiffness:

$$\delta = \delta_{\text{bending}} + \delta_{\text{shear}}$$

$$\frac{F}{2} = \left[ \frac{12 E I}{L^3} \right] \delta_{\text{bending}}$$

$$\frac{F}{2} = \left[ \frac{G A}{L} \right] \delta_{\text{shear}}$$

$$\delta = \left[ \frac{L^3}{24 E I} + \frac{L}{2 G A} \right] F$$

$$\left[ \frac{1}{K_{\text{gimbal}}} \right]_{\text{hard}} = \left[ \frac{L^3}{24 E I} \right] + \left[ \frac{L}{2 G A} \right] \dots\dots\dots (3.17)$$

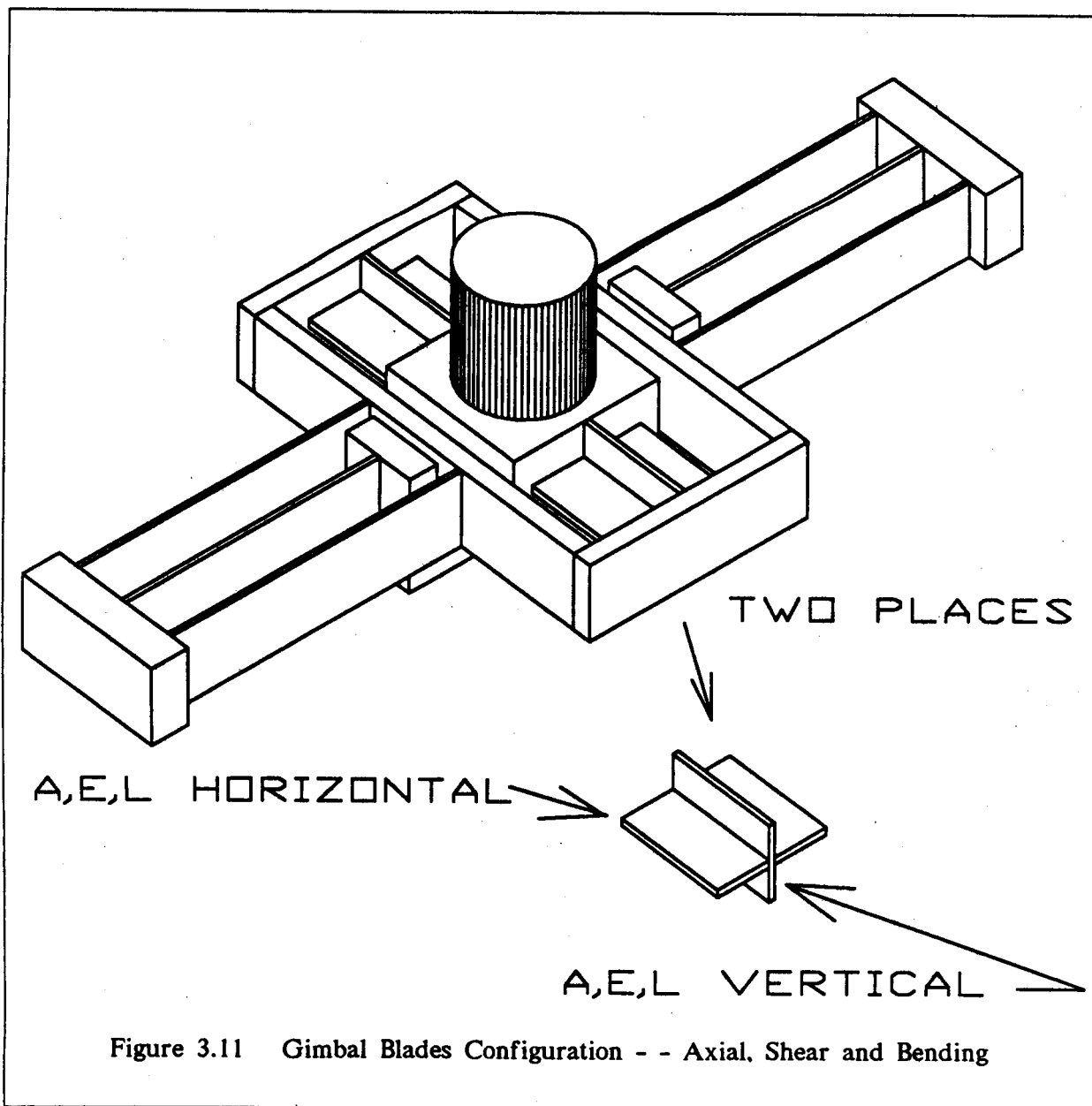


Figure 3.11 Gimbal Blades Configuration - - Axial, Shear and Bending

### *Develop frame stiffness*

The frame stiffness described in Figure 3.12 and by Equations 3.18 and 3.19 was not included in the SDOF analysis, as it was assumed that the frame was rigid in comparison to the other structural elements in the flexure assembly. When the NASTRAN model was assembled, actual section properties of all members were input. When the NASTRAN model predicted significantly lower natural frequencies than those predicted by the SDOF model, the hand analysis described in Chapter 4 which included the flexibility of the frame structure was performed. The results of the hand analysis confirmed the NASTRAN model, but because the NASTRAN model was so close to a final design, the SDOF model in the FORTRAN program in Appendix I was never updated. Equations 3.18 and 3.19 are therefore included here for completeness of the SDOF model.

From Figure 3.12

Bending and shear :

$$F = K \delta$$

$$\delta = \delta_1 + \delta_2 + \delta_3 + \delta_4$$

$$\delta_1 = \frac{\left(\frac{F}{4}\right)\left(\frac{L_1}{2}\right)^3}{3 E I} = \left[\frac{L_1^3}{96 E I}\right] F$$

$$\delta_2 = \left(\frac{F}{4}\right) \left[\frac{1}{12 E I}\right] \left[\frac{L_3}{2} - \frac{L_1}{2}\right]^2 \left[\frac{L_3}{2} + L_1\right] \quad (\text{Reference 6})$$

$$\delta_2 = \left[ \frac{1}{48 E I} \right] \left( \frac{L_3}{2} - \frac{L_1}{2} \right)^2 \left( \frac{L_3}{2} + L_1 \right) F$$

$$\delta_3 = \left[ \frac{1}{A G} \right] \left( \frac{F}{4} \right) \left( \frac{L_1}{2} \right) = \left[ \frac{L_1}{8 A G} \right] F$$

$$\delta_4 = \left[ \frac{1}{A G} \right] \left( \frac{F}{4} \right) \left( \frac{L_3}{2} - \frac{L_1}{2} \right) = \left[ \frac{L_3 - L_1}{8 A G} \right] F$$

$$\left[ \frac{1}{K_{\text{frame}}} \right]_{\text{soft}} = \left[ \frac{1}{96 E I} \right] \left[ L_1^3 + 2 \left( \frac{L_3}{2} - \frac{L_1}{2} \right)^2 \left( \frac{L_3}{2} + L_1 \right) \right] + \frac{L_3}{8 A G} \dots\dots\dots (3.18)$$

From Figure 3.12

Axial :

$$F = K \delta$$

$$\delta = \delta_1 + \delta_2$$

$$\delta_1 = \frac{\left( \frac{F}{4} \right) \left( \frac{L_1}{2} \right)}{A E} = \left[ \frac{L_1}{8 A E} \right] F$$

$$\delta_2 = \frac{\left( \frac{F}{4} \right) \left( \frac{L_3}{2} - \frac{L_1}{2} \right)}{A E} = \left[ \frac{L_3 - L_1}{8 A E} \right] F$$

$$\left[ \frac{1}{K_{\text{frame}}} \right]_{\text{axial}} = \frac{L_3}{8 A E} \dots\dots\dots (3.19)$$

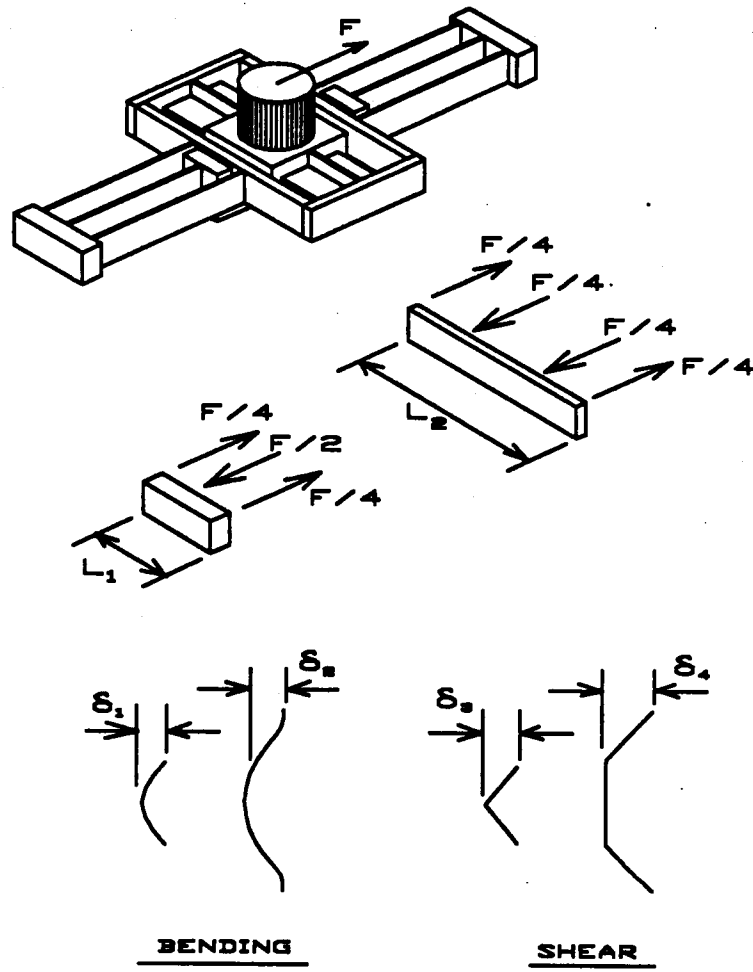


Figure 3.12 Frame Configuration

### *Develop stability model*

The flexure blades were designed to be as thin as possible to minimize the radial stiffness, but the blades are still required to react the vertical shear and bending moment imposed by the mass of the mirror vibrating parallel to the optical axis. Critical buckling loads therefore had to be determined for each configuration considered. Although closed form solutions with the proper boundary conditions were not available, the closed form solutions which were available were all of the following form<sup>7</sup>:

$$F_{cr} = C B \frac{t^3}{L^2} \dots \dots \dots (3.20)$$

where:

$F_{cr}$  = critical shear load

$B$  = blade height

$t$  = blade thickness

$L$  = blade length

$C$  = constant, a function of boundary constraints  
and material properties

Elastic stability models of selected flexure and gimbal blade configurations were run on the NASTRAN finite element program. It was observed that the constant,  $C$ , in Equation 3.20 could be extracted from the runs already made and that the deviation of the critical load predicted from run to run was within five percent. Equation 3.20 was incorporated into the SDOF parametric study program, thereby allowing the critical buckling load for each configuration studied to be calculated and compared with the current working load without the need of making a NASTRAN run. Of course, the final design configuration was analyzed for stability with NASTRAN, and a typical NASTRAN input file for buckling is included in Appendix V.



### *Finalize SDOF program*

All terms in Equations 3.7 and 3.8 have been determined and are described by Equations 3.13 through 3.19. The remainder of the new program now takes on a rearranged form of the old one. In summary:

Equation 3.4 gives the system stiffness:

$$\begin{aligned} K &= 1.5 ( K_{\text{soft}} + K_{\text{hard}} ) \\ &= 1.5 ( SKSSS + SKSSH ) \end{aligned}$$

Equation 3.3 gives the system natural frequency:

$$f = \left[ \frac{1}{2\pi} \right] \sqrt{\frac{K}{M}}$$

Equation 3.2 gives the value of the PSDF:

$$\text{PSD} = \left[ \begin{array}{ll} .02 \times (386.4)^2 & ; \text{ if } f \leq 250 \text{ hz} \\ \text{or} & \\ .02 \times (386.4)^2 \times \left[ \frac{f}{250} \right]^{-1.993} & ; \text{ if } f > 250 \text{ hz} \end{array} \right]$$

if  $f \leq 250$  hz, PSDF has slope of 0

if  $f > 250$  hz, PSDF has slope of  $-6 \frac{\text{dB}}{\text{octave}}$

Equation 3.1 gives the RMS single axis PSDF displacement:

$$\delta_{\text{RMS}} = \sqrt{\frac{\text{PSD}(f)}{(4\pi f)^3 \zeta}}$$

$$\zeta = 0.004$$

$$\delta_{3\sigma} = 3 \delta_{\text{RMS}}$$

For two axis PSDF:

$$\delta_{\text{design}} = \sqrt{2} \delta_{3\sigma}$$

Loads and stresses are then determined from the displacements. The output of the updated parametric design program consists of the following items:

- A. Header: presents information on the current PSDF, damping ratio, flexure material, cryogenic deflection, mirror weight and allowable operational bending moment for the mirror.
- B. Listing: following design parameters for each iteration considered.
1. Flexure blade length, width, and thickness.
  2. Gimbal horizontal blade length, width, and thickness.
  3. Horizontal displacement,  $(3\sigma)$
  4. Vertical displacement,  $(3\sigma)$
  5. Vertical natural frequency of SDOF system
  6. Horizontal natural frequency of SDOF system
  7. Vertical post load
  8. Horizontal post load
  9. Margins of safety for:
    - a. Flexure in the hard direction
    - b. Flexure in the soft direction
    - c. Gimbal in the hard direction
    - d. Gimbal in the soft direction
    - e. Bending moment at the mirror during cryogenic cooldown
    - f. Bending on vertical post
    - g. Manufacturing tolerances
    - h. Blade elastic stability (buckling)
- C. The FORTRAN listing of the program used for the final design of the SDOF system is presented in Appendix I.

### A numerical example

The geometry of the final design submitted to NASA Ames is shown in Figure 1.5. That geometry will be used in determining the numerical values for SKSSS and SKSSH in Equations 3.7 and 3.8. First the torsional stiffnesses,  $K_{rh}$  and  $K_{rs}$  will be determined.

From Equation 3.5 :

$$\begin{aligned}
 K_{rh} &= \left[ \frac{2 G B_1 t_1^3}{3 L_1} \right] + \left[ \frac{2 G B_2 t_2^3}{3 L_2} \right] \dots\dots\dots (3.5 \text{ repeated}) \\
 &= \frac{2.0 \times 6.92 \times 10^6 \times 3.0 \times 0.19^3}{3 \times 3} + \frac{2.0 \times 6.92 \times 10^6 \times 2.0 \times 0.14^3}{3 \times 3} \\
 &= 3.164 \times 10^4 + 8.439 \times 10^3 \\
 &= 4.008 \times 10^4 \frac{\text{in-lb}}{\text{rad}} \dots\dots\dots (3.21)
 \end{aligned}$$

From Equation 3.6 :

$$\begin{aligned}
 K_{rs} &= \frac{4 G B_1 t_1^3 B_2 t_2^3}{3 B_1 t_1^3 L_2 + 6 B_2 t_2^3 L_1} \dots\dots\dots (3.6 \text{ repeated}) \\
 &= \frac{4.0 \times 6.92 \times 10^6 \times 2.225 \times 0.18^3 \times 2.0 \times 0.14^3}{3.0 \times 2.225 \times 0.18^3 \times 7.0 + 6.0 \times 2.0 \times 0.14^3 \times 6.0} \\
 &= 4.193 \times 10^3 \frac{\text{in-lb}}{\text{rad}} \dots\dots\dots (3.22)
 \end{aligned}$$

Now the vertical post stiffnesses:

From Equation 3.12 :

$$\left[ \frac{1}{K_{\text{post}}} \right] = \frac{\left[ \frac{L K_r}{4 E I} + 1 \right]}{\left[ \frac{12 E I}{L^3} \right] \left[ \frac{L K_r}{4 E I} + \frac{1}{4} \right]} + \frac{L}{G A} \dots\dots\dots (3.12 \text{ repeated})$$

Where :

$$K_r = K_{rs} \text{ or } K_{rh} \text{ , depending on direction}$$

From Equation 3.12 :

$$\begin{aligned}\frac{4 E I}{L} &= \frac{4.0 \times 18 \times 10^6 \times \pi \times 3.0^4}{64 \times 3} \\ &= 9.538 \times 10^7 \frac{\text{in-lb}}{\text{rad}} \dots\dots\dots ( 3.23 )\end{aligned}$$

As shown by Equations 3.21, 3.22, and 3.23 :

$$K_{rs} \text{ and } K_{rh} \ll \left[ \frac{4 E I}{L} \right] :$$

Therefore from Equation 3.13

$$\begin{aligned}\left[ \frac{1}{K_{\text{post}}} \right]_{\text{soft}} &= \left[ \frac{1}{K_{\text{post}}} \right]_{\text{hard}} = \left[ \frac{1}{K_{\text{post}}} \right] \cong \left[ \frac{L^3}{3 E I} + \frac{L}{G A} \right] \dots\dots\dots ( 3.13 \text{ repeated} ) \\ \left[ \frac{1}{K_{\text{post}}} \right] &= \frac{3.0^3 \times 64.0}{3.0 \times 18.0 \times 10^6 \times 3.0^4} + \frac{3.0 \times 4.0}{6.92 \times 10^6 \times \pi \times 3^2} \\ &= 3.951 \times 10^{-7} + 6.136 \times 10^{-8} \\ &= 4.564 \times 10^{-7} \frac{\text{in}}{\text{lb}} \dots\dots\dots ( 3.24 )\end{aligned}$$

Now the horizontal blade stiffnesses :

From Equation 3.14 :

$$\begin{aligned}\left[ \frac{1}{K_{\text{blades}}} \right]_{\text{soft}} &= \left[ \frac{L_{\text{outer}}^3 I_{\text{inner}} + 2 L_{\text{inner}}^3 I_{\text{outer}}}{48 E I_{\text{inner}} I_{\text{outer}}} \right] \dots\dots\dots ( 3.14 \text{ repeated} ) \\ &= \frac{7.0^3 \times 2.225 \times 0.18^3 \times 12.0 + 2.0 \times 6^3 \times 2.0 \times 0.14^3 \times 12.0}{48.0 \times 18.0 \times 10^6 \times 2.225 \times 0.18^3 \times 2.0 \times 0.14^3} \\ &= 1.330 \times 10^{-3} \frac{\text{in}}{\text{lb}} \dots\dots\dots ( 3.25 )\end{aligned}$$

From Equation 3.15 :

$$\begin{aligned}\left[ \frac{1}{K_{\text{blades}}} \right]_{\text{axial}} &= \left[ \frac{L_{\text{inner}} A_{\text{outer}} + 2 L_{\text{outer}} A_{\text{inner}}}{4 E A_{\text{inner}} A_{\text{outer}}} \right] \dots\dots\dots ( 3.15 \text{ repeated} ) \\ &= \frac{6.0 \times 2.0 \times 0.14 + 2.0 \times 7.0 \times 2.225 \times 0.18}{4.0 \times 18.0 \times 10^6 \times 2.225 \times 0.18 \times 2.0 \times 0.14} \\ &= 9.025 \times 10^{-7} \frac{\text{in}}{\text{lb}} \dots\dots\dots ( 3.26 )\end{aligned}$$

Now the gimbal blade stiffnesses :

From Equation 3.16 :

$$\begin{aligned} \left[ \frac{1}{K_{\text{gimbal}}} \right]_{\text{axial}} &= \frac{L}{2 E (A_{\text{vertical}} + A_{\text{horizontal}})} \dots\dots\dots ( 3.16 \text{ repeated } ) \\ &= \frac{3.0}{(2.0 \times 18.0 \times 10^6)(2.0 \times 0.14 + 3.0 \times 0.19)} \\ &= 9.804 \times 10^{-8} \frac{\text{in}}{\text{lb}} \dots\dots\dots ( 3.27 ) \end{aligned}$$

From Equation 3.17 :

$$\begin{aligned} \left[ \frac{1}{K_{\text{gimbal}}} \right]_{\text{hard}} &= \left[ \frac{L^3}{24 E I} \right] + \left[ \frac{L}{2 G A} \right] \dots\dots\dots ( 3.17 \text{ repeated } ) \\ &= \frac{3.0^3 \times 12.0}{24.0 \times 18.0 \times 10^6 \times 3^3 \times 0.19} + \frac{3.0}{2.0 \times 6.92 \times 10^6 \times 3.0 \times 0.19} \\ &= 1.462 \times 10^{-7} + 3.803 \times 10^{-7} \\ &= 5.265 \times 10^{-7} \dots\dots\dots ( 3.28 ) \end{aligned}$$

From Equation 3.18 :

$$\begin{aligned} \left[ \frac{1}{K_{\text{frame}}} \right]_{\text{soft}} &= \left[ \frac{1}{96 E I} \right] \left[ L_1^3 + 2 \left[ \frac{L_3}{2} - \frac{L_1}{2} \right]^2 \left[ \frac{L_3}{2} + L_1 \right] \right] + \frac{L_3}{8 A G} \dots\dots\dots ( 3.18 \text{ repeated } ) \\ &= \left[ \frac{1.0}{96.0 \times 18.0 \times 10^6 \times 0.0703} \right] (2.88^3 + 2 \times (4.5 - 1.44)^2 (4.5 + 2.88)) \\ &\quad + \frac{9}{8.0 \times 1.5 \times 6.92 \times 10^6} \\ &= 1.334 \times 10^{-6} + 1.084 \times 10^{-7} \\ &= 1.443 \times 10^{-6} \frac{\text{in}}{\text{lb}} \dots\dots\dots ( 3.29 ) \end{aligned}$$

From Equation 3.19 :

$$\begin{aligned} \left[ \frac{1}{K_{\text{frame}}} \right]_{\text{axial}} &= \frac{L_3}{8 A E} \dots\dots\dots ( 3.19 \text{ repeated } ) \\ &= \frac{9.0}{8.0 \times 1.5 \times 18.0 \times 10^6} \\ &= 4.167 \times 10^{-8} \frac{\text{in}}{\text{lb}} \dots\dots\dots ( 3.30 ) \end{aligned}$$

Now substituting Equations 3.24, 3.25 3.27 and 3.30 into Equation 3.7 :

$$\begin{aligned} \frac{1}{SKSSS} &= \left[ \frac{1}{K_{\text{post}}} \right]_{\text{soft}} + \left[ \frac{1}{K_{\text{blades}}} \right]_{\text{soft}} + \left[ \frac{1}{K_{\text{gimbal}}} \right]_{\text{axial}} + \left[ \frac{1}{K_{\text{frame}}} \right]_{\text{axial}} \\ &\dots\dots\dots ( 3.7 \text{ repeated } ) \\ &= 4.564 \times 10^{-7} + 1.33 \times 10^{-3} + 9.804 \times 10^{-8} + 4.167 \times 10^{-8} \\ &= 1.331 \times 10^{-3} \frac{\text{in}}{\text{lb}} \\ SKSSS &= 751.5 \frac{\text{lb}}{\text{in}} \dots\dots\dots ( 3.31 ) \end{aligned}$$

And substituting Equations 3.24, 3.26, 3.28 and 3.29 into Equation 3.8 :

$$\begin{aligned} \frac{1}{SKSSH} &= \left[ \frac{1}{K_{\text{post}}} \right]_{\text{hard}} + \left[ \frac{1}{K_{\text{blades}}} \right]_{\text{axial}} + \left[ \frac{1}{K_{\text{gimbal}}} \right]_{\text{hard}} + \left[ \frac{1}{K_{\text{frame}}} \right]_{\text{soft}} \\ &\dots\dots\dots ( 3.8 \text{ repeated } ) \\ &= 4.564 \times 10^{-7} + 9.025 \times 10^{-7} + 5.265 \times 10^{-7} + 1.443 \times 10^{-6} \\ &= 3.328 \times 10^{-6} \frac{\text{in}}{\text{lb}} \\ SKSSH &= 3.004 \times 10^5 \frac{\text{lb}}{\text{in}} \dots\dots\dots ( 3.32 ) \end{aligned}$$

At this point in the SDOF program, Equation 3.4 would be used to calculate the system stiffness and Equation 3.3 would be used to calculate the natural frequency of the system. When this is done with the values of SKSSH and SKSSS calculated above, the frequency calculated is high by a factor of 1.89 when compared to the NASTRAN results. This is explained by the coupling of the lateral translation mode with the rotation mode which is discussed in detail in Chapter 4 and observed in the NASTRAN plots. The torsional mode of the mirror about its optical axis, however, is due entirely to the SKSSH stiffnesses of each of the three flexure assemblies. Using NASTRAN this torsional frequency is calculated to be 175 Hz as shown in Table 5.1. The following analytical calculation to determine the natural frequency of the torsional mode using the value of SKSSH calculated above demonstrates the validity of the modeling used in the

SDOF analysis.

From Figure 3.13 :

$$M = J \theta, \quad \text{and; } \theta = \frac{\delta}{R} \quad \text{so; } M = J \frac{\delta}{R}$$

And:

$$M = 3 \times F \times R, \quad \text{and; } F = K \delta \quad \text{so; } M = 3 \times K \times \delta \times R$$

Giving:

$$J \frac{\delta}{R} = 3 \times K \times \delta \times R$$

$$J = 3 \times K \times R^2$$

Where :

$$R = 13.0 \text{ inches}$$

From Equation 3.32 :

$$K = SKSSH = 3.004 \times 10^5 \frac{\text{lb}}{\text{in}}$$

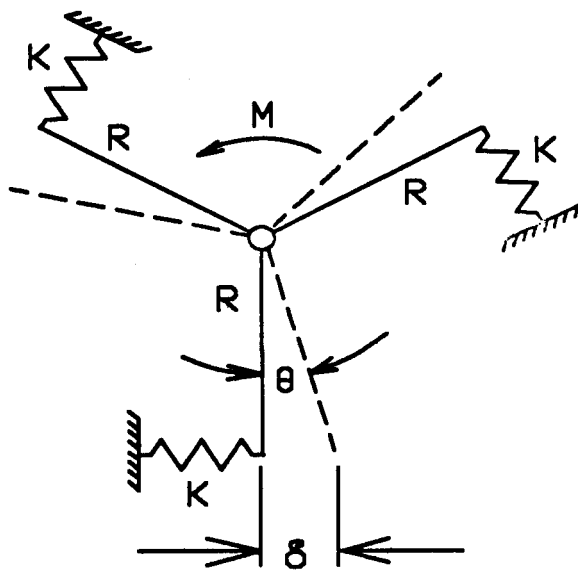
$$J = 1.523 \times 10^8 \frac{\text{in-lb}}{\text{rad}}$$

$$f = \frac{1}{2\pi} \sqrt{\frac{J}{I_{\text{polar}}}}$$

Where :

$$I_{\text{polar}} = 114.05 \text{ mugs-in}^2$$

$$f = 184 \text{ hz} \quad (\text{NASTRAN analysis predicted } 175 \text{ Hz})$$



$J$  - Torsional Stiffness

$M$  - Applied Torque

$F$  - Force in Each Assembly

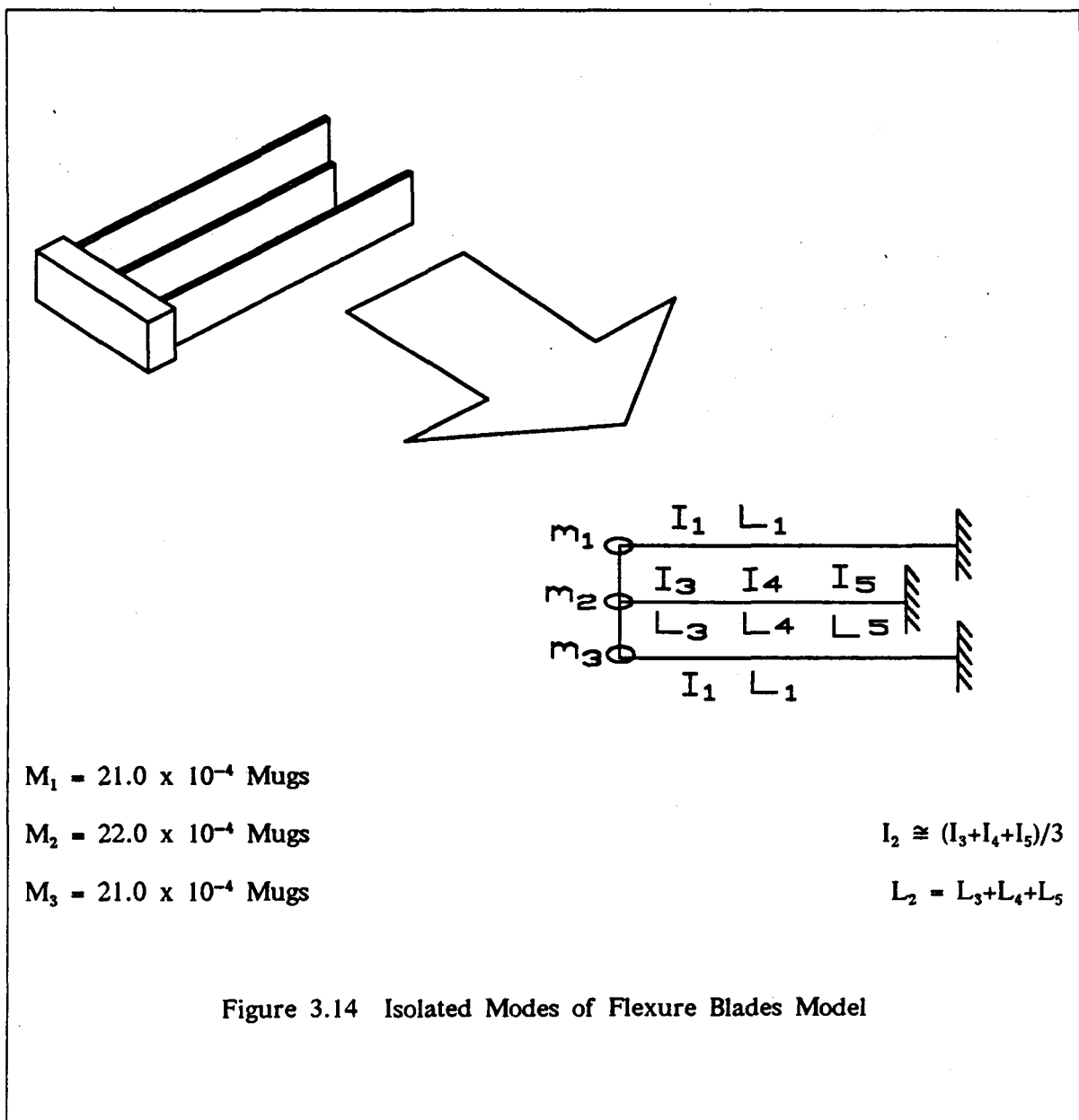
$I_{\text{polar}}$  - Mirror's Polar Mass Moment of Inertia

Figure 3.13 Free Body for Torsion Model



### *Isolated modes of the flexure blades*

Modes 4 through 9, as shown previously in Table 5.1, represent isolated motions of the flexure blades only. Although no motion of the mirror occurs in these modes, calculations of these frequencies are included here for completeness. The model used to calculate those frequencies is shown in Figure 3.14.



### Bending Stiffness

$$V_b = V_{1b} + V_{2b} + V_{3b}$$

$$\delta = \delta_1 = \delta_2 = \delta_3$$

$$V_{1b} = 12 \frac{EI_1}{L_1^3} \delta_1$$

$$V_{3b} = 12 \frac{EI_1}{L_1^3} \delta_3$$

$$V_{2b} = 12 \frac{EI_2}{L_2^3} \delta_2$$

$$V_b = \left[ 24 \frac{EI_1}{L_1^3} + 12 \frac{EI_2}{L_2^3} \right] \delta$$

$$K_b = 24 \frac{EI_1}{L_1^3} + 12 \frac{EI_2}{L_2^3}$$

$$= \frac{24 \times 18 \times 10^6 \times 4.6 \times 10^{-4}}{7^3} + \frac{12 \times 18 \times 10^6 \times 0.001}{6^3}$$

$$= 1579 \frac{\text{lb}}{\text{in}}$$

### Shear Stiffness

$$V_s = V_{1s} + V_{2s} + V_{3s}$$

$$\delta = \delta_1 = \delta_2 = \delta_3$$

$$V_{1s} = \frac{A_1 G}{L_1} \delta_1$$

$$V_{3s} = \frac{A_1 G}{L_1} \delta_3$$

$$V_{2s} = \frac{A_2 G}{L_2} \delta_2$$

$$V_s = \left[ \frac{2A_1 G}{L_1} + \frac{A_2 G}{L_2} \right] \delta$$

$$K_s = \frac{2A_1 G}{L_1} + \frac{A_2 G}{L_2}$$

$$= \frac{2 \times 0.28 \times 18 \times 10^6}{7 \times 2.6} + \frac{0.414 \times 18 \times 10^6}{6 \times 2.6}$$

$$= 1.03 \times 10^6 \frac{\text{lb}}{\text{in}}$$

#### Total Stiffness

$$\begin{aligned}\frac{1}{K} &= \frac{1}{K_b} + \frac{1}{K_s} \\ &= \frac{1}{1579} + \frac{1}{1.03 \times 10^4} \\ &= 6.34 \times 10^{-4} \frac{\text{in}}{\text{lb}} \\ K &= 1577 \frac{\text{lb}}{\text{in}}\end{aligned}$$

#### Total Mass on Appendage

$$\begin{aligned}M &= M_1 + M_2 + M_3 \\ &= 64.0 \times 10^{-4} \text{ mugs}\end{aligned}$$

#### System Frequency

$$\begin{aligned}f &= \frac{1}{2\pi} \sqrt{\frac{K}{M}} \\ &= \frac{1}{2\pi} \sqrt{\frac{1577}{64.0 \times 10^{-4}}} \\ &= 79.04 \text{ Hz} \dots\dots\dots (\text{NASTRAN analysis predicted } 81 \text{ Hz})\end{aligned}$$

## CHAPTER 4

### DYNAMIC ANALYSIS WITH A THREE DEGREE OF FREEDOM MODEL

The single degree of freedom model used during the parametric study of the SIRTf design provided an accurate tool for analyzing the flexure system as long as the vertical stiffness in the direction of the optical axis was much greater than the lateral stiffness. With the design evolution to the system of horizontal flexures, the vertical stiffness decreased to a value less than the lateral stiffness which violated the basic assumption of the SDOF model. As discussed in Chapter 3, the single degree of freedom model still provided a configuration that allowed the final design to be completed with very few NASTRAN iterations and it was not necessary to further update the FORTRAN program. The numerical example presented in Chapter 3 demonstrated the accuracy of the modeling by predicting the natural frequency of the torsional mode to be within 5.1 percent of the natural frequency predicted by the NASTRAN analysis. Work presented in this chapter was completed following the final design of the SIRTf configuration and was prompted by the objective to better define the coupling between the lateral and the rotational modes.

Although a FORTRAN program was not developed for the three degree of freedom model discussed in this chapter, all stiffness equations developed could be programmed for further parametric design studies should new requirements develop from NASA Ames that would cause that effort to become necessary.

#### *Develop the three DOF stiffness matrix*

By inspection, the torsional mode is seen to be decoupled from the other modes. That decoupling was confirmed numerically in Chapter 3 as well as with the NASTRAN program. Similarly, the vertical mode along the optical axis is seen to be

decoupled from the other modes. However, the vertical mode will be included as one of the degrees of freedom in this three degree of freedom model to consider the effects of the dependence of the rotational stiffness on the vertical stiffness. Although those two mode shapes are independent, the stiffnesses which determine their eigenvalues are not. The three degree of freedom model is shown in Figure 4.1. The development of the stiffness matrix for this system follows:

$$\begin{bmatrix} F_x \\ F_y \\ M_\theta \end{bmatrix} = \begin{bmatrix} K_{11} & K_{12} & K_{13} \\ K_{21} & K_{22} & K_{23} \\ K_{31} & K_{32} & K_{33} \end{bmatrix} \begin{bmatrix} x \\ y \\ \theta \end{bmatrix}$$

As shown in Figure 4.1 :

Unit displacement in the x-direction:  $\delta_x = 1$ , all other displacements = 0.

$$F_x = K_{11} = K_h \delta_x = K_h$$

$$F_y = K_{21} = 0$$

$$M_\theta = K_{31} = F_x L = K_h \delta_x L = K_h L$$

Unit displacement in the y-direction:  $\delta_y = 1$ , all other displacements = 0.

$$F_x = K_{12} = 0$$

$$F_y = K_{22} = K_v \delta_y = K_v$$

$$M_\theta = K_{32} = 0$$

Unit displacement in the  $\theta$ -direction:  $\theta = 1$ , all other displacements = 0.

$$F_x = K_{13} = K_h L \theta = K_h L$$

$$F_y = K_{23} = 0$$

$$M_\theta = K_{33} = K_t \theta + F_x L = K_t \theta + K_h L^2 \theta = K_t + K_h L^2$$

Therefore :

$$[K] = \begin{bmatrix} K_h & 0 & LK_h \\ 0 & K_v & 0 \\ LK_h & 0 & K_t + L^2 K_h \end{bmatrix}$$

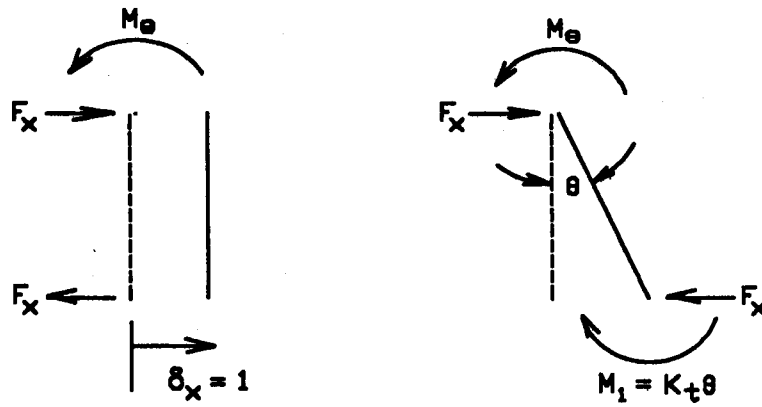
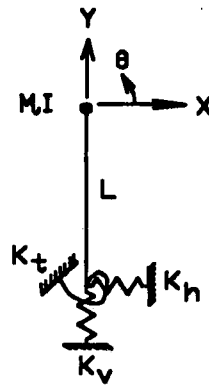


Figure 4.1 Free Body Diagram of Three Degree of Freedom Model

Develop the eigenvalues

$$[K] = \begin{bmatrix} K_h & 0 & LK_h \\ 0 & K_v & 0 \\ LK_h & 0 & K_t + L^2K_h \end{bmatrix} ; [M] = \begin{bmatrix} m & 0 & 0 \\ 0 & m & 0 \\ 0 & 0 & I \end{bmatrix}$$

$$|K - \lambda M| = \det \begin{bmatrix} K_h - \lambda m & 0 & LK_h \\ 0 & K_v - \lambda m & 0 \\ LK_h & 0 & K_t + L^2K_h - \lambda I \end{bmatrix}$$

Characteristic equation :

$$(K_h - \lambda m)(K_v - \lambda m)(K_t + L^2K_h - \lambda I) - LK_h (K_v - \lambda m)LK_h = 0$$

Factor  $(K_v - \lambda m)$  :

$$(K_v - \lambda m)(K_h - \lambda m)(K_t + L^2K_h - \lambda I) - (LK_h)^2 = 0$$

$$(K_v - \lambda m)(Im\lambda^2 - (IK_h + mK_t + mL^2K_h)\lambda + K_h K_t) = 0$$

$$\lambda_1 = \frac{K_v}{m} \dots \dots \dots (4.1)$$

$$\lambda_{2,3} = \frac{IK_h + mL^2K_h + mK_t \pm \sqrt{(IK_h + mL^2K_h + mK_t)^2 - 4mIK_h K_t}}{2Im} \dots \dots \dots (4.2)$$

Develop the relationship between  $K_t$  and  $K_v$

From Figure 4.2 :

$$M = K_t \theta \dots \dots \dots (4.3)$$

And :

$$M = F_1 R + F_2 \frac{R}{2} \dots \dots \dots (4.4)$$

$$F_1 = \frac{1}{3} K_V \delta_1$$

$$= \frac{1}{3} K_V R \theta$$

$$F_2 = \frac{2}{3} K_V \delta_2$$

$$= \frac{2}{3} K_V \frac{R}{2} \theta = \frac{1}{3} K_V R \theta$$

From Equations 4.3 and 4.4 :

$$M = R \left[ \frac{1}{3} K_V R \theta \right] + \frac{R}{2} \left[ \frac{1}{3} K_V R \theta \right]$$

$$= K_t \theta$$

$$K_t = \left[ \frac{1}{3} K_V R^2 + \frac{1}{6} K_V R^2 \right]$$

$$K_t = \frac{1}{2} R^2 K_V \dots\dots\dots (4.5)$$

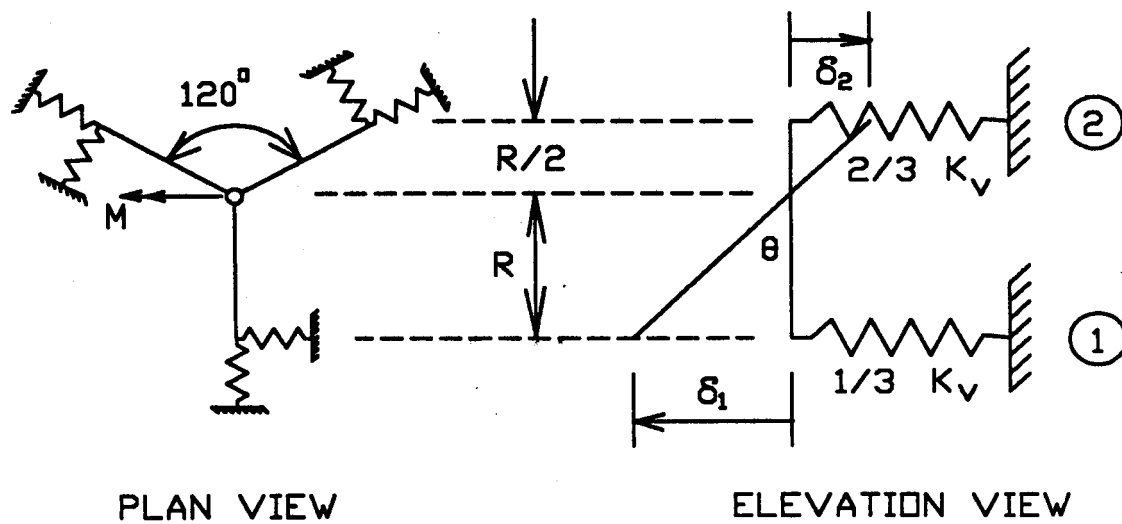


Figure 4.2 Relationship Between  $K_V$  and  $K_t$



### *A numerical example*

Determine the vertical stiffness of a single flexure assembly as shown in Figure 4.3. The geometry of the final design submitted to NASA Ames will be used in numerically determining the vertical stiffness. The load distribution throughout the assembly is identified in Table 4.1 :

Axial deflection in post :

$$\begin{aligned}\delta_1 &= \frac{L}{A E} F \\ &= \frac{3 \times 4}{\pi \times 3^2 \times 18 \times 10^6} F = 2.36 \times 10^{-8} F\end{aligned}$$

Bending deflection in gimbal cruciform :

$$\begin{aligned}\delta_2 &= \frac{L^3}{12 E I} \frac{F}{2} \\ &= \frac{3^3 \times 12}{24 \times 18 \times 10^6 \times 0.14 \times 8} F = 6.696 \times 10^{-7} F\end{aligned}$$

Shear deflection in gimbal cruciform :

$$\begin{aligned}\delta_3 &= \frac{L}{A G} \frac{F}{2} \\ &= \frac{3}{0.14 \times 6.92 \times 10^6 \times 2} F = 1.548 \times 10^{-6} F\end{aligned}$$

Bending deflection in frame :

$$\begin{aligned}\delta_4 &= \frac{1}{12 E I} \left[ \frac{L_3}{2} - \frac{L_1}{2} \right]^2 (l_3 + L_1) \frac{F}{4} + \frac{L_1^3}{24 E I} \frac{F}{4} \\ &= \frac{12}{96 \times 18 \times 10^6 \times 0.75 \times 8} (2.88^3 + 2 \times (4.5 - 1.44)^2 (4.5 + 2.88)) F \\ &= 1.876 \times 10^{-7} F\end{aligned}$$

Shear deflection in frame :

$$\begin{aligned}\delta_5 &= \frac{L_3}{2 A G} \frac{F}{4} \\ &= \frac{9}{8 \times 1.5 \times 6.92 \times 10^6} F = 1.084 \times 10^{-7} F\end{aligned}$$

Bending deflection in outer blade :

$$\begin{aligned}\delta_6 &= \frac{L^3}{12 E I} \frac{F}{4} \\ &= \frac{7_3 \times 12}{12 \times 18 \times 10^6 \times 0.14 \times 8 \times 4} F = 4.253 \times 10^{-6} F\end{aligned}$$

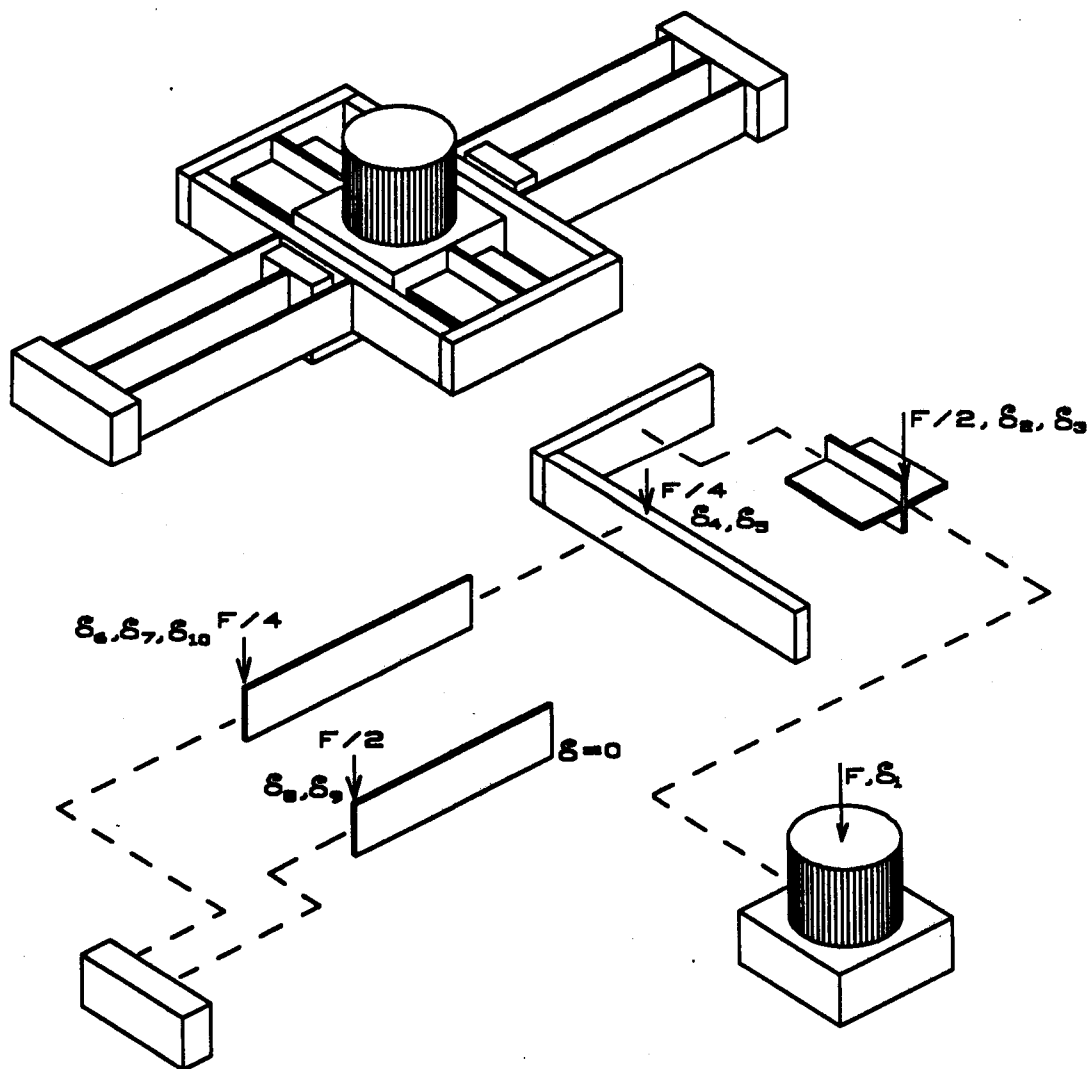


Figure 4.3 Vertical Stiffness of Single Flexure Assembly

Shear deflection in outer blade :

$$\delta_7 = \frac{L}{A G} \frac{F}{4}$$

$$= \frac{7}{4 \times 2 \times 0.14 \times 6.92 \times 10^6} F = 9.032 \times 10^{-7} F$$

Bending deflection in inner blade :

$$\delta_8 = \frac{L^3}{12 EI} \frac{F}{2}$$

$$= \frac{6^3 \times 12}{24 \times 18 \times 10^6 \times 0.18 \times 2.225^3} F = 3.026 \times 10^{-6} F$$

Shear deflection in inner blade :

$$\delta_9 = \frac{L}{AG} \frac{F}{2}$$

$$= \frac{6}{0.18 \times 2.225 \times 6.92 \times 10^6 \times 2} F = 1.082 \times 10^{-6} F$$

Deflection due to torsional deflection of frame :

$$\theta = \frac{ML}{JG}$$

$$M = \left[ \frac{F}{4} \times 7 \right] \times \frac{1}{2} \text{ in-lb}$$

$$J = 0.2813 \text{ in}^4$$

$$L = 3.06 \text{ in}$$

$$\delta_{10} = 7 \times \theta$$

Therefore :

$$\delta_{10} = \frac{7^2 \times 3.06}{8 \times 0.2813 \times 6.92 \times 10^6} F = 9.628 \times 10^{-6} F$$

LOCATION	FORCE	LOCATION	FORCE
$\delta_1 = \delta(\text{post})$	F	$\delta_6 = \delta(\text{bending, outer blade})$	F/4
$\delta_2 = \delta(\text{bending, gimbal})$	F/2	$\delta_7 = \delta(\text{shear, outer blade})$	F/4
$\delta_3 = \delta(\text{shear, gimbal})$	F/2	$\delta_8 = \delta(\text{bending, inner blade})$	F/2
$\delta_4 = \delta(\text{bending, frame})$	F/4	$\delta_9 = \delta(\text{shear, inner blade})$	F/2
$\delta_5 = \delta(\text{shear, frame})$	F/4	$\delta_{10} = \delta(\text{torsion, frame})$	F/4

Table 4.1 Element loads for vertical stiffness

Flexure assembly vertical deflection :

$$\begin{aligned}\delta &= \delta_1 + \delta_2 + \delta_3 + \delta_4 + \delta_5 + \delta_6 + \delta_7 + \delta_8 + \delta_9 + \delta_{10} \\ &= 2.143 \times 10^{-5} F\end{aligned}$$

So, single flexure assembly force :

$$F = 4.666 \times 10^4 \delta$$

Vertical stiffness of SIRTf system :

$$K_v = 3 \times 4.666 \times 10^5 = 1.40 \times 10^5 \frac{\text{lb}}{\text{in}}$$

Vertical natural frequency of SIRTf system :

$$\begin{aligned}f_1 &= \frac{1}{2\pi} \sqrt{\frac{1.40 \times 10^5}{0.668}} \\ &= 72.9 \text{ Hz} \dots\dots\dots (\text{NASTRAN analysis predicted 73 Hz})\end{aligned}$$

$$\begin{aligned}K_t &= \frac{R^2}{2} K_v \dots\dots\dots (4.5 \text{ repeated}) \\ &= \frac{169}{2} \times 1.40 \times 10^5 = 1.183 \times 10^7 \frac{\text{lb}}{\text{in}}\end{aligned}$$

From Equations 3.4 and 3.32 :

$$K_h = 3.004 \times 10^5 \times 1.5 = 4.506 \times 10^5 \frac{\text{lb}}{\text{in}}$$

$$M = 0.668 \text{ mugs}$$

$$I = 57.47 \text{ mugs-in}^2$$

From Equation 4.2

$$\lambda_2 = 1.801 \times 10^5$$

Therefore :

$$f_2 = 67.6 \text{ Hz} \dots\dots\dots (\text{NASTRAN analysis predicted 69 Hz})$$

And :

$$\lambda_3 = 7.709 \times 10^5$$

Therefore :

$$f_3 = 140.0 \text{ Hz} \dots\dots\dots (\text{NASTRAN analysis predicted 129 Hz})$$

## CHAPTER 5

### DYNAMIC ANALYSIS WITH A NASTRAN FINITE ELEMENT MODEL

The structural model used for the NASTRAN analysis is shown in Figure 5.1. It has the center of the global coordinate system coinciding with the center post on one of the flexure assemblies. It has the x-axis passing through the mid-plane of the right center blade and the y-axis passing through the vertical projection of the mirror's center of mass. Geometries for the other two flexure assemblies were obtained by using the identical coordinates but in two newly defined coordinate systems. One coordinate system is rotated 120° clockwise about the optical axis of the mirror and the other is rotated 240° clockwise about the same axis. Flexure assemblies were modeled with beam (CBEAM) elements that included both flexure and shear stiffness. Fixity was assigned to the center blade elements that interface with the SIRTf baseplate. Rigid bar (RBAR) elements were attached to the center posts of each of the three flexure assemblies and connected at the center of mass of the mirror. Lumped translational mass and mass moments of inertia were placed at the mirror's center of mass to simulate the inertial effects of the mirror. Inherent in this modeling is the assumption that the mirror and baseplate are much stiffer than the flexure assemblies, as was established early in the system analysis.

#### *Solution Type 3 -- Normal Modes Analysis*

Natural frequencies, mode shapes, and plots are available as output from SOL 3. Plots of the first twelve mode shapes are presented in Figures 5.2 through 5.13. Mode 1, shown in Figure 5.2, is a lateral in-plane translation coupled with out-of-plane rotation. It is one of the coupled modes discussed in Chapter 4. One flexure assembly moves up while the other two move down. Mode 2, shown in Figure 5.3,

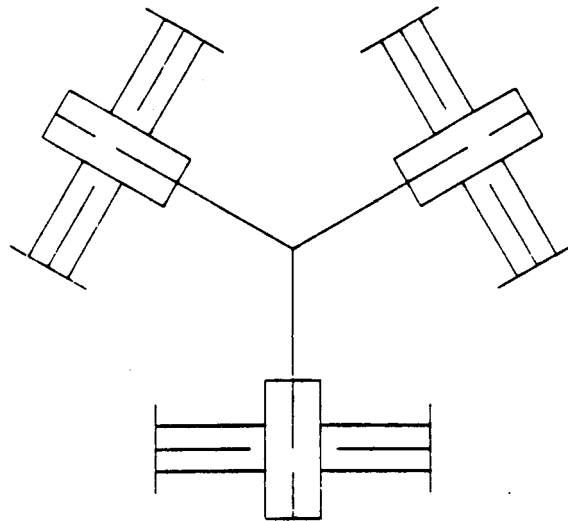
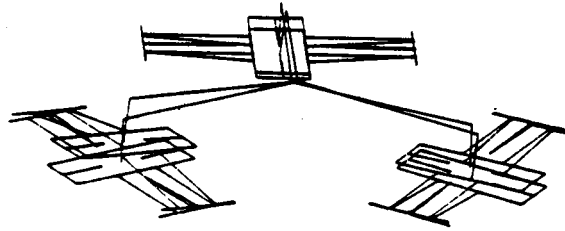
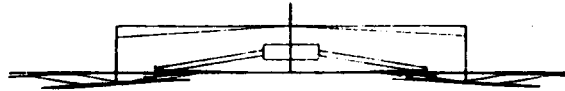


Figure 5.1 NASTRAN Finite Element Model

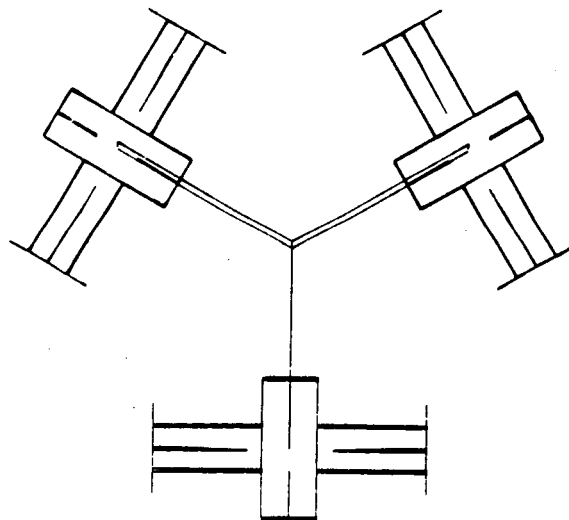
has the same frequency as Mode 1 but is orthogonal to it. One flexure assembly is essentially stationary while the other two are moving out of phase with each other with equal amplitudes. These mode shapes occur at the same frequency because, as was shown in the SDOF model, the stiffness of the entire support system is independent of its orientation. This gives complete symmetry to the lateral and rotational deflections even though the structure has three-fold structural symmetry because of the three identical assemblies located  $120^\circ$  apart. Identical frequencies are



Isometric View

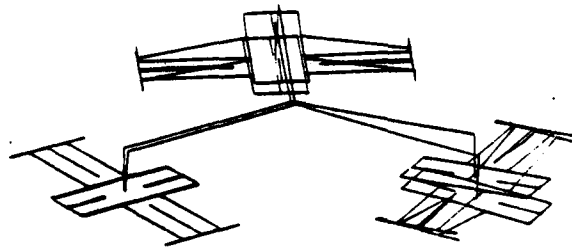


Elevation View

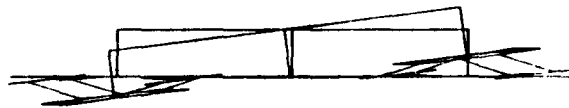


Plan View

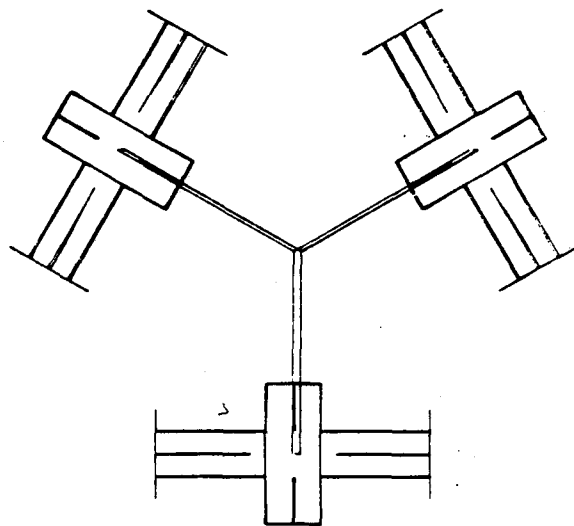
Figure 5.2 NASTRAN Plot of Mode Shape 1 -- 69 Hz



Isometric View



Elevation View

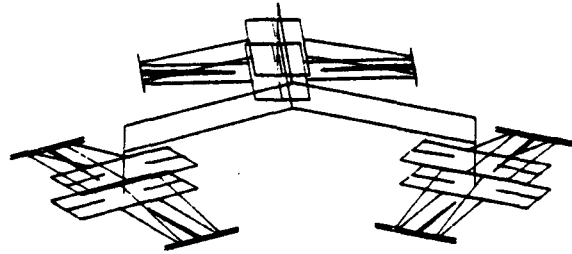


Plan View

Figure 5.3 NASTRAN Plot of Mode Shape 2 -- 69 Hz



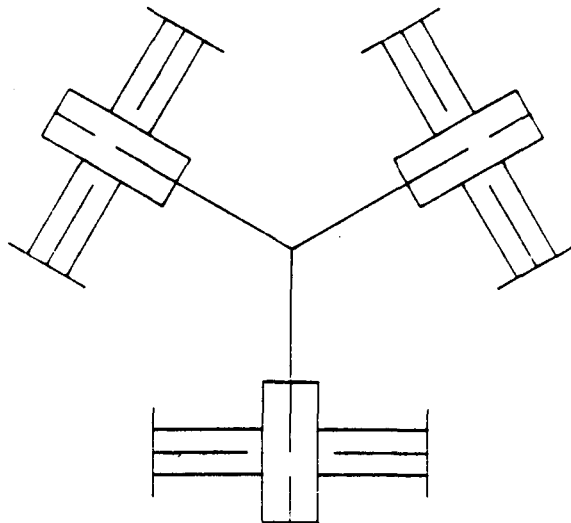
to be expected with any axes orientation used to model the assembly and the mode shapes could be expected to change as a function of that orientation. The frequency of mode shapes 1 and 2 was predicted by the three DOF model to within two percent of the value calculated by NASTRAN. Mode 3, shown in Figure 5.4, is a pure translation mode along the mirror's optical axis. The frequency of this mode shape was predicted by the SDOF model to within one percent of the value calculated by NASTRAN. Modes 4 through 9, shown in Figures 5.5 through 5.10, are modes with the outer appendages of the gimbal oscillating. No motion of the mirror occurs in those modes. The frequencies of modes 4 through 9 were determined analytically to within three percent of the values predicted by the NASTRAN analysis. Modes 10 and 11, shown in Figures 5.11 and 5.12, are the orthogonal complements of modes 1 and 2 in that they represent the coupled modes associated with the second root of the quadratic characteristic equation. In both modes, one flexure assembly has very little motion while the other two have larger motions of approximately the same magnitude. In mode 10, the other two assemblies have motions that are in phase and in mode 11, the other two assemblies have motions that are out of phase. The frequency of these mode shapes was predicted by the three DOF model to within nine percent of the value calculated using NASTRAN. Mode 12, shown in Figure 5.13, is a pure torsional mode about the mirror's optical axis. The frequency of this mode shape was predicted by the SDOF model to within six percent of the value calculated using NASTRAN. Summarized in Table 5.1 are the values of the first twelve natural frequencies of the flexure and gimbal assembly that were used to evaluate the system's stresses and displacements. The input file for the SOL 3 analysis used for the final analysis of the SIRTf configuration is listed in Appendix II.



Isometric View

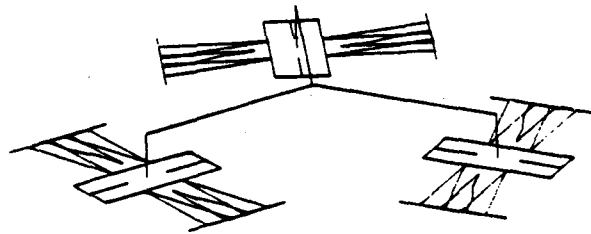


Elevation View

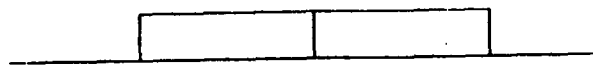


Plan View

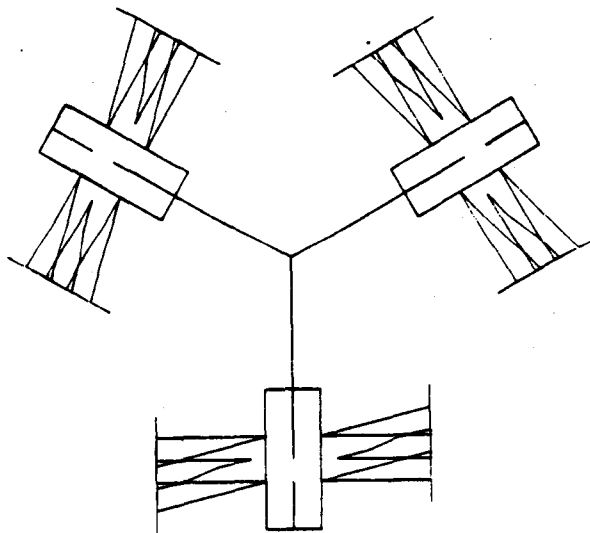
Figure 5.4 NASTRAN Plot of Mode Shape 3 -- 73 Hz



Isometric View

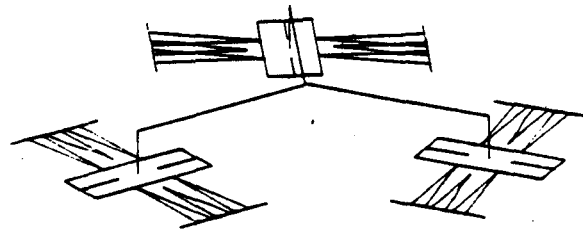


Elevation View



Plan View

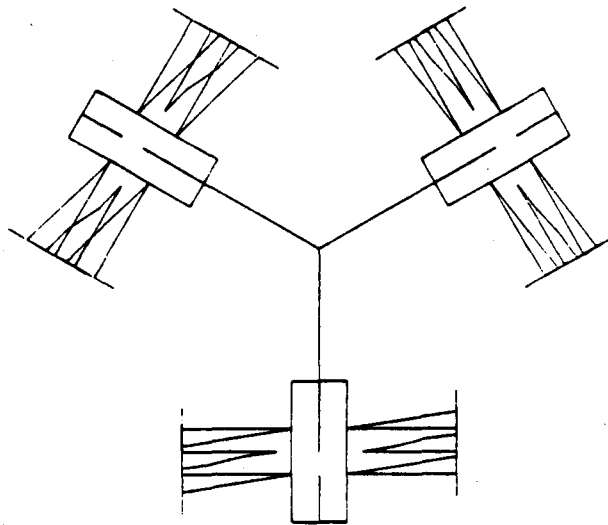
Figure 5.5 NASTRAN Plot of Mode Shape 4 -- 81 Hz



Isometric View

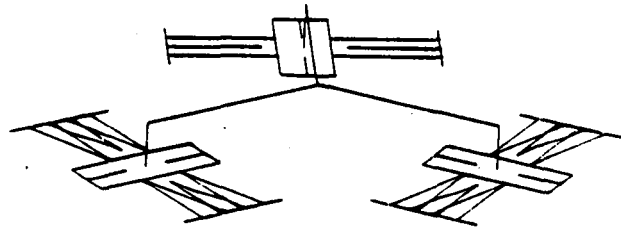


Elevation View

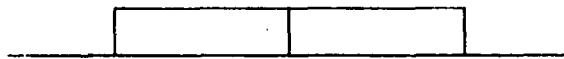


Plan View

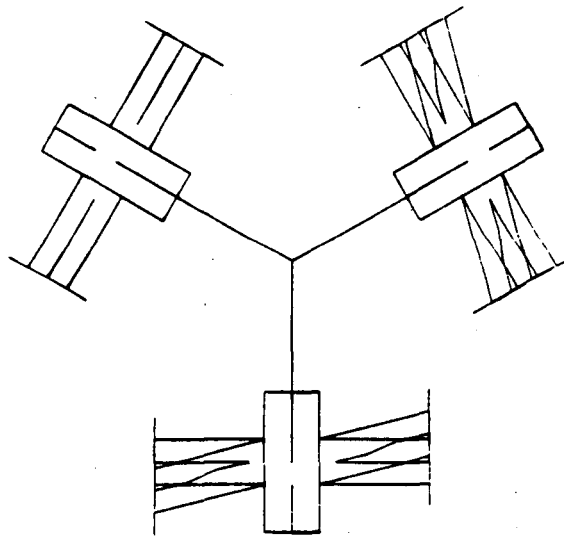
Figure 5.6 NASTRAN Plot of Mode Shape 5 -- 81 Hz



Isometric View

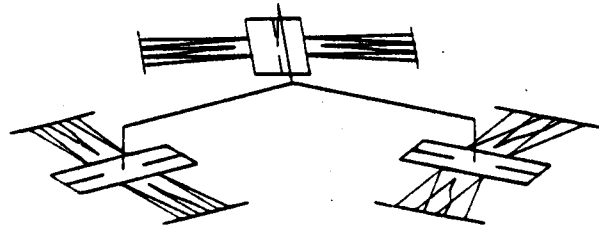


Elevation View

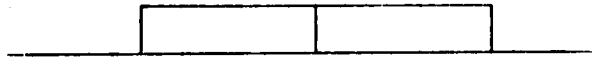


Plan View

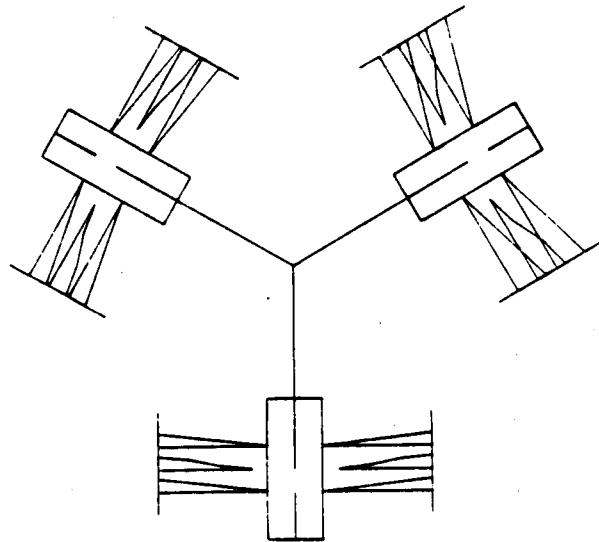
Figure 5.7 NASTRAN Plot of Mode Shape 6 -- 81 Hz



Isometric View

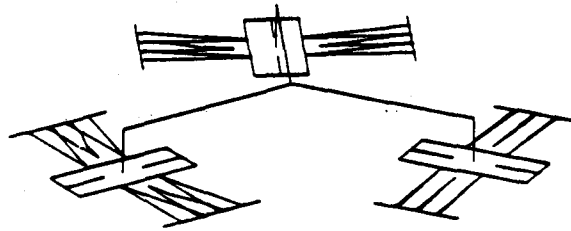


Elevation View



Plan View

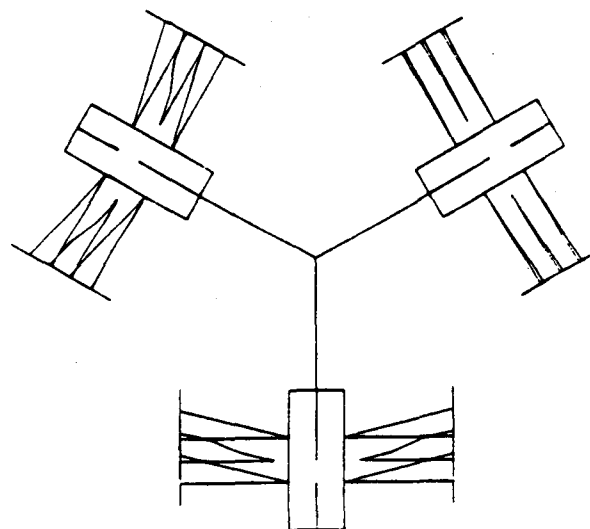
Figure 5.8 NASTRAN Plot of Mode Shape 7 -- 81 Hz



Isometric View

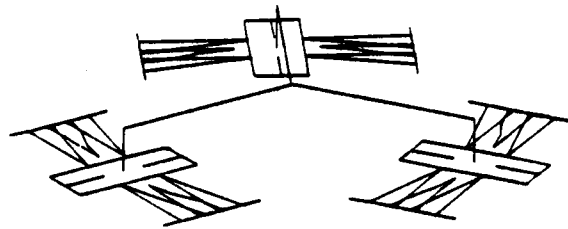


Elevation View

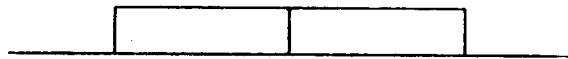


Plan View

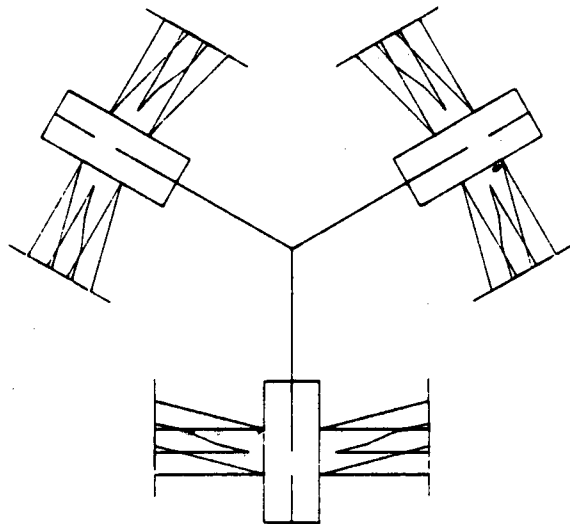
Figure 5.9 NASTRAN Plot of Mode Shape 8 -- 81 Hz



Isometric View



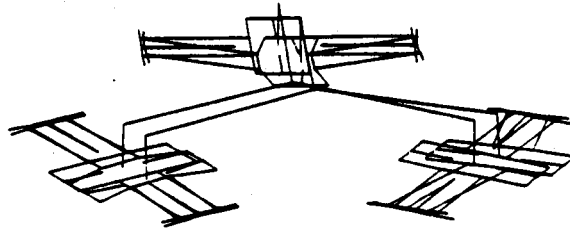
Elevation View



Plan View

Figure 5.10 NASTRAN Plot of Mode Shape 9 -- 81 Hz

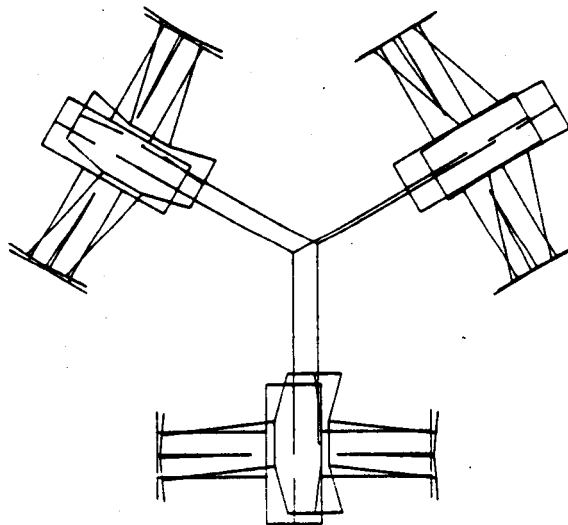




Isometric View

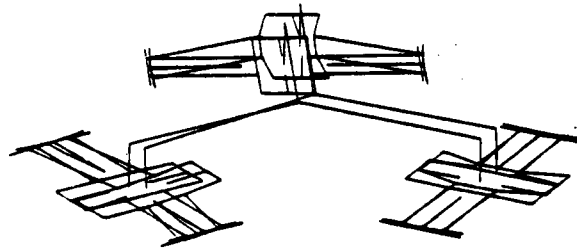


Elevation View

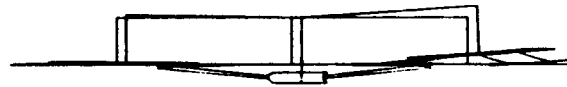


Plan View

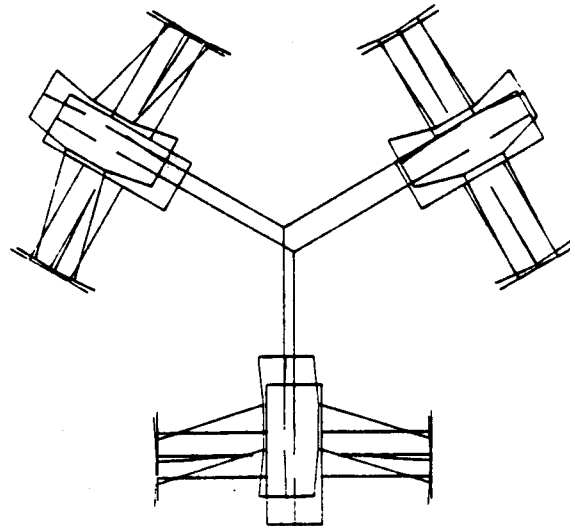
Figure 5.11 NASTRAN Plot of Mode Shape 10 -- 129 Hz



Isometric View

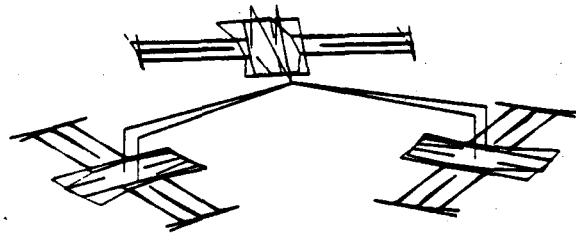


Elevation View

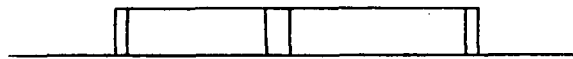


Plan View

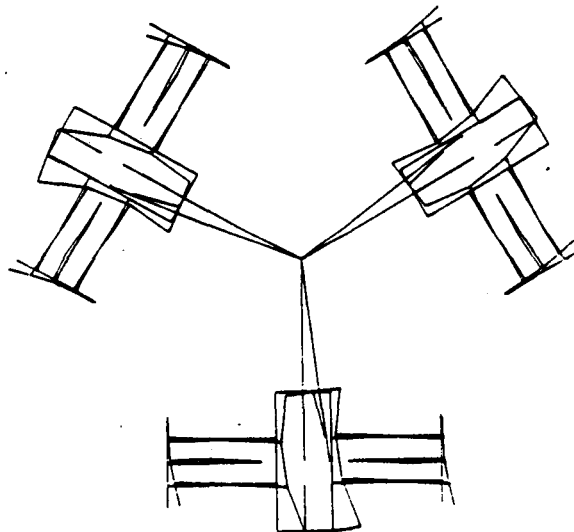
Figure 5.12 NASTRAN Plot of Mode Shape 11 -- 129 Hz



Isometric View



Elevation View



Plan View

Figure 5.13 NASTRAN Plot of Mode Shape 12 -- 175 Hz

Mode	Natural Frequency (Hz)		Comments
	SDOF/3DOF	NASTRAN	
1	68	69	Lateral in-plane translation
2	68	69	and out-of-plane rotation
3	73	73	Optical axis translation
4	79	81	Flexure motion only
5	79	81	Flexure motion only
6	79	81	Flexure motion only
7	79	81	Flexure motion only
8	79	81	Flexure motion only
9	79	81	Flexure motion only
10	140	129	Lateral in-plane translation
11	140	129	and out-of-plane rotation
12	184	175	Torsion

Table 5.1 First Twelve Natural Frequencies of SIRTf

*Solution Type 63 -- Superelement Normal Modes Analysis*

Solution Type 63 (SOL 63) was used to perform a complete dynamic design analysis based on the design criteria response spectrum. Applying the displacement response spectrum described by Equation 3.1 to the structure in each of the three mutually orthogonal directions, a mode shape was determined by NASTRAN for each of the twelve natural frequencies given in Table 5.1. Because of the symmetry of the assembly, there are multiple eigenvalues as shown in Table 5.1. Consequently, the method of combining modal maxima effects becomes a significant concern. Combining

modal maxima effects by the square root of the sum of squares (SRSS) gives RMS values providing that the eigenvalues are well spaced, however the SRSS method is unconservative for systems that have repeated eigenvalues. Combining modal maxima effects by the sum of the absolutes (ABS) is appropriate if all of the eigenvalues are essentially equal. The Naval Research Laboratory (NRL) method of combining modal maxima effects applies if the lowest mode is the dominant mode and the remaining modes are well dispersed. Each of the above three methods is available in NASTRAN but none of them are actually appropriate for the SIRTf assembly. A fourth method called CLOSE is also available in NASTRAN. The user is required to define a value for the variable "close". Each eigenvalue is compared to the one that precedes it and if their difference is equal to or less than the value "close", then those two modal maxima associated with those two eigenvalues are added absolutely. If the eigenvalue difference is greater than "close", the modal maxima associated with the larger eigenvalue is included in an SRSS combination and the procedure is repeated for the next eigenvalue comparison.

The limited methods of combining modal maxima is not unique to the NASTRAN program. It is a problem that exists for most large computer programs in use today<sup>7</sup>. A method for combining modal maxima effects using a displacement response spectrum that gives essentially the same results as obtained using a power spectral density criteria was developed in this design study. This result<sup>8</sup> is the Modified Root of the Sum of the Squares (MRSS) method. It is a variation of the CLOSE method available in NASTRAN. The value for "close" in MRSS is determined from the cross-modal coefficients,  $\rho_{ij}$ . For SIRTf, the coefficients can be approximated<sup>9</sup> as the cross-correlations between modal responses given by:

$$\rho_{ij} = \frac{8 \sqrt{(\zeta_i)(\zeta_j)} (\zeta_i + r\zeta_j) r^{3/2}}{(1-r^2)^2 + 4(\zeta_i)(\zeta_j)r(1+r^2) + 4(\zeta_i^2 + \zeta_j^2)r^2} \dots\dots\dots (5.1)$$

where  $r = \frac{\omega_i}{\omega_j}$ . For constant modal damping,  $\zeta$ , this becomes:

$$\rho_{ij} = \frac{8\zeta^2 (1+r)r^{3/2}}{(1-r^2)^2 + 4\zeta^2 r(1+r)^2} \dots\dots\dots (5.2)$$

For a given damping ratio, these equations may be used to determine when the eigenvalues are essentially equal.

The procedure for using MRSS is as follows:

- 1: Make a SOL 3 run on NASTRAN to determine the system's eigenvalue distribution.
- 2: Identify eigenvalues that are "close".
- 3: Make the following analysis using SOL 63:
  - a: Identify in the NASTRAN input file, those specific eigenvalues that are close and select the option in NASTRAN that combines their modal maxima effects with ABS.
  - b: Identify in the NASTRAN input file, those specific eigenvalues that are well spaced. For each individual eigenvalue, select the option in NASTRAN that calculates its modal maxima effects. Either ABS or SRSS can be selected here as they give the same result for a single eigenvalue selection.
  - c: External to NASTRAN, using data obtained above, combine by SRSS the results of the ABS combinations with the results of the distinct eigenvalue cases.

The accuracy of the MRSS method of combining modal maxima for the SIRTFF flexure assembly is demonstrated in Table 7.1 where the MRSS design loads are summarized with the SOL 30 design loads. Equations that define the methods for combining modal maxima effects are shown in Figure 5.14.

$$\text{SRSS method: } (U_p) = \left[ \sum_{p=1}^H (u_p^2) \right]^{\frac{1}{2}}$$

$$\text{Absolute method: } (U_p) = \sum_{p=1}^H (|u_p|)$$

$$\text{NRL method: } (U_p) = [|u_1|] + \left[ \sum_{p=2}^H (u_p^2) \right]^{\frac{1}{2}}$$

$$\text{CLOSE method: } (U_p) = \sum_{p=1}^Z (|u_p|) + \left[ \sum_{p=Z+1}^{H-Z} (u_p^2) \right]^{\frac{1}{2}}$$

$$\text{MRSS method: } (U_p) = \left[ \sum_{j=1}^N \left[ \sum_{p=1}^K (|u_p|) \right]^2 + \sum_{p=Z+1}^{H-Z} (u_p^2) \right]^{\frac{1}{2}}$$

Where:

$U_p$  = Combined response

$u_p$  = Response of mode  $p$

$H$  = Number of modes considered in the analysis

$Z$  = Total number of modes determined to be close

$N$  = Number of sets of equal or close eigenvalues

$K$  = Number of equal or close eigenvalues in any set

Figure 5.14 Modal Response Combinations

A numerical example follows that demonstrates the methods for combining modal maxima that have been presented. The histogram of the first twelve frequencies for SIRTf is shown in Figure 5.15 to emphasize the MRSS combination scheme. After each grouping is summed absolutely, the summations of each group are combined by SRSS. For the example, it will be assumed that the effect of each modal maxima is the same and that each has a value equal to one. The results indicate that the conclusion of a response spectrum analysis depends strongly on the modal maxima combination scheme selected.

$$\text{SRSS} = (1^2 + 1^2 + 1^2 + 1^2 + 1^2 + 1^2 + 1^2 + 1^2 + 1^2 + 1^2 + 1^2 + 1^2)^{1/2} = \sqrt{12} = 3.46$$

$$\text{ABS} = 1 + 1 + 1 + 1 + 1 + 1 + 1 + 1 + 1 + 1 + 1 + 1 = 12.00$$

$$\text{NRL} = 1 + (1^2 + 1^2 + 1^2 + 1^2 + 1^2 + 1^2 + 1^2 + 1^2 + 1^2 + 1^2 + 1^2 + 1^2)^{1/2} = 1 + \sqrt{11} = 4.31$$

$$\text{CLOSE} = 10 + (1^2 + 1^2)^{1/2} = 11.41$$

$$\text{MRSS} = (2^2 + 1^2 + 6^2 + 2^2 + 1^2)^{1/2} = \sqrt{46} = 6.78$$

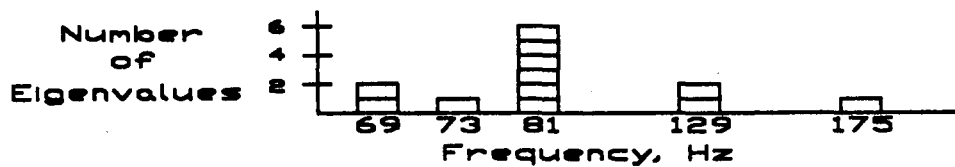


Figure 5.15 Histogram of SIRTf Natural Frequencies

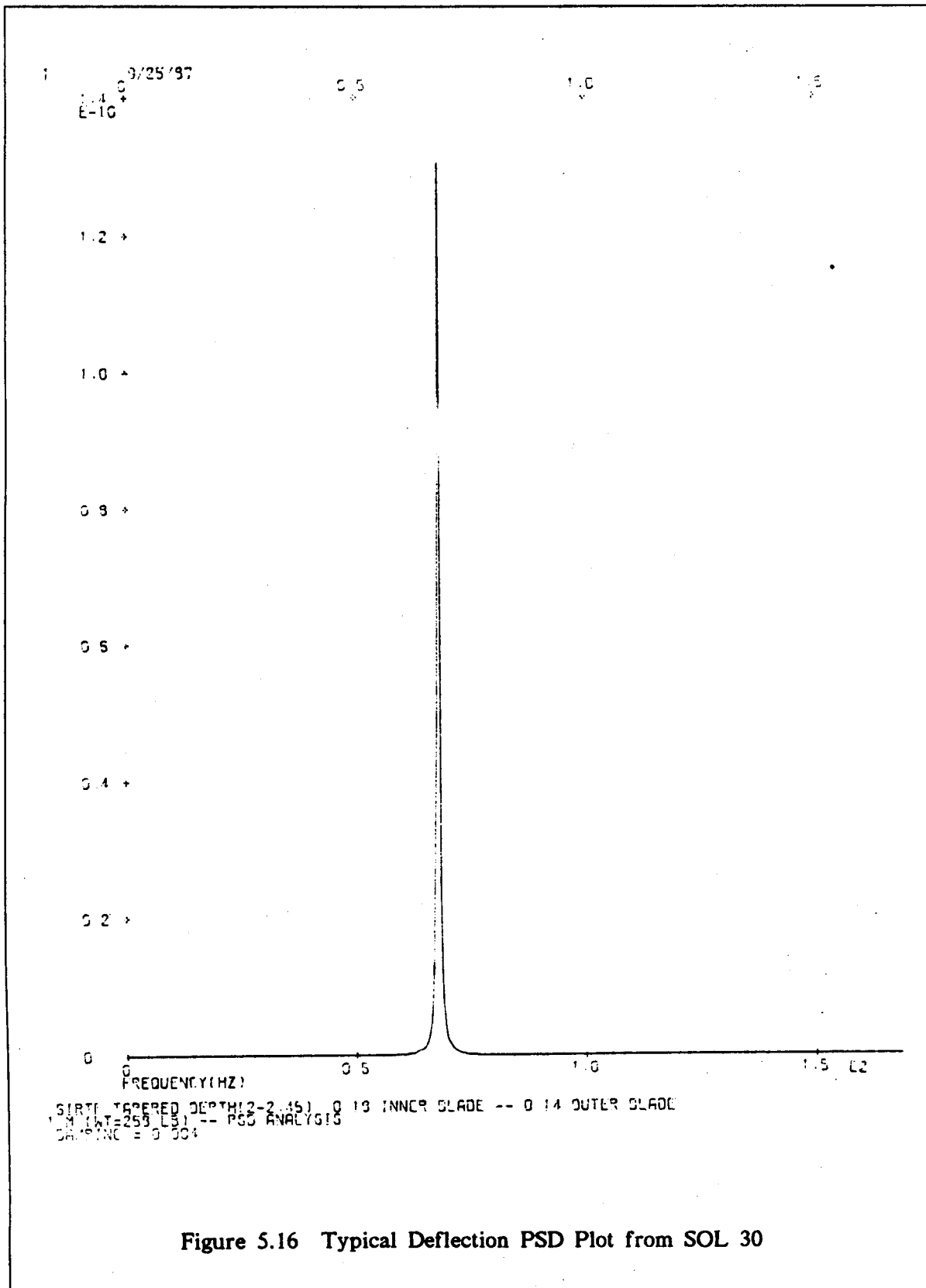


### *Solution Type 30 -- Modal Frequency Response Analysis*

Solution Type 30 is both more complex and more expensive to use than SOL 63 to perform random vibration analysis in a design mode, but SOL 30 is also expected to provide the more accurate solution. The significant difference in effort and complexity between SOL 63 and SOL 30 is in the post processing of the frequency response analysis. Following the SOL 30 frequency response analysis, the power spectral density curves of the response quantities are determined based directly on the input PSDF and are integrated to provide the RMS values of the response quantities. For the SIRTf analysis those response quantities were displacements and loads. The SOL 30 analysis is expected to produce the best solution of all the solution types considered, with the only error resulting from the numerical integration scheme within the computing process. A comparison of results is shown in Table 7.1.

The burden of defining the integration intervals of the power spectral density curves is left to the user of NASTRAN. This requires that a plot of the function to be integrated be made in order to determine the frequency range over which the function has significant magnitude as well as to determine the integration intervals. Two typical PSD plots from the SIRTf analysis are shown in Figures 5.16 and 5.17. As can be explicitly seen from those plots, the curves to be integrated are essentially spikes and care must be taken to insure that the integration is done accurately. Small errors in the selection of the integrating parameters for systems such as SIRTf with low damping can easily result in large errors in the final design parameters.

ORIGINAL PAGE IS  
OF POOR QUALITY



143 2/25/87 0.5 1.0 1.5

3  
E3 +

7. +

5 +

5 +

4 +

3 +

2 +

1 +

0

0 0.5 1.0 1.5

FREQUENCY(HZ)

GIRTH TAPERED DEPTH(2-2.45) 0.19 INNER BLADE -- 0.14 OUTER BLADE  
MOUNT=255 LBI -- PSD ANALYSIS  
DAMPING = 0.004

**Figure 5.17 Typical Internal Load PSD Plot from SOL 30**

## CHAPTER 6

### A COST COMPARISON OF THE SIRTf DYNAMIC ANALYSIS

Although designing an acceptable configuration for the support structure of the SIRTf primary mirror was the main objective of this study, minimizing the costs involved in performing the dynamic analysis was an issue that became a secondary objective. Many flexure assembly configurations were considered in this design study. Clearly, the budget constraints for this project would not have allowed those iterations to have been made using only NASTRAN. This chapter contains a summary of the costs incurred for each of the solution types used in this study. The value received for a given investment of resources is highest for the SDOF/3DOF models providing that accurate modeling is assured. The modest cost of a full NASTRAN analysis using the MRSS combination scheme with SOL 63 is attractive when compared to the costs of a SOL 30 NASTRAN analysis. That is especially so when the results are shown to be nearly the same as demonstrated in Figure 7.1. The MRSS combination scheme with SOL 63 provides the best NASTRAN alternative based on the SIRTf design study.

A subjective cost item not included in this summary is the hourly manpower rate of the user in applying the various methods discussed. Once the SDOF/3DOF design model is constructed, it requires the least amount of experience of the user. SOL 63 could easily be used by a junior level engineer provided proper supervision is available. SOL 30 is difficult to use with many different ways to obtain an erroneous conclusion. A clear understanding of random vibrations is required of the user as this portion of NASTRAN is not well documented. Manpower costs, then, can vary in the progression just presented based solely on the experience required of the user.

### *Cost of analysis with the FORTRAN model*

Previous work<sup>9</sup> on the SIRTf configuration had just developed a preliminary FORTRAN program that considered the system to behave as a single degree of freedom. That program was modified to FORTRAN 77 for the VAX computer. It could have as easily been written to operate on a PC as very little storage is required for its operation. On the University of Arizona computer center's VAX, each iteration of several hundred configurations cost less than two dollars. On a PC the cost would be zero if the initial cost of the PC is ignored. As all data input to the computer systems were input through a PC, the initial cost of the PC is common to all of the procedures considered and will be ignored. Manpower costs for preparing input to the FORTRAN model is negligible when cost per configuration evaluated is considered. A thirty minute session could result in as many as five hundred configurations being analyzed. The manpower costs for evaluating the output are also minimal as only those configurations that passed all of the system requirements are presented in the output. The primary manpower cost was in developing the initial program and then updating it for the different fundamental configurations. Each major update required a supplemental hand analysis for confirmation of the programming accuracy. Over the eighteen month duration of this design effort, approximately five major programming iterations took place with approximately sixty manhours of programming and confirmation calculations per iteration. An estimated three thousand configurations were considered and most of them were unacceptable. That is approximately 0.1 manhour per configuration studied.

### *Cost of analysis with the NASTRAN SOL 3 model*

The cost of the typical SIRTf configuration on a SOL 3 NASTRAN analysis was approximately three dollars on the University's Cyber system. SOL 3 models are

very similar to static analysis models and they provided the nodal geometry and connectivity for the SOL 63 and SOL 30 models that followed. Geometry plots were obtained from this model as well as mode shape plots for each natural frequency. No specific dynamic loads analysis is performed with SOL 3, however, the frequencies calculated are useful in checking both the FORTRAN model and the other NASTRAN models. A direct comparison can be made with the frequency calculated with the SDOF/3DOF models and if they agree, it can be concluded that both were modeled correctly. The check with the other NASTRAN models has value because the eigenvalues result from different analytical models within NASTRAN. SOL 3 models have the ground points fixed as in a statics analysis. That is equivalent to the support being a stiff spring, resulting in a high frequency mode that is ignored in the output. SOL 30 and SOL 63 models require the introduction of a large mass to represent ground. All fixed points must be attached to the large mass by rigid members. The introduction of the large mass results in a low frequency, essentially zero, mode shape for each degree of freedom associated with the large mass. Reproducing the frequencies calculated with the SOL 3 option provides conformation that the SOL 63 and SOL 30 input file have been correctly assembled because the determination of the values of that large mass and its mass moments of inertia are non-trivial efforts. The cost of the SOL 3 analysis is included in the model development costs of the SOL 63 and SOL 30 costs, so the SOL 3 analyses will not be summarized separately in this cost comparison.

#### *Cost of analysis with the NASTRAN SOL 63 model*

The time required to develop a NASTRAN model of a typical SIRTf model is approximately forty hours. Each analysis requesting the SRSS or ABS combination scheme cost eleven dollars. Minor changes in configuration do not require an

accompanying SOL 3 analysis. For each SOL 63 analysis, six deflections were calculated at each node and all loads within each element were calculated. This is important in comparing costs with SOL 30 as the cost for a comparable amount of output with SOL 30 would have been prohibitive for this project.

As stated in Chapter 5, neither the SRSS nor the ABS combination schemes are applicable to SIRTf. Although the MRSS scheme introduces slightly higher costs than SRSS or ABS, the MRSS combination scheme provided a more accurate solution for SIRTf. From the SOL 3 analyses, the modal groupings are determined for the SOL 63 MRSS analyses. Following those analyses, an SRSS combination is done by hand. Automating that combination scheme could easily be done, but for the SIRTf design it was done by hand. Each ABS combination scheme grouping cost approximately nine dollars resulting in a composite MRSS cost of forty-five dollars per analysis. The manhours to manually perform the subsequent SRSS by hand was approximately four hours for SIRTf. Automating that process would allow the same amount of data to be combined as is obtained from a normal SOL 63 analysis and it would take significantly less than four hours to accomplish. For SIRTf, only that data that was determined to be important was actually combined by SRSS following the SOL 63 ABS analyses.

#### *Cost of analysis with the NASTRAN SOL 30 model*

The SOL 30 option in NASTRAN is difficult to use. It performs the same frequency response analysis used in SOL 63 but it then integrates the power spectral density function of the response desired producing an RMS value of that response. Those integrating parameters are left for the user to define. For SIRTf the functions being integrated were typically spike functions where a small error in defining the tip of the spike or a small error in the integrating interval resulted in a very significant

error in the value of the integral. Plots of the power spectral density functions of the desired responses were required in order to define the range and the value of the integrating intervals. Although raster plots are relatively inexpensive, their quality was generally not acceptable so Calcomp plots were required. Procedures for requesting output from SOL 30 analyses are awkward. Each deflection desired and each load desired is a special request and each requires an individual plot for defining the integrating parameters. The primary cost of this solution type is in the integrating scheme. Of the 2,568 responses available that were all reported by the SOL 63 analysis, 148 responses were requested in the SOL 30 analysis. The cost of the SOL 30 analysis was \$68.00 for CPU and \$320.00 for plots. Actual manhours devoted to establishing the first acceptable analysis are not included in this cost comparison as a significant amount of time was spent in learning to use the SOL 30 option in NASTRAN. The preprocessing time presented is an estimate of the time that it would take to do it a second time. It must be kept in mind that even though SOL 30 is the hardest option to use of those considered; properly applied, it is expected to give the most reliable output for design.

#### *Cost summary of analyses*

The summary of the discussions of the previous sections is presented in Table

6.1.



*Manhour summary*

Model	Model Development New configuration (manhours)	Pre-processing Per iteration (manhours)	Post-processing Per iteration (manhours)
SDOF/3DOF	60.0	0.0	0.0
SOL 63 - SRSS	40.0	8.0	0.0
SOL 63 - ABS	40.0	8.0	0.0
SOL 63 - MRSS	40.0	12.0	4.0
Sol 30	50.0	16.0	16.0

*Cost summary*

Model	Computer (dollar)	Plotter (dollar)	Number of Iterations Analyzed	Processing Costs per Iteration (*) mh/iteration    dollar/iteration
SDOF/3DOF	0.0	0.0	3,000	≈0.0    0.0
SOL 63 - SRSS	11.0	4.0	10	8.0    15.0
SOL 63 - ABS	11.0	4.0	10	8.0    15.0
SOL 63 - MRSS	45.0	4.0	5	16.0    49.0
Sol 30	68.0	320.0	1	32.0    388.0

\* Assumes basic configuration already exists  
and only an iteration analysis is made.

Table 6.1 Cost Comparison of the SIRTf Dynamic Analysis

## CHAPTER 7

### SUMMARY AND CONCLUSIONS

Methods used in developing the final design configuration of the support structure for the primary mirror of the Space Infrared Telescope Facility (SIRTF) have been presented.

A brief description of the work performed with FRINGE was presented in Chapter 2. This work was necessary in order to establish the maximum loads that the support structure could apply to the mirror during operation at cryogenic temperatures. This began by modifying the program FRINGE to accept as its input, the output from the structural analysis program NASTRAN. The interfacing of these two programs allows an optical evaluation to be made of the structural deflections on the optical surface of the mirror. By applying unit loads to a finite element model of the mirror at the points which interface with the support structure, influence coefficients were obtained relating surface deflections on the mirror to unit loads at the support interface. For SIRTF, NASA had prepared an optical error budget that established the limit of the RMS deflections allowed on the optical surface. Comparing those limits with the results of the FRINGE program allowed the unit loads to be ratioed to establish a set of design loads for the support structure. In performing that analysis it was determined that the bending moment at the plane of the mirror's centroid was the load of concern. The shear accompanying the bending moment has a negligible influence with respect to that of the bending moment. Combining the maximum load that the mirror can withstand during optical operation with the known deflection that occurs during cryogenic cooldown leaves only the stiffness of each flexure assembly as the design variable. Radial compliance was a constant consideration throughout this

design effort.

The dynamic design analysis began using the three point support concept established on previous work performed at the University of Arizona for NASA Ames. A presentation demonstrating that the three point support system behaves as a single degree of freedom is shown in detail in Chapter 3. It is further shown that the system stiffness in the lateral direction can be expressed as a function of the sum of the radial stiffness and tangential stiffness of a single leg in the three leg support. If the radial stiffness is significantly less than the tangential stiffness, the system stiffness becomes a function of only the tangential stiffness. This approach was taken in the selection of some of the early design considerations as it was necessary to limit the radial stiffness to meet the cryogenic cooldown requirements. Early attempts were made to decouple the radial stiffness and the tangential stiffness by using the concept of a parallel spring guide. The inherent coupling of that configuration made it an unacceptable design. Manufacturing tolerances generated constraints that had to be satisfied. Mismatch of components during manufacturing caused the same type of aberrations to the optics as the moments resulting from cryogenic cooldown. A torsionally compliant gimbal structure placed between each leg of the flexure assembly and the baseplate solved the manufacturing tolerance problem. This gimbal structure evolved into a successful configuration for significantly decoupling the radial and tangential stiffnesses. Buckling of the various components was fully considered. Euler buckling was a problem for the long blade design, but the folded back configuration solved that problem. Out of plane buckling due to shear remained an item of concern throughout this design effort. An algorithm for predicting the critical buckling load was developed for the FORTRAN parametric analysis and the final design was analyzed for stability with a special NASTRAN analysis.

Demonstrating that the system could be considered as a SDOF allowed a straight forward parametric design program to be written in FORTRAN. Expense in both manhours and computer time was minimized by using this program to parametrically identify available design space. Accuracy of the simplified FORTRAN analysis was checked regularly with a NASTRAN model. In the early designs that had a relatively simple structure, the results of the FORTRAN analysis were consistently within five percent of the results predicted by the NASTRAN model. As the configurations became more complex, the accuracy decreased. Specifically, as the design approached its final configuration, the stiffness of each flexure assembly along the mirror's optical axis decreased, thereby allowing the rotational mode of the mirror assembly to couple with the lateral mode. The coupling modes and frequencies were described by a three degree of freedom model shown in Chapter 4. Although the equations presented were not programmed, the hand calculations presented demonstrate that the problem is well understood. If new design constraints were to be applied to the SIRTf telescope, these equations could be programmed and used for further parametric studies. Developing the FORTRAN program to investigate preliminary designs provided a cost effective method to evaluate many different configurations. Developing the stiffness equations for the FORTRAN program further resulted in a more thorough understanding of the effect of each element in the SIRTf support structure. Typical of the insights provided by the SDOF was the ability to decouple the radial and translational stiffnesses and still have a structurally stable system.

In addition to the SDOF and the three DOF models, dynamic analysis was performed using three different capabilities of NASTRAN. SOL 3 was used to determine the natural frequencies and mode shape plots of the system. SOL 63 was used to perform a displacement response spectrum analysis, which led to the subject of combining modal maxima of closely spaced modes. The SRSS, ABS, and CLOSE

methods available within NASTRAN were discussed. None of the available methods offer satisfactory results. ABS is inherently too conservative for modes with well spaced natural frequencies. SRSS is unpredictable for modes with clustered natural frequencies and can predict unconservative results. CLOSE was considered and a similar approach to CLOSE was developed for the SIRTf design which is presented as MRSS. SOL 30 was used to perform the final dynamic analysis. It can be expected to give near exact solutions, however it offered its own set of complications. Establishing the integrating interval for SOL 30 is a non-trivial procedure.

In summary, the MRSS method of combining modal maxima effects resulting from a SOL 63 analysis with NASTRAN gave almost identical results as the SOL 30 results. The comparisons were made on the design loads at the glass to titanium interface at the mirror socket and on the maximum design moments on the flexure support assembly. These results are shown in Table 7.1.

*Socket loads*

	<b>Moment</b>	<b>Shear</b>	<b>Axial</b>
<b>Method</b>	<b>(in-lb)</b>	<b>(lb)</b>	<b>(lb)</b>
SRSS	35,500	11,800	5,300
ABS	69,600	23,300	9,400
MRSS	45,100	15,100	5,800
SOL 30	45,000	15,000	5,600

*Blade loads*

	<b>Outer moment</b>	<b>Inner moment</b>
<b>Method</b>	<b>(in-lb)</b>	<b>(in-lb)</b>
SRSS	5,987	11,922
ABS	11,100	22,149
MRSS	6,783	13,560
SOL 30	6,336	12,650

**Table 7.1 Numerical Summary of Dynamic Analysis**

## REFERENCES

1. Melugin, R. K. and Miller, J. H., *Infrared Telescope Design: Implications from Cryogenic Tests of Fused-silica Mirrors*, SPIE Proc. 433 (1983). Contemporary Methods of Optical Manufacturing and Testing.
2. Vukobratovich, D., Iraninejad, B., Richard, R. M., Hansen, Q. M., and Melugin, R., *Optimum Shape for Lightweighted Mirrors*, SPIE Proc. 332 (1982). International Conference on Advanced Technology Optical Telescopes.
3. Iraninejad, Bijan and Vukobratovich, Daniel, *Double Arch Mirror Study*, Engineering Analysis Report, NASA Grant 2-220, NASA Ames Research Center, Mail Stop 244-7, Moffett Field, California 94035, May 1983.
4. Neugebauer, George H., *Designing Springs For Parallel Motion*, Machine Design, Volume 52:119-120, August 7, 1980.
5. Crandall, Stephen H. and Mark, William D., *Random Vibration*, Academic Press, Inc., Orlando, Florida, 1963.
6. Roark, Raymond J., *Formulas For Stress And Strain*, Fifth Edition, McGraw-Hill, New York, 1975.
7. Timoshenko, Stephen P. and Gere, James M., *Theory Of Elastic Stability*, McGraw-Hill, New York, 1961.
8. Richard, R. M., Private Communication, University of Arizona, 1987.
9. Wilson, E. L., Der Kiureghian, A., and Bayo, E. P., *A Replacement for the SRSS Method in Seismic Analysis*, Publication of University of California, Berkeley, California.

## APPENDIX I

### FORTTRAN LISTING OF SDOF DESIGN STUDY

```
C  VANMARCKE'S EQUATION FOR A SDOF SYSTEM
C  EQUATIONS ASSUME SINGLE CYLINDER VERTICAL POST, A TWO
C  CRUCIFORM GIMBAL, AND TWO SOFT FLEXURES, EACH
C  CONSISTING OF 3 BLADES
C  MAY 6, 1987
C
C  BY WAYNE POLLARD AND MYUNG CHO
C
C      PROGRAM BLOCK
C      CHARACTER ITIME*5,IDATE*14
C      CHARACTER*19 CHA,CHB,CHC,CHD,CHE,CHF,CHG,CHH,CHI,CHJ,CHK,CHL
C
C  P0=MAXIMUM VALUE OF PSD INPUT (IN/SEC2)2/HZ
C  YM=YOUNG'S MODULUS  PSI
C  SIGMA=ALLOWABLE STRESS  PSI
C  F0=LIMIT OF CONSTAN SPECTRAL DENSITY
C  SL=SLOPE OF PSD
C  E=PERCENT CRITICAL DAMPING
C  WEIGHT=MIRROR WEIGHT
C  ZARM=MOMENT ARM FROM GIMBAL PLANE TO MIRROR CG
C  CRYDEL= RADIAL THERMAL SHRINKAGE OF BASEPLATE
C  GM= SHEAR MOD (SET TO LARGE VALUE TO EXCLUDE SHEAR
DEFORMATION)
C
C      OPEN(UNIT=6,FILE='BLOCK.DAT',STATUS='OLD')
C      OPEN(UNIT=7,FILE='BLOCK.OUT',STATUS='NEW')
C
C      READ(6,111) ISIZE,JUMPSF,ALL,STB,IOPT
C
C      IF ISIZE ==
C          EQ.1 ONE METER MIRROR
C          NE.1 HALF METER MIRROR
C
C      IF JUMPSF ==
C          EQ.1 CHECK FACTOR OF SAFETY
C          EQ.0 NO CHECK
C
C      ALL -- ALLOWABLE SAFETY FACTOR (DEFAULT = 1.0)
C
C      STA -- SAFETY FACTOR FOR STABILITY (3 SIGMA)
C
C      IF IOPT ==
C          EQ.1 VERTICAL BLADE OF CRUCIFORM IDENTICAL TO HORIZ
BLADE
C          EQ.0 VERTICAL BLADE OF CRUCIFORM IDENTICAL TO SOFT
```



BLADE

C

111 FORMAT(/2I5,2F5.0,I5)

IF(ISIZE.EQ.1) THEN

CRYDEL=.062

WEIGHT=258.

CRYMOM=74.7

WRITE(7, '(///,25H \*\*\* ONE METER MIRROR \*\*\*)')

WRITE(7, '( 15H NOTE: CRYDEL =,F6.3)') CRYDEL

ELSE

CRYDEL=.0324

WEIGHT=35.

CRYMOM=30.4

WRITE(7, '(///,26H \*\*\* HALF METER MIRROR \*\*\*)')

ENDIF

C

C\*\* CONSTANTS

C

XMASS=WEIGHT/386.

PSD=.02

E=.004

P0=PSD\*386.\*386.

YM=18000000.

GM=YM/2.6

SIGMA=129000.

F0=250.

SL=-6.0

C

WRITE(7,89)PSD,YM,GM,SIGMA,E,CRYMOM,WEIGHT,CRYDEL

89 FORMAT(//,' PSD= 'F8.3,/, ' MODULUS OF ELASTICITY= 'E10.5,

+/,' SHEAR MODULUS= 'E8.3,/, ' ALLOWABLE STRESS= 'E8.3,/,

+' CRITICAL DAMPING RATIO= 'F7.4,/, ' ALLOWABLE CRYO MOMENT= ',

+F7.3,/, ' MIRROR WEIGHT= 'F7.3,/,

+' THERMAL SHRINKAGE OF BASEPLATE= 'F7.3,

+//,' VERTICAL FLEXURE IS A SINGLE CIRCULAR POST')

CALL DATE(IDATE)

CALL TIME(ETIME)

WRITE(7,899) ETIME,IDATE

899 FORMAT(///1X,30(1H\*))' THIS RAN AT 'A5,' ON 'A14/1X,30(1H\*))

WRITE(7,114) ISIZE,JUMPSF,ALL,STB,IOPT

114 FORMAT(///,' ISIZE =',I2,3X,'JUMPSF =',I2,3X,'ALL =',F5.2,

+ 3X,'STB =',F5.2,3X,'IOPT =',I2)

C POST DIMENSIONS

READ(6,999) FL1,FL2,FL3,FB1,FB2,FB3,FT1,FT2,FT3

C SELECT OUTER FLEXURE BLADE DIMENSIONS, SOFT

READ(6,999) GL1,GL2,GL3,GB1,GB2,GB3,GT1,GT2,GT3

C SELECT GIMBAL BLADE DIMENSIONS, HARD — HORZ. CRUCIFORM BLADES

READ(6,999) GLX1,GLX2,GLX3,GBX1,GBX2,GBX3,GTX1,GTX2,GTX3

C SELECT INNER FLEXURE BLADE DIMENSIONS

READ(6,999) GLC1,GLC2,GLC3,GBC1,GBC2,GBC3,GTC1,GTC2,GTC3

C

CHA=' POST LENGTH'

```

CHB=' POST      DIAMETER'
CHC=' POST      THICK'
CHD=' FLEX      SOFT LENGTH'
CHE=' FLEX      SOFT WIDTH'
CHF=' FLEX      SOFT THICK'
CHI=' GIMBAL    HARD LENGTH'
CHG=' GIMBAL    HARD WIDTH'
CHH=' GIMBAL    HARD THICK'
CHJ=' FLEX      CENT LENGTH'
CHK=' FLEX      CENT WIDTH'
CHL=' FLEX      CENT THICK'
WRITE(7,997)
WRITE(7,998) CHA,FL1,FL2,FL3,CHB,FB1,FB2,FB3,CHC,FT1,FT2,FT3
WRITE(7,998) CHD,GL1,GL2,GL3,CHE,GB1,GB2,GB3,CHF,GT1,GT2,GT3
WRITE(7,998) CHI,GLX1,GLX2,GLX3,CHG,GBX1,GBX2,GBX3,
+           CHH,GTX1,GTX2,GTX3
WRITE(7,998) CHJ,GLC1,GLC2,GLC3,CHK,GBC1,GBC2,GBC3,
+           CHL,GTC1,GTC2,GTC3
997      FORMAT(///,22X,' START   LAST   STEP')
998      FORMAT(/,A19,3X,3F8.3)
999      FORMAT(/,3F5.0)

C
C** JUMPSF=1 NO CHECK FOR SAFETY FACTORS, OTHERWISE CHECK
C** ALL IS ALLOWABLE SAFETY FACTOR, SET ALL=1.0
C
C FL=POST LENGTH
DO 100 FL=FL1,FL2,FL3
C FB=POST OD
DO 100 FB=FB1,FB2,FB3
C FT=POST WALL THICKNESS
DO 100 FT=FT1,FT2,FT3
ZARM=FL
WRITE(7,901) FL,FB,FT
901      FORMAT(////,' FL = ',F5.2,' FB = ',F5.2,' FT = ',F5.3)
C GLX=GIMBAL LENGTH, HARD
DO 100 GLX=GLX1,GLX2,GLX3
C GBX=GIMBAL WIDTH, HARD
DO 100 GBX=GBX1,GBX2,GBX3
C GTX=GIMBAL THICKNESS, HARD
DO 100 GTX=GTX1,GTX2,GTX3
WRITE(7,902) GLX,GBX,GTX
902      FORMAT(////,' GLX = ',F5.2,' GBX = ',F5.2,' GTX = ',F5.3)
WRITE(7,900)
900      FORMAT(/,' GL  GB  GT  GLC  GBC  GTC  VDISP
+      ,      'HDISP  VFREQ  HFREQ  VUNIT  HUNIT  FH'
+      ,      ' GH  GS  CC  VBH  VBS  TM  SS')
C SELECT OUTER FLEXURE BLADE DIMENSIONS
C GL=FLEXURE LENGTH, SOFT
DO 100 GL=GL1,GL2,GL3
C GB=FLEXURE WIDTH, SOFT

```

```

DO 100 GB=GB1,GB2,GB3
C GT=FLEXURE THICKNESS, SOFT
DO 100 GT=GT1,GT2,GT3
C SELECT INNER FLEXURE BLADE DIMENSIONS
C GLX=FLEXURE LENGTH, CENTER
C DO 100 GLC=GLC1,GLC2,GLC3
GLC=GL-1.
C GBX=FLEXURE WIDTH, CENTER
C DO 100 GBC=GBC1,GBC2,GBC3
GBC=GB
C GTX=FLEXURE THICKNESS, CENTER
DO 100 GTC=GTC1,GTC2,GTC3
C GIMBAL ROTATIONAL STIFFNESS SOFT, GKRS
GJ1=GB*(GT**3)/3.0
GJ2=GBC*(GTC**3)/3.0
GKRS=(GM*4.0*GJ1*GJ2)/(GL*GJ2+2.0*GLC*GJ1)
C GIMBAL ROTATIONAL STIFFNESS HARD, GKRH
GKRH=(GM*4.0*GBX*GTX**3.)/(3.0*GLX)
IF (IOPT .NE. 1) GKRH=GKRH/2.+(GM*2.0*GB*GT**3.)/(3.0*GLX)
C GIMBAL TRANSLATIONAL STIFFNESS, 1/KT, SOFT
GINER1=GB*GT**3./12.
GINER2=GBC*GTC**3/12.
GKTSSA=((GL**3)*GINER2+2.*(GLC**3)*GINER1)/(48.*YM*GINER1*GINER2)
1 +(GL*GBC*GTC+2.0*GLC*GB*GT)/(4.0*GM*GBC*GTC*GB*GT)
C INCLUDE STIFFNESS OF BLADE LENGTH
GKTSS=GKTSSA+GLX/(4*YM*GBX*GTX)
IF (IOPT .NE.
1)GKTSS=GKTSSA+GLX/(2*YM*GB*GT)+GLX/(2*YM*GBX*GTX)
C GIMBAL TRANSLATIONAL STIFFNESS, 1/KT, HARD
GINER=(GTX*(GBX)**3.+GBX*GTX**3.)/12.
IF (IOPT .NE. 1)GINER=(GTX*(GBX)**3.+GB*GT**3.)/12.
GKTSH=GLX**3./(24.*YM*GINER)+GLX/(2.*(GBX)*GTX*GM)
C INCLUDE STIFFNESS OF BLADE LENGTH
GKTSH=GKTSH+(GL*GBC*GTC+2.0*GLC*GB*GT)/(4.0*YM*GB*GT*GBC*GTC)
C FLEXURE INERTIA, HARD
FIH=(3.14159/4.)*((FB/2.)**4.-(FB/2.-FT)**4.)
C FLEXURE INERTIA, SOFT
FIS=FIH
C POST HEIGHT
PH=-(FL-ZARM)
C ASSEMBLY STIFFNESS, HARD
PAR1=3.0*PH/(2.*FL)
C WRITE(7, '(6H PAR1=,G11.3)') PAR1
PAR2=1.0+GKRH*FL/(4.0*YM*FIH)
C WRITE(7, '(6H PAR2=,G11.3)') PAR2
PAR3=FL**3./(12.*YM*FIH)
C WRITE(7, '(6H PAR3=,G11.3)') PAR3
SKSSHI=(1.+PAR1/PAR2)*PAR3*(PAR2+PAR1)/(PAR2-.75)
C WRITE(7, '(8H SKSSHI=,G11.3)') SKSSHI
SKSSHI=SKSSHI+(PH**2.*FL/(4.*YM*FIH))/PAR2+GKTSH
C WRITE(7, '(8H SKSSHI=,G11.3)') SKSSHI

```

```

      SKSSHI=SKSSHI+FL/(3.14*((FB/2.)**2-(FB/2.-FT)**2.)*GM)
C  WRITE(7,(/8H SKSSHI=,G11.3)) SKSSHI
      SKSSH=1./SKSSHI
C  WRITE(7,(/8H SKSSH =,G11.3)) SKSSH
C  ASSEMBLY STIFFNESS, SOFT
      PAR2=1.+GKRS*FL/(4.0*YM*FIS)
C  WRITE(7,(/6H PAR2=,G11.3)) PAR2
      PAR3=FL**3./(12.*YM*FIS)
C  WRITE(7,(/6H PAR3=,G11.3)) PAR3
      SKSSSI=(1.+PAR1/PAR2)*PAR3*(PAR2+PAR1)/(PAR2-.75)
C  WRITE(7,(/8H SKSSSI=,G11.3)) SKSSSI
      SKSSSI=SKSSSI+(PH**2.*FL/(4.*YM*FIS))/PAR2+GKTSS
C  WRITE(7,(/8H SKSSSI=,G11.3)) SKSSSI
      SKSSSI=SKSSSI+FL/(3.14*((FB/2.)**2-(FB/2.-FT)**2.)*GM)
C  WRITE(7,(/8H SKSSSI=,G11.3)) SKSSSI
      SKSSS=1./SKSSSI
C  WRITE(7,(/8H SKSSS =,G11.3)) SKSSS
C  WRITE(7,81)EL
C  81  FORMAT(////////,' LENGTH='F6.3,/)
C  WRITE(7,99)
C  99  FORMAT(2X,'FREQUENCY',6X,'PSD',5X,'DISPLACEMENT',2X,
C  + ' I11 ',4X,'SHEAR',7X,'MOMENT',8X,'B',10X,'H',
C  +10X,'I22',8X,'AREA',6X,' J',.39X,'(LARGE)',17X,'(CRYO)')
C
C  SYSTEM STIFFNESS
      SYS=1.5*(SKSSS+SKSSH)
C  SDOF FREQUENCY
      F=1./(2.*3.14159)*SQRT(SYS/XMASS)
C  PSD VALUE
      IF(F.LE.250.)GO TO 90
      S=P0*(F/F0)**(SL*3.3219/10.0)
      GO TO 91
90  S=P0
91  CONTINUE
C  RMS DEFLECTION, SINGLE AXIS PSD
      D=(S/(1984.*E*F**3.))**.5
C  RMS DEFLECTION, TWO AXIS PSD
      DSYS=1.414*D
C  3 SIGMA DEFLECTION, 2 AXIS PSD
      DSYS=3.*DSYS
C  SYSTEM SHEAR TO BE COMPARED TO EIGENVALUE IN STABILITY RUN
      SYSSHR=DSYS*SYS
C  ASSEMBLY SHEAR, TWO AXIS PSD
      ASHEAR=DSYS*SKSSH
C  BENDING STRESS IN FLEXURE, HARD
      BM=ASHEAR*FL/2.
C  WRITE(7,(/6H BMFH=,G11.3)) BM
      FSH=BM*FB/(2.0*FIH)
      SAFEFH=SIGMA/FSH
      IF(JUMPSF.NE.1 .AND. SAFEFH.LT.ALL) GOTO 100
C  BENDING STRESS IN GIMBAL, HARD: SHEAR DIVIDES TO TWO BLADES

```

```

      BM=(ASHEAR*GLX/2.)/2.
C  WRITE(7, '(6H BMGH=,G11.3)') BM
      GSH=BM*(GBX/(2.))/(((GBX)**3.*GTX+GTX**3.*GBX)/12.)
      IF (IOPT .NE. 1)GSH=BM*(GBX/(2.))/(((GBX)**3.*GTX+GT**3.*GB)/12.)
      SAFEGH=SIGMA/GSH
      IF(JUMPSF.NE.1 .AND. SAFEGH.LT.ALL) GOTO 100
C  RADIAL SHEAR FOR CRY COOLDOWN
      RSHEAR=CRYDEL*SKSSS
C  BENDING STRESS IN FLEXURE, SOFT
C      BM=RSHEAR*FL/2.
C  WRITE(7, '(6H BMFS=,G11.3)') BM
C      FSS=BM*FB/(2.*FIS)
C      SAFEFS=SIGMA/FSS
C  BENDING STRESS IN GIMBAL, SOFT: SHEAR DIVIDES TO TWO BLADES
      BM=(RSHEAR*GLC/2.)/2.
C  WRITE(7, '(6H BMGS=,G11.3)') BM
      GSS=BM*(GT/2.)/(GB*GT**3./12.)
      SAFEGS=SIGMA/GSS
      IF(JUMPSF.NE.1 .AND. SAFEGS.LT.ALL) GOTO 100
C  BENDING MOMENT AT MIRRORS CG
C  INCLUDES GB/2.
      CGMOM=RSHEAR*(ZARM+GB/2.)
      SAFECC=CRYMOM/CGMOM
      IF(JUMPSF.NE.1 .AND. SAFECC.LT.ALL) GOTO 100
C  VERTICAL STIFFNESS OF A GIMBAL ASSEMBLY
      GINER1=GT*GB**3/12.0
      GINER2=GTC*GBC**3/12.0
      GKVII=(2.*GLC**3.*GINER1+GL**3.*GINER2)/(48.*YM*GINER1*GINER2)
      1 +(2.*GLC*GB*GT+GL*GBC*GTC)/(4.*GT*GB*GM*GBC*GTC)
      GKVI=GKVII+GLX**3./(2.*YM*GTX*GBX**3.)+GLX/(2.*GTX*GBX*GM)
      IF (IOPT .NE. 1) GKVI=GKVII+GLX**3./(2.*YM*GT*GB**3.)
      1 +GLX/(2.*GT*GB*GM)
      GKV=1./GKVI
C  VERTICAL STIFFNESS OF SYSTEM
      SYSGKV=3.*GKV
C  VERTICAL NATURAL FREQUENCY
      VF=(1./(2.*3.14159))*(SYSGKV/XMASS)**.5
C  CHECK POINT ON PSD CURVE
      IF (VF.LE.250.)GO TO 700
      VS=P0*(VF/F0)**(SL*3.3219/10.)
      GOTO 910
700  VS=P0
910  CONTINUE
C  VERTICAL RMS DISPLACEMENT
      VD=(VS/(1984.*E*VF**3.))**.5
C  VERTICAL 3 SIGMA DISPLACEMENT
      VD=3.*VD
C  VERTICAL SHEAR, SINGLE ASSEMBLY
      VSHEAR=SYSGKV*VD/3.
C  VERTICAL BENDING MOMENT SOFT: SHEAR DIVIDES TO TWO BLADES
      VBMS=(VSHEAR*GLC/2.)/2.
C  VERTICAL BENDING STRESS SOFT

```

```

      VBSS=VBMS*(GB/2.)/((GT*(GB)**3./12.))
      SAFVBS=SIGMA/VBSS
      IF(JUMPSF.NE.1 .AND. SAFVBS.LT.ALL) GOTO 100
C VERTICAL BENDING MOMENT HARD: SHEAR DIVIDES TO TWO BLADES
      VBMH=(VSHEAR*GLX/2.)/2.
C VERTICAL BENDING STRESS HARD
      VBSH=VBMH*(GBX/2.)/((GT*(GBX)**3./12.))
      IF (IOPT . NE. 1)VBSH=VBMH*(GB/2.)/((GT*GB**3.+GBX*GT**3.)/12.)
      SAFVBH=SIGMA/VBSH
      IF(JUMPSF.NE.1 .AND. SAFVBH.LT.ALL) GOTO 100
C TORSIONAL MOMENT ON GIMBAL/MIRROR DUE TO .001 RAD
MISALIGNMENT
      TMMH=GKRH*.001
      TMMS=GKRS*.001
      TMM=AMAX1(TMMH, TMMS)
      TMM=TMM/2.
      SAFTMM=CRYMOM/TMM
      IF(JUMPSF.NE.1 .AND. SAFTMM.LT.ALL) GOTO 100
C STABILITY ALGORITHM
      SSYS=VSHEAR/(2.*GB*GT**3/GL**2)
      SK=2837./6.173E-5
C FACTOR OF SAFETY ON STABILITY
      FS1=SK/SSYS
C
      SSYS=VSHEAR/(GBC*GTC**3/GLC**2)
      SK=2837./6.173E-5
C FACTOR OF SAFETY ON STABILITY
      FS2=SK/SSYS
      FS=FS1
      IF (FS1 .GT. FS2)FS=FS2
C
      IF(SAFEFH .GT. 9.) SAFEFH=9.0
      IF(SAFEGH .GT. 9.) SAFEGH=9.0
      IF(SAFEGS .GT. 9.) SAFEGS=9.0
      IF(SAFECC .GT. 9.) SAFECC=9.0
      IF(SAFVBH .GT. 9.) SAFVBH=9.0
      IF(SAFVBS .GT. 9.) SAFVBS=9.0
      IF(SAFTMM .GT. 9.) SAFTMM=9.0
      IF(FS .GT. 9.) FS =9.0
      IF(FS .LT. STB) GOTO 903
888 WRITE(7,905) GL,GB,GT,GLC,GBC,GTC,VD,DSYS,VF,F,VSHEAR,ASHEAR
      +,
SAFEFH,SAFEGH,SAFEGS,SAFECC,SAFVBH,SAFVBS,SAFTMM,FS
903 CONTINUE
905 FORMAT(1X,2(2F5.2,F6.3),6E10.3,7F5.1,F4.1)
100 CONTINUE
      STOP
      END

```

## APPENDIX II

### NASTRAN INPUT FILE - - SOLUTION TYPE 3

ID SIRTF,FREQ  
 SOL 3  
 TIME 50  
 CEND  
 TITLE= SIRTF 1.0 M — TAPERED(2.00-2.45), INNER=0.18; OUTER=0.14 THICK  
 SUBTITLE=DYNAMICS FOR Wt=258 LB MIRROR  
 SPC=23  
 DISPLACEMENT = ALL  
 METHOD=1  
 OUTPUT(PLOT)  
 PLOTTER NAST  
 SET 1 = ALL

-----UNDEFORMED MESH

FIND SCALE, ORIGIN 1, SET 1  
 PLOT,SET 1,ORIGIN 1

-----DEFORMED MESH

PLOT MODAL DEFORMATION 0 RANGE 0.,300.,SET 1,SHAPE

AXES Y,Z,X

VIEW 0.,0.,0.

FIND SCALE,ORIGIN 2,SET 1

PLOT MODAL DEFORMATION 0 RANGE 0.,300.,SET 1,ORIGIN 2,SHAPE

AXES Z,X,Y

VIEW 0.,0.,0.

FIND SCALE,ORIGIN 4,SET 1

PLOT MODAL DEFORMATION 0 RANGE 0.,300.,SET 1,ORIGIN 4,SHAPE

BEGIN BULK

*Program listing begins double column here*

CBEAM ,191,4,112,191,501

CBEAM ,192,5,191,192,501

CBEAM ,193,5,193,194,501

CBEAM ,194,4,194,131,501

CBEAM ,291,4,212,291,501

CBEAM ,292,5,291,292,501

CBEAM ,293,5,293,294,501

CBEAM ,294,4,294,231,501

CBEAM ,391,4,312,391,501

CBEAM ,392,5,391,392,501

CBEAM ,393,5,393,394,501

CBEAM ,394,4,394,331,501

GRID ,191,0,-6.75,0.0,0.0

GRID ,192,0,-4.75,0.0,0.0

GRID ,193,0, 4.75,0.0,0.0

GRID ,194,0, 6.75,0.0,0.0

GRID ,291,1,-6.75,0.0,0.0

GRID ,292,1,-4.75,0.0,0.0

GRID ,293,1, 4.75,0.0,0.0

GRID ,294,1, 6.75,0.0,0.0

GRID ,391,2,-6.75,0.0,0.0

GRID ,392,2,-4.75,0.0,0.0

GRID ,393,2, 4.75,0.0,0.0

GRID ,394,2, 6.75,0.0,0.0

CORD2R,1,0,11.26,19.50,0.0,11.26,19.5,1.0,+  
 RD1

+RD1,0.0,39.0,0.0

CORD2R,2,0,-11.26,19.5,0.0,-11.26,19.5,1.0,+  
 RD2

+RD2,-15.01,13.0,0.0

PBEAM ,1,1,1.500,.0703,.5000,0.0,.2813

= ,2,1, .280,4.6-4,.0933,0.0,.0018

= ,3,1, .387,.0010,.1491,0.0,.0042

= ,4,1, .441,.0012,.2206,0.0,.0048

= ,5,1, .414,.0011,.1825,0.0,.0045

= ,6,1,1.838,.0861,.9191,0.0,.3445

- .7,1, .850,.4280,.0950,0.0,.0087  
 - .9,1,7.069,3.976,3.976,0.0,7.952

CONM2,101,500,0,0.668,,,,,+CONM2  
 +CONM2,57.4761,,57.4761,,,114.0531  
 EIGR,1,MHOU,10.0,600,,,,,+EIGR1  
 +EIGR1,MAX

MAT1,1,18.0+6,...3  
 SPC1,23 ,123456,116,127  
 SPC1,23 ,123456,216,227  
 SPC1,23 ,123456,316,327

PARAM,AUTOSPC,YES  
 RBAR, 101,500,121,123456,,,123456  
 RBAR, 102,500,221,123456,,,123456  
 RBAR, 103,500,321,123456,,,123456  
 RBAR, 112,120,122,123456,,,123456  
 RBAR, 114,122,123,123456,,,123456  
 RBAR, 212,220,222,123456,,,123456  
 RBAR, 214,222,223,123456,,,123456  
 RBAR, 312,320,322,123456,,,123456  
 RBAR, 314,322,323,123456,,,123456  
 PLOTTEL,5001,500,121  
 PLOTTEL,5002,500,221  
 PLOTTEL,5003,500,321

----- 1 ST  
 CMASS2,1111,21.0-4,111,3

- \*(1),= ,113,3  
 - \*(1),= ,130,3  
 - \*(1),= ,132,3  
 - \*(1),22.0-4,112,3  
 - \*(1),= ,131,3  
 - \*(1),16.8-4,114,3  
 - \*(1),= ,118,3  
 - \*(1),= ,125,3  
 - \*(1),= ,129,3  
 - \*(1),27.6-4,115,3  
 - \*(1),= ,117,3  
 - \*(1),= ,126,3  
 - \*(1),= ,128,3  
 - \*(1),18.2-4,119,3  
 - \*(1),= ,124,3  
 - \*(1),5.94-4,120,3  
 - \*(1),= ,123,3  
 - \*(1),18.3-3,122,3  
 - \*(1),5.60-4,116,3  
 - \*(1),= ,127,3

----- 2 ND  
 CMASS2,2111,21.0-4,211,3  
 - \*(1),= ,213,3  
 - \*(1),= ,230,3

- \*(1),= ,232,3  
 - \*(1),22.0-4,212,3  
 - \*(1),= ,231,3  
 - \*(1),16.8-4,214,3  
 - \*(1),= ,218,3  
 - \*(1),= ,225,3  
 - \*(1),= ,229,3  
 - \*(1),27.6-4,215,3  
 - \*(1),= ,217,3  
 - \*(1),= ,226,3  
 - \*(1),= ,228,3  
 - \*(1),18.2-4,219,3  
 - \*(1),= ,224,3  
 - \*(1),5.94-4,220,3  
 - \*(1),= ,223,3  
 - \*(1),18.3-3,222,3  
 - \*(1),5.60-4,216,3  
 - \*(1),= ,227,3

----- 3 RD  
 CMASS2,3111,21.0-4,311,3

- \*(1),= ,313,3  
 - \*(1),= ,330,3  
 - \*(1),= ,332,3  
 - \*(1),22.0-4,312,3  
 - \*(1),= ,331,3  
 - \*(1),16.8-4,314,3  
 - \*(1),= ,318,3  
 - \*(1),= ,325,3  
 - \*(1),= ,329,3  
 - \*(1),27.6-4,315,3  
 - \*(1),= ,317,3  
 - \*(1),= ,326,3  
 - \*(1),= ,328,3  
 - \*(1),18.2-4,319,3  
 - \*(1),= ,324,3  
 - \*(1),5.94-4,320,3  
 - \*(1),= ,323,3  
 - \*(1),18.3-3,322,3  
 - \*(1),5.60-4,316,3  
 - \*(1),= ,327,3

----- 2-1  
 CMASS2,1211,21.0-4,111,2

- \*(1),= ,113,2  
 - \*(1),= ,130,2  
 - \*(1),= ,132,2  
 - \*(1),22.0-4,112,2  
 - \*(1),= ,131,2  
 - \*(1),16.8-4,114,2  
 - \*(1),= ,118,2  
 - \*(1),= ,125,2  
 - \*(1),= ,129,2  
 - \*(1),27.6-4,115,2



- \*(1),= ,117,2  
 - \*(1),= ,126,2  
 - \*(1),= ,128,2  
 - \*(1),18.2-4,119,2  
 - \*(1),= ,124,2  
 - \*(1),5.94-4,120,2  
 - \*(1),= ,123,2  
 - \*(1),18.3-3,122,2  
 - \*(1),5.60-4,116,2  
 - \*(1),= ,127,2

----- 2 ND  
 CMASS2,2211,21.0-4,211,2

- \*(1),= ,213,2  
 - \*(1),= ,230,2  
 - \*(1),= ,232,2  
 - \*(1),22.0-4,212,2  
 - \*(1),= ,231,2  
 - \*(1),16.8-4,214,2  
 - \*(1),= ,218,2  
 - \*(1),= ,225,2  
 - \*(1),= ,229,2  
 - \*(1),27.6-4,215,2  
 - \*(1),= ,217,2  
 - \*(1),= ,226,2  
 - \*(1),= ,228,2  
 - \*(1),18.2-4,219,2  
 - \*(1),= ,224,2  
 - \*(1),5.94-4,220,2  
 - \*(1),= ,223,2  
 - \*(1),18.3-3,222,2  
 - \*(1),5.60-4,216,2  
 - \*(1),= ,227,2

----- 3 RD  
 CMASS2,3211,21.0-4,311,2

- \*(1),= ,313,2  
 - \*(1),= ,330,2  
 - \*(1),= ,332,2  
 - \*(1),22.0-4,312,2  
 - \*(1),= ,331,2  
 - \*(1),16.8-4,314,2  
 - \*(1),= ,318,2  
 - \*(1),= ,325,2  
 - \*(1),= ,329,2  
 - \*(1),27.6-4,315,2  
 - \*(1),= ,317,2  
 - \*(1),= ,326,2  
 - \*(1),= ,328,2  
 - \*(1),18.2-4,319,2  
 - \*(1),= ,324,2  
 - \*(1),5.94-4,320,2  
 - \*(1),= ,323,2  
 - \*(1),18.3-3,322,2

- \*(1),5.60-4,316,2  
 - \*(1),= ,327,2

----- 3-1  
 CMASS2,1311,21.0-4,111,1

- \*(1),= ,113,1  
 - \*(1),= ,130,1  
 - \*(1),= ,132,1  
 - \*(1),22.0-4,112,1  
 - \*(1),= ,131,1  
 - \*(1),16.8-4,114,1  
 - \*(1),= ,118,1  
 - \*(1),= ,125,1  
 - \*(1),= ,129,1  
 - \*(1),27.6-4,115,1  
 - \*(1),= ,117,1  
 - \*(1),= ,126,1  
 - \*(1),= ,128,1  
 - \*(1),18.2-4,119,1  
 - \*(1),= ,124,1  
 - \*(1),5.94-4,120,1  
 - \*(1),= ,123,1  
 - \*(1),18.3-3,122,1  
 - \*(1),5.60-4,116,1  
 - \*(1),= ,127,1

----- 2 ND  
 CMASS2,2311,21.0-4,211,1

- \*(1),= ,213,1  
 - \*(1),= ,230,1  
 - \*(1),= ,232,1  
 - \*(1),22.0-4,212,1  
 - \*(1),= ,231,1  
 - \*(1),16.8-4,214,1  
 - \*(1),= ,218,1  
 - \*(1),= ,225,1  
 - \*(1),= ,229,1  
 - \*(1),27.6-4,215,1  
 - \*(1),= ,217,1  
 - \*(1),= ,226,1  
 - \*(1),= ,228,1  
 - \*(1),18.2-4,219,1  
 - \*(1),= ,224,1  
 - \*(1),5.94-4,220,1  
 - \*(1),= ,223,1  
 - \*(1),18.3-3,222,1  
 - \*(1),5.60-4,216,1  
 - \*(1),= ,227,1

----- 3 RD  
 CMASS2,3311,21.0-4,311,1

- \*(1),= ,313,1  
 - \*(1),= ,330,1  
 - \*(1),= ,332,1  
 - \*(1),22.0-4,312,1

- \*(1),= ,331,1  
 - \*(1),16.8-4,314,1  
 - \*(1),= ,318,1  
 - \*(1),= ,325,1  
 - \*(1),= ,329,1  
 - \*(1),27.6-4,315,1  
 - \*(1),= ,317,1  
 - \*(1),= ,326,1  
 - \*(1),= ,328,1  
 - \*(1),18.2-4,319,1  
 - \*(1),= ,324,1  
 - \*(1),5.94-4,320,1  
 - \*(1),= ,323,1  
 - \*(1),18.3-3,322,1  
 - \*(1),5.60-4,316,1  
 - \*(1),= ,327,1

1ST

CBEAM , 111,6,111,112,501

- \*(1),6,112,113,-  
 - \*(1),2,111,115,-  
 - \*(1),3,192,116,-  
 - \*(1),2,113,117,-  
 - \*(1),1,114,115,-  
 - \*(1),-,115,117,-  
 - \*(1),-,117,118,-  
 - \*(1),-,114,119,-  
 - \*(1),-,119,125,-  
 - \*(1),7,119,120,131  
 - , 123,9,121,122,501  
 - , 125,7,123,124,131  
 - , 127,1,118,124,501  
 - \*(1),-,124,129,-  
 - \*(1),-,125,126,-  
 - \*(1),-,126,128,-  
 - \*(1),-,128,129,-  
 - \*(1),2,126,130,-  
 - \*(1),3,127,193,-  
 - \*(1),2,128,132,-  
 - \*(1),6,131,130,112  
 - \*(1),6,132,131,112

2 ND

CBEAM , 211,6,211,212,501

- \*(1),6,212,213,-  
 - \*(1),2,211,215,-  
 - \*(1),3,292,216,-  
 - \*(1),2,213,217,-  
 - \*(1),1,214,215,-  
 - \*(1),-,215,217,-  
 - \*(1),-,217,218,-  
 - \*(1),-,214,219,-  
 - \*(1),-,219,225,-

- \*(1),7,219,220,231  
 - , 223,9,221,222,501  
 - , 225,7,223,224,231  
 - , 227,1,218,224,501  
 - \*(1),-,224,229,-  
 - \*(1),-,225,226,-  
 - \*(1),-,226,228,-  
 - \*(1),-,228,229,-  
 - \*(1),2,226,230,-  
 - \*(1),3,227,293,-  
 - \*(1),2,228,232,-  
 - \*(1),6,231,230,212  
 - \*(1),6,232,231,212

3 RD

CBEAM , 311,6,311,312,501

- \*(1),6,312,313,-  
 - \*(1),2,311,315,-  
 - \*(1),3,392,316,-  
 - \*(1),2,313,317,-  
 - \*(1),1,314,315,-  
 - \*(1),-,315,317,-  
 - \*(1),-,317,318,-  
 - \*(1),-,314,319,-  
 - \*(1),-,319,325,-  
 - \*(1),7,319,320,331  
 - , 323,9,321,322,501  
 - , 325,7,323,324,331  
 - , 327,1,318,324,501  
 - \*(1),-,324,329,-  
 - \*(1),-,325,326,-  
 - \*(1),-,326,328,-  
 - \*(1),-,328,329,-  
 - \*(1),2,326,330,-  
 - \*(1),3,327,393,-  
 - \*(1),2,328,332,-  
 - \*(1),6,331,330,312  
 - \*(1),6,332,331,312

CBEAM , 101,6,101,111,501

- \*(1),-,113,102,-  
 - \*(1),-,130,103,-  
 - \*(1),-,104,132,-

CBEAM , 201,6,201,211,501

- \*(1),-,213,202,-  
 - \*(1),-,230,203,-  
 - \*(1),-,204,232,-

CBEAM , 301,6,301,311,501

- \*(1),-,313,302,-  
 - \*(1),-,330,303,-  
 - \*(1),-,304,332,-

GRID, 101,0,-8.75 , 2.88 ,0.0

- \*(1),-,= , -2.88 ,=

```

- ,*(1),=-, 8.75 , 2.88 ,
- ,*(1),=-, -2.88 ,
GRID, 201,1,-8.75 , 2.88 ,0.0
- ,*(1),=-, -2.88 ,
- ,*(1),=-, 8.75 , 2.88 ,
- ,*(1),=-, -2.88 ,

```

```

GRID, 301,2,-8.75 , 2.88 ,0.0

```

```

- ,*(1),=-, -2.88 ,
- ,*(1),=-, 8.75 , 2.88 ,
- ,*(1),=-, -2.88 ,

```

```

GRID, 500,0, 0.0 ,13.0 ,3.0

```

```

GRID, 501,0, 0.0 ,13.0 ,0.0

```

```

----- 1 ST

```

```

GRID, 111,0,-8.75 , 1.44 ,0.0

```

```

- ,*(1),=-, , 0.0 ,==
- ,*(1),=-, -1.44 ,==
- , 130,-, 8.75 , 1.44 ,==
- ,*(1),=-, , 0.0 ,==
- ,*(1),=-, -1.44 ,==
- , 114,-,-1.75 , 4.5 ,0.0
- ,*(1),=-, , 1.44 ,=
- ,*(1),=-,-2.75 , 0.0 ,=
- ,*(1),=-,-1.75 , -1.44 ,
- ,*(1),=-, -4.5 ,=
- , 125,-, 1.75 , 4.5 ,=
- ,*(1),=-, , 1.44 ,=
- ,*(1),=-, 2.75 , 0.0 ,=
- ,*(1),=-, 1.75 , -1.44 ,=
- ,*(1),=-, -4.5 ,=
- , 119,-, 0.0 , 4.5 ,=
- ,*(1),=-, , 1.5 ,=
- ,*(1),=-, , 0.0 ,3.0
- ,*(1),=-, , 0.0 ,0.0
- ,*(1),=-, -1.5 ,=
- ,*(1),=-, -4.5 ,=

```

```

----- 2 ND

```

```

GRID, 211,1,-8.75 , 1.44 ,0.0

```

```

- ,*(1),=-, , 0.0 ,==
- ,*(1),=-, -1.44 ,==
- , 230,-, 8.75 , 1.44 ,==
- ,*(1),=-, , 0.0 ,==
- ,*(1),=-, -1.44 ,==
- , 214,-,-1.75 , 4.5 ,0.0
- ,*(1),=-, , 1.44 ,=
- ,*(1),=-,-2.75 , 0.0 ,=
- ,*(1),=-,-1.75 , -1.44 ,=
- ,*(1),=-, -4.5 ,=
- , 225,-, 1.75 , 4.5 ,=
- ,*(1),=-, , 1.44 ,=
- ,*(1),=-, 2.75 , 0.0 ,=
- ,*(1),=-, 1.75 , -1.44 ,=
- ,*(1),=-, -4.5 ,=

```

```

- , 219,-, 0.0 , 4.5 ,
- ,*(1),=-, , 1.5 ,=
- ,*(1),=-, , 0.0 ,3.0
- ,*(1),=-, , 0.0 ,0.0
- ,*(1),=-, -1.5 ,=
- ,*(1),=-, -4.5 ,=

```

```

----- 3 RD

```

```

GRID, 311,2,-8.75 , 1.44 ,0.0

```

```

- ,*(1),=-, , 0.0 ,==
- ,*(1),=-, -1.44 ,==
- , 330,-, 8.75 , 1.44 ,==
- ,*(1),=-, , 0.0 ,==
- ,*(1),=-, -1.44 ,==
- , 314,-,-1.75 , 4.5 ,0.0
- ,*(1),=-, , 1.44 ,=
- ,*(1),=-,-2.75 , 0.0 ,=
- ,*(1),=-,-1.75 , -1.44 ,=
- ,*(1),=-, -4.5 ,=
- , 325,-, 1.75 , 4.5 ,=
- ,*(1),=-, , 1.44 ,=
- ,*(1),=-, 2.75 , 0.0 ,=
- ,*(1),=-, 1.75 , -1.44 ,=
- ,*(1),=-, -4.5 ,=
- , 319,-, 0.0 , 4.5 ,=
- ,*(1),=-, , 1.5 ,=
- ,*(1),=-, , 0.0 ,3.0
- ,*(1),=-, , 0.0 ,0.0
- ,*(1),=-, -1.5 ,=
- ,*(1),=-, -4.5 ,=

```

```

ENDDATA

```

# APPENDIX III

## NASTRAN INPUT FILE - - SOLUTION TYPE 63

```
ID SIRTF,SPECTRUM
SOL 63
TIME 10
ALTER 5
DBSTORE SPECSEL//V,Y,SOLID/0
CEND
TITLE= SIRTF TAPERED DEPTH(2-2.45); 0.18 INNER BLADE -- 0.14 OUTER
BLADES
SUBTITLE=SPECTRUM 1 M (Wt=258 LB) -- ABS (0 - 200 HZ)
DISPLACEMENT = ALL
ELFO = ALL
DLOAD = 1
METHOD= 1
SET 1 = 0
SEALL = 1
BEGIN BULK
```

*Program listing begins double column here*

```
CBEAM ,191,4,112,191,501
CBEAM ,192,5,191,192,501
CBEAM ,193,5,193,194,501
CBEAM ,194,4,194,131,501
CBEAM ,291,4,212,291,501
CBEAM ,292,5,291,292,501
CBEAM ,293,5,293,294,501
CBEAM ,294,4,294,231,501
CBEAM ,391,4,312,391,501
CBEAM ,392,5,391,392,501
CBEAM ,393,5,393,394,501
CBEAM ,394,4,394,331,501
GRID ,191,0,-6.75,0.0,0.0
GRID ,192,0,-4.75,0.0,0.0
GRID ,193,0, 4.75,0.0,0.0
GRID ,194,0, 6.75,0.0,0.0
GRID ,291,1,-6.75,0.0,0.0
GRID ,292,1,-4.75,0.0,0.0
GRID ,293,1, 4.75,0.0,0.0
GRID ,294,1, 6.75,0.0,0.0
GRID ,391,2,-6.75,0.0,0.0
GRID ,392,2,-4.75,0.0,0.0
GRID ,393,2, 4.75,0.0,0.0
GRID ,394,2, 6.75,0.0,0.0

CORD2R,1,0,11.26,19.50,0.0,11.26,19.5,1.0,+
RD1
+RD1,0.0,39.0,0.0

CORD2R,2,0,-11.26,19.5,0.0,-11.26,19.5,1.0,+
RD2
+RD2,-15.01,13.0,0.0

PBEAM ,1,1,1.500,.0703,.5000,0.0,.2813
= ,2,1, .280,4.6-4,.0933,0.0,.0018
= ,3,1, .387,.0010,.1491,0.0,.0042
= ,4,1, .441,.0012,.2206,0.0,.0048
= ,5,1, .414,.0011,.1825,0.0,.0045
= ,6,1,1.838,.0861,.9191,0.0,.3445
= ,7,1, .850,.4280,.0950,0.0,.0087
= ,9,1,7.069,3.976,3.976,0.0,7.952
MAT1,1,18.0+6,..3
SUPORT,501,123456
CMASS2,333,1.+6 ,501,1
= ,334,= ,= ,2
= ,335,= ,= ,3
CMASS2,336,1.+8 ,501,4
= ,337,= ,= ,5
= ,338,= ,= ,6

CONM2,101,500,0.0,668,.....+CONM2
+CONM2,57.4761,,57.4761,,,114.0531
EIGR,1,MGIV,10.0,300,.....+EIGR1
+EIGR1,MASS
DLOAD,1,1,,1,,1,1.0,1,1.0,1,+DLOAD
+DLOAD,0.0,1,0.0,1,0.0,1
DTI,SPECSEL,0
```

DTI,SPECSEL,1,,D,1,,004,ENDREC  
RBE2,901,501,123456,116,127,216,227,316,+R  
BE  
+RBE,327  
TABLED1,1,,,,,,+TAB1  
+TAB1, 40.,7.668-2, 50.,5.487-2, 60.,4.174-2,  
80.,2.711-2,+TAB2  
+TAB2,100.,1.940-2,150.,1.056-2,200.,6.858-3  
,230.,5.561-3,+TAB3  
+TAB3,260.,4.450-3,290.,3.388-3,320.,2.650-3  
,350.,2.118-3,+TAB4  
+TAB4,ENDT  
PARAM,SCRSPEC,0  
PARAM,LFREQ,0.  
PARAM,HFREQ,200.  
PARAM,OPTION,ABS

————— 1 ST  
CMASS2,1111,21.0-4,111,3

- \*(1),= ,113,3  
- \*(1),= ,130,3  
- \*(1),= ,132,3  
- \*(1),22.0-4,112,3  
- \*(1),= ,131,3  
- \*(1),16.8-4,114,3  
- \*(1),= ,118,3  
- \*(1),= ,125,3  
- \*(1),= ,129,3  
- \*(1),27.6-4,115,3  
- \*(1),= ,117,3  
- \*(1),= ,126,3  
- \*(1),= ,128,3  
- \*(1),18.2-4,119,3  
- \*(1),= ,124,3  
- \*(1),5.94-4,120,3  
- \*(1),= ,123,3  
- \*(1),18.3-3,122,3  
- \*(1),5.60-4,116,3  
- \*(1),= ,127,3

————— 2 ND  
CMASS2,2111,21.0-4,211,3

- \*(1),= ,213,3  
- \*(1),= ,230,3  
- \*(1),= ,232,3  
- \*(1),22.0-4,212,3  
- \*(1),= ,231,3  
- \*(1),16.8-4,214,3  
- \*(1),= ,218,3  
- \*(1),= ,225,3  
- \*(1),= ,229,3  
- \*(1),27.6-4,215,3  
- \*(1),= ,217,3  
- \*(1),= ,226,3

- \*(1),= ,228,3  
- \*(1),18.2-4,219,3  
- \*(1),= ,224,3  
- \*(1),5.94-4,220,3  
- \*(1),= ,223,3  
- \*(1),18.3-3,222,3  
- \*(1),5.60-4,216,3  
- \*(1),= ,227,3

————— 3 RD  
CMASS2,3111,21.0-4,311,3

- \*(1),= ,313,3  
- \*(1),= ,330,3  
- \*(1),= ,332,3  
- \*(1),22.0-4,312,3  
- \*(1),= ,331,3  
- \*(1),16.8-4,314,3  
- \*(1),= ,318,3  
- \*(1),= ,325,3  
- \*(1),= ,329,3  
- \*(1),27.6-4,315,3  
- \*(1),= ,317,3  
- \*(1),= ,326,3  
- \*(1),= ,328,3  
- \*(1),18.2-4,319,3  
- \*(1),= ,324,3  
- \*(1),5.94-4,320,3  
- \*(1),= ,323,3  
- \*(1),18.3-3,322,3  
- \*(1),5.60-4,316,3  
- \*(1),= ,327,3

————— 2-1  
CMASS2,1211,21.0-4,111,2

- \*(1),= ,113,2  
- \*(1),= ,130,2  
- \*(1),= ,132,2  
- \*(1),22.0-4,112,2  
- \*(1),= ,131,2  
- \*(1),16.8-4,114,2  
- \*(1),= ,118,2  
- \*(1),= ,125,2  
- \*(1),= ,129,2  
- \*(1),27.6-4,115,2  
- \*(1),= ,117,2  
- \*(1),= ,126,2  
- \*(1),= ,128,2  
- \*(1),18.2-4,119,2  
- \*(1),= ,124,2  
- \*(1),5.94-4,120,2  
- \*(1),= ,123,2  
- \*(1),18.3-3,122,2  
- \*(1),5.60-4,116,2  
- \*(1),= ,127,2

----- 2 ND  
CMASS2,2211,21.0-4,211,2

- \*(1),= ,213,2  
- \*(1),= ,230,2  
- \*(1),= ,232,2  
- \*(1),22.0-4,212,2  
- \*(1),= ,231,2  
- \*(1),16.8-4,214,2  
- \*(1),= ,218,2  
- \*(1),= ,225,2  
- \*(1),= ,229,2  
- \*(1),27.6-4,215,2  
- \*(1),= ,217,2  
- \*(1),= ,226,2  
- \*(1),= ,228,2  
- \*(1),18.2-4,219,2  
- \*(1),= ,224,2  
- \*(1),5.94-4,220,2  
- \*(1),= ,223,2  
- \*(1),18.3-3,222,2  
- \*(1),5.60-4,216,2  
- \*(1),= ,227,2

----- 3 RD  
CMASS2,3211,21.0-4,311,2

- \*(1),= ,313,2  
- \*(1),= ,330,2  
- \*(1),= ,332,2  
- \*(1),22.0-4,312,2  
- \*(1),= ,331,2  
- \*(1),16.8-4,314,2  
- \*(1),= ,318,2  
- \*(1),= ,325,2  
- \*(1),= ,329,2  
- \*(1),27.6-4,315,2  
- \*(1),= ,317,2  
- \*(1),= ,326,2  
- \*(1),= ,328,2  
- \*(1),18.2-4,319,2  
- \*(1),= ,324,2  
- \*(1),5.94-4,320,2  
- \*(1),= ,323,2  
- \*(1),18.3-3,322,2  
- \*(1),5.60-4,316,2  
- \*(1),= ,327,2

----- 3-1  
CMASS2,1311,21.0-4,111,1

- \*(1),= ,113,1  
- \*(1),= ,130,1  
- \*(1),= ,132,1  
- \*(1),22.0-4,112,1  
- \*(1),= ,131,1  
- \*(1),16.8-4,114,1

- \*(1),= ,118,1  
- \*(1),= ,125,1  
- \*(1),= ,129,1  
- \*(1),27.6-4,115,1  
- \*(1),= ,117,1  
- \*(1),= ,126,1  
- \*(1),= ,128,1  
- \*(1),18.2-4,119,1  
- \*(1),= ,124,1  
- \*(1),5.94-4,120,1  
- \*(1),= ,123,1  
- \*(1),18.3-3,122,1  
- \*(1),5.60-4,116,1  
- \*(1),= ,127,1

----- 2 ND  
CMASS2,2311,21.0-4,211,1

- \*(1),= ,213,1  
- \*(1),= ,230,1  
- \*(1),= ,232,1  
- \*(1),22.0-4,212,1  
- \*(1),= ,231,1  
- \*(1),16.8-4,214,1  
- \*(1),= ,218,1  
- \*(1),= ,225,1  
- \*(1),= ,229,1  
- \*(1),27.6-4,215,1  
- \*(1),= ,217,1  
- \*(1),= ,226,1  
- \*(1),= ,228,1  
- \*(1),18.2-4,219,1  
- \*(1),= ,224,1  
- \*(1),5.94-4,220,1  
- \*(1),= ,223,1  
- \*(1),18.3-3,222,1  
- \*(1),5.60-4,216,1  
- \*(1),= ,227,1

----- 3 RD  
CMASS2,3311,21.0-4,311,1

- \*(1),= ,313,1  
- \*(1),= ,330,1  
- \*(1),= ,332,1  
- \*(1),22.0-4,312,1  
- \*(1),= ,331,1  
- \*(1),16.8-4,314,1  
- \*(1),= ,318,1  
- \*(1),= ,325,1  
- \*(1),= ,329,1  
- \*(1),27.6-4,315,1  
- \*(1),= ,317,1  
- \*(1),= ,326,1  
- \*(1),= ,328,1  
- \*(1),18.2-4,319,1

```

-      *(1),=      ,324,1
-      *(1),5.94-4,320,1
-      *(1),=      ,323,1
-      *(1),18.3-3,322,1
-      *(1),5.60-4,316,1
-      *(1),=      ,327,1

```

PARAM,AUTOSPC,YES

```

RBAR, 112,120,122,123456,...,123456
RBAR, 114,122,123,123456,...,123456
RBAR, 212,220,222,123456,...,123456
RBAR, 214,222,223,123456,...,123456
RBAR, 312,320,322,123456,...,123456
RBAR, 314,322,323,123456,...,123456
RBAR, 101,500,121,123456,...,123456
RBAR, 102,500,221,123456,...,123456
RBAR, 103,500,321,123456,...,123456

```

PLOTEL,5001,500,121

PLOTEL,5002,500,221

PLOTEL,5003,500,321

----- 1ST

CBEAM , 111,6,111,112,501

```

-      *(1),6,112,113,=
-      *(1),2,111,115,=
-      *(1),3,192,116,=
-      *(1),2,113,117,=
-      *(1),1,114,115,=
-      *(1),=,115,117,=
-      *(1),=,117,118,=
-      *(1),=,114,119,=
-      *(1),=,119,125,=
-      *(1),7,119,120,131
-      , 123,9,121,122,501
-      , 125,7,123,124,131
-      , 127,1,118,124,501
-      *(1),=,124,129,=
-      *(1),=,125,126,=
-      *(1),=,126,128,=
-      *(1),=,128,129,=
-      *(1),2,126,130,=
-      *(1),3,127,193,=
-      *(1),2,128,132,=
-      *(1),6,131,130,112
-      *(1),6,132,131,112

```

----- 2 ND

CBEAM , 211,6,211,212,501

```

-      *(1),6,212,213,=
-      *(1),2,211,215,=
-      *(1),3,292,216,=
-      *(1),2,213,217,=
-      *(1),1,214,215,=
-      *(1),=,215,217,=

```

```

-      *(1),=,217,218,=
-      *(1),=,214,219,=
-      *(1),=,219,225,=
-      *(1),7,219,220,231
-      , 223,9,221,222,501
-      , 225,7,223,224,231
-      , 227,1,218,224,501
-      *(1),=,224,229,=
-      *(1),=,225,226,=
-      *(1),=,226,228,=
-      *(1),=,228,229,=
-      *(1),2,226,230,=
-      *(1),3,227,293,=
-      *(1),2,228,232,=
-      *(1),6,231,230,212
-      *(1),6,232,231,212

```

----- 3 RD

CBEAM , 311,6,311,312,501

```

-      *(1),6,312,313,=
-      *(1),2,311,315,=
-      *(1),3,392,316,=
-      *(1),2,313,317,=
-      *(1),1,314,315,=
-      *(1),=,315,317,=
-      *(1),=,317,318,=
-      *(1),=,314,319,=
-      *(1),=,319,325,=
-      *(1),7,319,320,331
-      , 323,9,321,322,501
-      , 325,7,323,324,331
-      , 327,1,318,324,501
-      *(1),=,324,329,=
-      *(1),=,325,326,=
-      *(1),=,326,328,=
-      *(1),=,328,329,=
-      *(1),2,326,330,=
-      *(1),3,327,393,=
-      *(1),2,328,332,=
-      *(1),6,331,330,312
-      *(1),6,332,331,312

```

CBEAM , 101,6,101,111,501

```

-      *(1),=,113,102,=
-      *(1),=,130,103,=
-      *(1),=,104,132,=

```

CBEAM , 201,6,201,211,501

```

-      *(1),=,213,202,=
-      *(1),=,230,203,=
-      *(1),=,204,232,=

```

CBEAM , 301,6,301,311,501

```

-      *(1),=,313,302,=
-      *(1),=,330,303,=
-      *(1),=,304,332,=

```

GRID, 101,0,-8.75 , 2.88 ,0.0

= ,\*(1),=- , -2.88 ,=

= ,\*(1),=- , 8.75 , 2.88 ,=

= ,\*(1),=- , -2.88 ,=

GRID, 201,1,-8.75 , 2.88 ,0.0

= ,\*(1),=- , -2.88 ,=

= ,\*(1),=- , 8.75 , 2.88 ,=

= ,\*(1),=- , -2.88 ,=

GRID, 301,2,-8.75 , 2.88 ,0.0

= ,\*(1),=- , -2.88 ,=

= ,\*(1),=- , 8.75 , 2.88 ,=

= ,\*(1),=- , -2.88 ,=

GRID, 500,0, 0.0 ,13.0 ,3.0

GRID, 501,0, 0.0 ,13.0 ,0.0

----- 1 ST

GRID, 111,0,-8.75 , 1.44 ,0.0

= ,\*(1),=- , 0.0 ,==

= ,\*(1),=- , -1.44 ,==

= , 130,=- , 8.75 , 1.44 ,==

= ,\*(1),=- , 0.0 ,==

= ,\*(1),=- , -1.44 ,==

= , 114,=- , -1.75 , 4.5 ,0.0

= ,\*(1),=- , 1.44 ,=

= ,\*(1),=- , -2.75 , 0.0 ,=

= ,\*(1),=- , -1.75 , -1.44 ,=

= ,\*(1),=- , -4.5 ,=

= , 125,=- , 1.75 , 4.5 ,=

= ,\*(1),=- , 1.44 ,=

= ,\*(1),=- , 2.75 , 0.0 ,=

= ,\*(1),=- , 1.75 , -1.44 ,=

= ,\*(1),=- , -4.5 ,=

= , 119,=- , 0.0 , 4.5 ,=

= ,\*(1),=- , 1.5 ,=

= ,\*(1),=- , 0.0 ,3.0

= ,\*(1),=- , 0.0 ,0.0

= ,\*(1),=- , -1.5 ,=

= ,\*(1),=- , -4.5 ,=

----- 2 ND

GRID, 211,1,-8.75 , 1.44 ,0.0

= ,\*(1),=- , 0.0 ,==

= ,\*(1),=- , -1.44 ,==

= , 230,=- , 8.75 , 1.44 ,==

= ,\*(1),=- , 0.0 ,==

= ,\*(1),=- , -1.44 ,==

= , 214,=- , -1.75 , 4.5 ,0.0

= ,\*(1),=- , 1.44 ,=

= ,\*(1),=- , -2.75 , 0.0 ,=

= ,\*(1),=- , -1.75 , -1.44 ,=

= ,\*(1),=- , -4.5 ,=

= , 225,=- , 1.75 , 4.5 ,=

= ,\*(1),=- , 1.44 ,=

= ,\*(1),=- , 2.75 , 0.0 ,=

= ,\*(1),=- , 1.75 , -1.44 ,=

= ,\*(1),=- , -4.5 ,=

= , 219,=- , 0.0 , 4.5 ,=

= ,\*(1),=- , 1.5 ,=

= ,\*(1),=- , 0.0 ,3.0

= ,\*(1),=- , 0.0 ,0.0

= ,\*(1),=- , -1.5 ,=

= ,\*(1),=- , -4.5 ,=

----- 3 RD

GRID, 311,2,-8.75 , 1.44 ,0.0

= ,\*(1),=- , 0.0 ,==

= ,\*(1),=- , -1.44 ,==

= , 330,=- , 8.75 , 1.44 ,==

= ,\*(1),=- , 0.0 ,==

= ,\*(1),=- , -1.44 ,==

= , 314,=- , -1.75 , 4.5 ,0.0

= ,\*(1),=- , 1.44 ,=

= ,\*(1),=- , -2.75 , 0.0 ,=

= ,\*(1),=- , -1.75 , -1.44 ,=

= ,\*(1),=- , -4.5 ,=

= , 325,=- , 1.75 , 4.5 ,=

= ,\*(1),=- , 1.44 ,=

= ,\*(1),=- , 2.75 , 0.0 ,=

= ,\*(1),=- , 1.75 , -1.44 ,=

= ,\*(1),=- , -4.5 ,=

= , 319,=- , 0.0 , 4.5 ,=

= ,\*(1),=- , 1.5 ,=

= ,\*(1),=- , 0.0 ,3.0

= ,\*(1),=- , 0.0 ,0.0

= ,\*(1),=- , -1.5 ,=

= ,\*(1),=- , -4.5 ,=

ENDDATA



## APPENDIX IV

### NASTRAN INPUT FILE - - SOLUTION TYPE 30

ID CHO,PSD  
SOL 30  
TIME 9999  
CEND

TITLE= SIRTf TAPERED BLADES -- (FREQ. 0-180)  
SUBTITLE=1 M (Wt=258 LB) -- ALL 12 MODE SHAPES CONSIDERED  
LABEL= DAMPING = 0.004

*Program listing begins double column here*

MPC = 3  
METHOD = 4  
DLOAD = 5  
FREQUENCY = 6  
SDAMP = 7  
RANDOM = 8  
SVECTOR = ALL  
OUTPUT(XY PLOT)  
PLOTTER NAST  
XTITLE=FREQUENCY(HZ)  
X DISPLACEMENT  
XY PLOT DISP PSDF/612 (T1)  
XY PLOT DISP PSDF/613 (T1)  
XY PLOT DISP PSDF/614 (T1)  
XY PLOT DISP PSDF/615 (T1)  
XY PLOT DISP PSDF/616 (T1)  
XY PLOT DISP PSDF/617 (T1)  
XY PLOT DISP PSDF/622 (T1)  
XY PLOT DISP PSDF/623 (T1)  
XY PLOT DISP PSDF/624 (T1)  
XY PLOT DISP PSDF/625 (T1)  
XY PLOT DISP PSDF/626 (T1)  
XY PLOT DISP PSDF/627 (T1)  
XY PLOT DISP PSDF/632 (T1)  
XY PLOT DISP PSDF/633 (T1)  
XY PLOT DISP PSDF/634 (T1)  
XY PLOT DISP PSDF/635 (T1)  
XY PLOT DISP PSDF/636 (T1)  
XY PLOT DISP PSDF/637 (T1)  
Y DISPLACEMENT  
XY PLOT DISP PSDF/712 (T1)  
XY PLOT DISP PSDF/713 (T1)  
XY PLOT DISP PSDF/714 (T1)  
XY PLOT DISP PSDF/715 (T1)  
XY PLOT DISP PSDF/716 (T1)  
XY PLOT DISP PSDF/717 (T1)

XY PLOT DISP PSDF/722 (T1)  
XY PLOT DISP PSDF/723 (T1)  
XY PLOT DISP PSDF/724 (T1)  
XY PLOT DISP PSDF/725 (T1)  
XY PLOT DISP PSDF/726 (T1)  
XY PLOT DISP PSDF/727 (T1)  
XY PLOT DISP PSDF/732 (T1)  
XY PLOT DISP PSDF/733 (T1)  
XY PLOT DISP PSDF/734 (T1)  
XY PLOT DISP PSDF/735 (T1)  
XY PLOT DISP PSDF/736 (T1)  
XY PLOT DISP PSDF/737 (T1)  
Z DISPLACEMENT  
XY PLOT DISP PSDF/812 (T1)  
XY PLOT DISP PSDF/813 (T1)  
XY PLOT DISP PSDF/814 (T1)  
XY PLOT DISP PSDF/815 (T1)  
XY PLOT DISP PSDF/816 (T1)  
XY PLOT DISP PSDF/817 (T1)  
XY PLOT DISP PSDF/822 (T1)  
XY PLOT DISP PSDF/823 (T1)  
XY PLOT DISP PSDF/824 (T1)  
XY PLOT DISP PSDF/825 (T1)  
XY PLOT DISP PSDF/826 (T1)  
XY PLOT DISP PSDF/827 (T1)  
XY PLOT DISP PSDF/832 (T1)  
XY PLOT DISP PSDF/833 (T1)  
XY PLOT DISP PSDF/834 (T1)  
XY PLOT DISP PSDF/835 (T1)  
XY PLOT DISP PSDF/836 (T1)  
XY PLOT DISP PSDF/837 (T1)  
DISPLACEMENT OF CENTER OF  
MIRROR  
XY PLOT DISP PSDF/901 (T1)  
XY PLOT DISP PSDF/902 (T1)  
XY PLOT DISP PSDF/903 (T1)

XYPLOT DISP PSDF/904 (T1)  
XYPLOT DISP PSDF/905 (T1)  
XYPLOT DISP PSDF/906 (T1)

BLADE — MOMENT 1&2, AXIAL

XYPLOT ELFORCE PSDF/113 (4)  
XYPLOT ELFORCE PSDF/114 (4)  
XYPLOT ELFORCE PSDF/191 (4)  
XYPLOT ELFORCE PSDF/115 (4)  
XYPLOT ELFORCE PSDF/132 (4)  
XYPLOT ELFORCE PSDF/194 (4)  
XYPLOT ELFORCE PSDF/133 (4)  
XYPLOT ELFORCE PSDF/134 (4)  
XYPLOT ELFORCE PSDF/113 (5)  
XYPLOT ELFORCE PSDF/114 (5)  
XYPLOT ELFORCE PSDF/191 (5)  
XYPLOT ELFORCE PSDF/115 (5)  
XYPLOT ELFORCE PSDF/132 (5)  
XYPLOT ELFORCE PSDF/194 (5)  
XYPLOT ELFORCE PSDF/133 (5)  
XYPLOT ELFORCE PSDF/134 (5)  
XYPLOT ELFORCE PSDF/113 (8)  
XYPLOT ELFORCE PSDF/114 (8)  
XYPLOT ELFORCE PSDF/191 (8)  
XYPLOT ELFORCE PSDF/115 (8)  
XYPLOT ELFORCE PSDF/132 (8)  
XYPLOT ELFORCE PSDF/194 (8)  
XYPLOT ELFORCE PSDF/133 (8)  
XYPLOT ELFORCE PSDF/134 (8)

2 ND

XYPLOT ELFORCE PSDF/213 (4)  
XYPLOT ELFORCE PSDF/214 (4)  
XYPLOT ELFORCE PSDF/291 (4)  
XYPLOT ELFORCE PSDF/215 (4)  
XYPLOT ELFORCE PSDF/232 (4)  
XYPLOT ELFORCE PSDF/294 (4)  
XYPLOT ELFORCE PSDF/233 (4)  
XYPLOT ELFORCE PSDF/234 (4)  
XYPLOT ELFORCE PSDF/213 (5)  
XYPLOT ELFORCE PSDF/214 (5)  
XYPLOT ELFORCE PSDF/291 (5)  
XYPLOT ELFORCE PSDF/215 (5)  
XYPLOT ELFORCE PSDF/232 (5)  
XYPLOT ELFORCE PSDF/294 (5)  
XYPLOT ELFORCE PSDF/233 (5)  
XYPLOT ELFORCE PSDF/234 (5)  
XYPLOT ELFORCE PSDF/213 (8)  
XYPLOT ELFORCE PSDF/214 (8)  
XYPLOT ELFORCE PSDF/291 (8)  
XYPLOT ELFORCE PSDF/215 (8)  
XYPLOT ELFORCE PSDF/232 (8)  
XYPLOT ELFORCE PSDF/294 (8)

XYPLOT ELFORCE PSDF/233 (8)  
XYPLOT ELFORCE PSDF/234 (8)  
3RD

XYPLOT ELFORCE PSDF/313 (4)  
XYPLOT ELFORCE PSDF/314 (4)  
XYPLOT ELFORCE PSDF/391 (4)  
XYPLOT ELFORCE PSDF/315 (4)  
XYPLOT ELFORCE PSDF/332 (4)  
XYPLOT ELFORCE PSDF/394 (4)  
XYPLOT ELFORCE PSDF/333 (4)  
XYPLOT ELFORCE PSDF/334 (4)  
XYPLOT ELFORCE PSDF/313 (5)  
XYPLOT ELFORCE PSDF/314 (5)  
XYPLOT ELFORCE PSDF/391 (5)  
XYPLOT ELFORCE PSDF/315 (5)  
XYPLOT ELFORCE PSDF/332 (5)  
XYPLOT ELFORCE PSDF/394 (5)  
XYPLOT ELFORCE PSDF/333 (5)  
XYPLOT ELFORCE PSDF/334 (5)  
XYPLOT ELFORCE PSDF/313 (8)  
XYPLOT ELFORCE PSDF/314 (8)  
XYPLOT ELFORCE PSDF/391 (8)  
XYPLOT ELFORCE PSDF/315 (8)  
XYPLOT ELFORCE PSDF/332 (8)  
XYPLOT ELFORCE PSDF/394 (8)  
XYPLOT ELFORCE PSDF/333 (8)  
XYPLOT ELFORCE PSDF/334 (8)

POST — MOMENT 1&2, SHEAR 1&2,  
AXIAL

XYPLOT ELFORCE PSDF/123 (4)  
XYPLOT ELFORCE PSDF/123 (5)  
XYPLOT ELFORCE PSDF/123 (6)  
XYPLOT ELFORCE PSDF/123 (7)  
XYPLOT ELFORCE PSDF/123 (8)  
XYPLOT ELFORCE PSDF/223 (4)  
XYPLOT ELFORCE PSDF/223 (5)  
XYPLOT ELFORCE PSDF/223 (6)  
XYPLOT ELFORCE PSDF/223 (7)  
XYPLOT ELFORCE PSDF/223 (8)  
XYPLOT ELFORCE PSDF/323 (4)  
XYPLOT ELFORCE PSDF/323 (5)  
XYPLOT ELFORCE PSDF/323 (6)  
XYPLOT ELFORCE PSDF/323 (7)  
XYPLOT ELFORCE PSDF/323 (8)  
BEGIN BULK

SPOINT,612,THRU,617  
SPOINT,622,THRU,627  
SPOINT,632,THRU,637  
SPOINT,712,THRU,717  
SPOINT,722,THRU,727

SPOINT,732,THRU,737  
SPOINT,812,THRU,817  
SPOINT,822,THRU,827  
SPOINT,832,THRU,837  
SPOINT,901,THRU,906

— X DISPLACEMENT

MPC,3,612,1,1.0,112,1,-1.0,+,X2  
+X2, .501,1,1.0  
MPC,3,613,1,1.0,119,1,-1.0,+,X3  
+X3, .501,1,1.0  
MPC,3,614,1,1.0,122,1,-1.0,+,X4  
+X4, .501,1,1.0  
MPC,3,615,1,1.0,124,1,-1.0,+,X5  
+X5, .501,1,1.0  
MPC,3,616,1,1.0,131,1,-1.0,+,X6  
+X6, .501,1,1.0  
MPC,3,617,1,1.0,121,1,-1.0,+,X7  
+X7, .501,1,1.0

2 ND

MPC,3,622,1,1.0,212,1,-1.0,+,A2  
+A2, .501,1,1.0  
MPC,3,623,1,1.0,219,1,-1.0,+,A3  
+A3, .501,1,1.0  
MPC,3,624,1,1.0,222,1,-1.0,+,A4  
+A4, .501,1,1.0  
MPC,3,625,1,1.0,224,1,-1.0,+,A5  
+A5, .501,1,1.0  
MPC,3,626,1,1.0,231,1,-1.0,+,A6  
+A6, .501,1,1.0  
MPC,3,627,1,1.0,221,1,-1.0,+,A7  
+A7, .501,1,1.0

3 RD

MPC,3,632,1,1.0,312,1,-1.0,+,B2  
+B2, .501,1,1.0  
MPC,3,633,1,1.0,319,1,-1.0,+,B3  
+B3, .501,1,1.0  
MPC,3,634,1,1.0,322,1,-1.0,+,B4  
+B4, .501,1,1.0  
MPC,3,635,1,1.0,324,1,-1.0,+,B5  
+B5, .501,1,1.0  
MPC,3,636,1,1.0,331,1,-1.0,+,B6  
+B6, .501,1,1.0  
MPC,3,637,1,1.0,321,1,-1.0,+,B7  
+B7, .501,1,1.0

— Y DISPLACEMENT

MPC,3,712,1,1.0,112,2,-1.0,+,Y2  
+Y2, .501,2,1.0  
MPC,3,713,1,1.0,119,2,-1.0,+,Y3  
+Y3, .501,2,1.0  
MPC,3,714,1,1.0,122,2,-1.0,+,Y4  
+Y4, .501,2,1.0

MPC,3,715,1,1.0,124,2,-1.0,+,Y5  
+Y5, .501,2,1.0  
MPC,3,716,1,1.0,131,2,-1.0,+,Y6  
+Y6, .501,2,1.0  
MPC,3,717,1,1.0,121,2,-1.0,+,Y7  
+Y7, .501,2,1.0

2ND

MPC,3,722,1,1.0,212,2,-1.0,+,C2  
+C2, .501,2,1.0  
MPC,3,723,1,1.0,219,2,-1.0,+,C3  
+C3, .501,2,1.0  
MPC,3,724,1,1.0,222,2,-1.0,+,C4  
+C4, .501,2,1.0  
MPC,3,725,1,1.0,224,2,-1.0,+,C5  
+C5, .501,2,1.0  
MPC,3,726,1,1.0,231,2,-1.0,+,C6  
+C6, .501,2,1.0  
MPC,3,727,1,1.0,221,2,-1.0,+,C7  
+C7, .501,2,1.0

3 RD

MPC,3,732,1,1.0,312,2,-1.0,+,D2  
+D2, .501,2,1.0  
MPC,3,733,1,1.0,319,2,-1.0,+,D3  
+D3, .501,2,1.0  
MPC,3,734,1,1.0,322,2,-1.0,+,D4  
+D4, .501,2,1.0  
MPC,3,735,1,1.0,324,2,-1.0,+,D5  
+D5, .501,2,1.0  
MPC,3,736,1,1.0,331,2,-1.0,+,D6  
+D6, .501,2,1.0  
MPC,3,737,1,1.0,321,2,-1.0,+,D7  
+D7, .501,2,1.0

— Z DISPLACEMENT

MPC,3,812,1,1.0,112,3,-1.0,+,Z2  
+Z2, .501,3,1.0  
MPC,3,813,1,1.0,119,3,-1.0,+,Z3  
+Z3, .501,3,1.0  
MPC,3,814,1,1.0,122,3,-1.0,+,Z4  
+Z4, .501,3,1.0  
MPC,3,815,1,1.0,124,3,-1.0,+,Z5  
+Z5, .501,3,1.0  
MPC,3,816,1,1.0,131,3,-1.0,+,Z6  
+Z6, .501,3,1.0  
MPC,3,817,1,1.0,121,3,-1.0,+,Z7  
+Z7, .501,3,1.0

2 ND

MPC,3,822,1,1.0,212,3,-1.0,+,E2  
+E2, .501,3,1.0  
MPC,3,823,1,1.0,219,3,-1.0,+,E3  
+E3, .501,3,1.0  
MPC,3,824,1,1.0,222,3,-1.0,+,E4  
+E4, .501,3,1.0

MPC,3,825,1,1.0,224,3,-1.0.,+E5  
 +E5, .501,3,1.0  
 MPC,3,826,1,1.0,231,3,-1.0.,+E6  
 +E6, .501,3,1.0  
 MPC,3,827,1,1.0,221,3,-1.0.,+E7  
 +E7, .501,3,1.0  
 3 RD  
 MPC,3,832,1,1.0,312,3,-1.0.,+F2  
 +F2, .501,3,1.0  
 MPC,3,833,1,1.0,319,3,-1.0.,+F3  
 +F3, .501,3,1.0  
 MPC,3,834,1,1.0,322,3,-1.0.,+F4  
 +F4, .501,3,1.0  
 MPC,3,835,1,1.0,324,3,-1.0.,+F5  
 +F5, .501,3,1.0  
 MPC,3,836,1,1.0,331,3,-1.0.,+F6  
 +F6, .501,3,1.0  
 MPC,3,837,1,1.0,321,3,-1.0.,+F7  
 +F7, .501,3,1.0  
 DISPLACEMENTS OF CENTER OF  
 MIRROR  
 MPC,3,901,1,1.0,500,1,-1.0.,+G1  
 +G1, .501,1,1.0  
 MPC,3,902,1,1.0,500,2,-1.0.,+G2  
 +G2, .501,2,1.0  
 MPC,3,903,1,1.0,500,3,-1.0.,+G3  
 +G3, .501,3,1.0  
 MPC,3,904,1,1.0,500,4,-1.0.,+G4  
 +G4, .501,4,1.0  
 MPC,3,905,1,1.0,500,5,-1.0.,+G5  
 +G5, .501,5,1.0  
 MPC,3,906,1,1.0,500,6,-1.0.,+G6  
 +G6, .501,6,1.0  
  
 RLOAD1,5,24,..60  
 DAREA,24,501,1,1.+6  
 DAREA,24,501,2,=  
 DAREA,24,501,3,=  
 TABLED1,60,.....+TD1  
 +TD1,0.,1.0,2000.,1.0,ENDT  
  
 FREQ1,6,60.0,0.3,400  
 FREQ,  
 6,68.7224,68.7303,73.4666,80.4452,80.5297,80  
 .7655,80.8417,+FRQ  
 +FRQ,129.3772,129.4017,174.8084  
  
 TABDMP1,7,CRIT,.....+CD1  
 +CD1,1,0,0.004,1000.,0.004,ENDT  
  
 RANDPS,8,1,1,149305,..77

0.02 PSD W/6 DB-OCT  
  
 TABRND1,77,.....+T771  
 +T771, .25., 0.020,250.,  
 0.020,260.,1.850-2,280.,1.596-2,+T772  
 +T772,300.,1.391-2,320.,1.223-2,340.,1.084-3,  
 360.,9.669-3,+T773  
 +T773,380.,8.681-3,400.,7.838-3,420.,7.111-3,  
 440.,6.482-3,+T774  
 +T774,460.,5.932-3,480.,5.450-3,500.,5.024-3,  
 520.,4.646-3,+T775  
 +T775,540.,4.309-3,560.,4.008-3,580.,3.737-3,  
 600.,3.493-3,+T776  
 +T776,ENDT  
  
 EIGR,4,MGIV,10.0,300.0,.....+EIG1  
 +EIG1,MAX  
  
 SUPORT,501,123456  
 CMASS2,333,1,+6 .501,1  
 = .334,= ., .2  
 = .335,= ., .3  
 CMASS2,336,1,+8 .501,4  
 = .337,= ., .5  
 = .338,= ., .6  
  
 CONM2, 111, 101,0,1.0-7  
 = .\*(1),\*(1),0,1.0-7  
 =(2)  
 CONM2, 121, 191,0,1.0-7  
 = .\*(1),\*(1),0,1.0-7  
 =(2)  
 2 ND  
 CONM2, 211, 201,0,1.0-7  
 = .\*(1),\*(1),0,1.0-7  
 =(2)  
 CONM2, 221, 291,0,1.0-7  
 = .\*(1),\*(1),0,1.0-7  
 =(2)  
 3 RD  
 CONM2, 311, 301,0,1.0-7  
 = .\*(1),\*(1),0,1.0-7  
 =(2)  
 CONM2, 321, 391,0,1.0-7  
 = .\*(1),\*(1),0,1.0-7  
 =(2)  
 CONM2,101,500,0,0.668,.....+CONM2  
 +CONM2,57.4761,..57.4761,..114.0531  
 RBE2,901,501,123456,116,127,216,227,316,+R  
 BE  
 +RBE,327

# INPUT DATA

```
CORD2R,1,0,11.26,19.50,0.0,11.26,19.5,1.0,+
RD1
+RD1,0.0,39.0,0.0
CORD2R,2,0,-11.26,19.5,0.0,-11.26,19.5,1.0,+
RD2
+RD2,-15.01,13.0,0.0
```

```
PBEAM ,1,1,1.500,.0703,.5000,0.0,.2813
- ,2,1, .280,4.6-4,.0933,0.0,.0018
- ,3,1, .387,.0010,.1491,0.0,.0042
- ,4,1, .441,.0012,.2206,0.0,.0048
- ,5,1, .414,.0011,.1825,0.0,.0045
- ,6,1,1.838,.0861,.9191,0.0,.3445
- ,7,1, .850,.4280,.0950,0.0,.0087
- ,9,1,7.069,3.976,3.976,0.0,7.952
MAT1,1,18.0+6,..3
```

```
CBEAM ,191,4,112,191,501
CBEAM ,192,5,191,192,501
CBEAM ,193,5,193,194,501
CBEAM ,194,4,194,131,501
CBEAM ,291,4,212,291,501
CBEAM ,292,5,291,292,501
CBEAM ,293,5,293,294,501
CBEAM ,294,4,294,231,501
CBEAM ,391,4,312,391,501
CBEAM ,392,5,391,392,501
CBEAM ,393,5,393,394,501
CBEAM ,394,4,394,331,501
GRID ,191,0,-6.75,0.0,0.0
GRID ,192,0,-4.75,0.0,0.0
GRID ,193,0, 4.75,0.0,0.0
GRID ,194,0, 6.75,0.0,0.0
GRID ,291,1,-6.75,0.0,0.0
GRID ,292,1,-4.75,0.0,0.0
GRID ,293,1, 4.75,0.0,0.0
GRID ,294,1, 6.75,0.0,0.0
GRID ,391,2,-6.75,0.0,0.0
GRID ,392,2,-4.75,0.0,0.0
GRID ,393,2, 4.75,0.0,0.0
GRID ,394,2, 6.75,0.0,0.0
```

```
----- 1 ST
CMASS2,1111,21.0-4,111,3
- ,*(1),= ,113,3
- ,*(1),= ,130,3
- ,*(1),= ,132,3
- ,*(1),22.0-4,112,3
- ,*(1),= ,131,3
- ,*(1),16.8-4,114,3
- ,*(1),= ,118,3
```

```
- ,*(1),= ,125,3
- ,*(1),= ,129,3
- ,*(1),27.6-4,115,3
- ,*(1),= ,117,3
- ,*(1),= ,126,3
- ,*(1),= ,128,3
- ,*(1),18.2-4,119,3
- ,*(1),= ,124,3
- ,*(1),5.94-4,120,3
- ,*(1),= ,123,3
- ,*(1),18.3-3,122,3
- ,*(1),5.60-4,116,3
- ,*(1),= ,127,3
```

## 2 ND

```
CMASS2,2111,21.0-4,211,3
- ,*(1),= ,213,3
- ,*(1),= ,230,3
- ,*(1),= ,232,3
- ,*(1),22.0-4,212,3
- ,*(1),= ,231,3
- ,*(1),16.8-4,214,3
- ,*(1),= ,218,3
- ,*(1),= ,225,3
- ,*(1),= ,229,3
- ,*(1),27.6-4,215,3
- ,*(1),= ,217,3
- ,*(1),= ,226,3
- ,*(1),= ,228,3
- ,*(1),18.2-4,219,3
- ,*(1),= ,224,3
- ,*(1),5.94-4,220,3
- ,*(1),= ,223,3
- ,*(1),18.3-3,222,3
- ,*(1),5.60-4,216,3
- ,*(1),= ,227,3
```

## 3 RD

```
CMASS2,3111,21.0-4,311,3
- ,*(1),= ,313,3
- ,*(1),= ,330,3
- ,*(1),= ,332,3
- ,*(1),22.0-4,312,3
- ,*(1),= ,331,3
- ,*(1),16.8-4,314,3
- ,*(1),= ,318,3
- ,*(1),= ,325,3
- ,*(1),= ,329,3
- ,*(1),27.6-4,315,3
- ,*(1),= ,317,3
- ,*(1),= ,326,3
- ,*(1),= ,328,3
- ,*(1),18.2-4,319,3
- ,*(1),= ,324,3
```

- \*(1),5.94-4,320,3  
 - \*(1),= ,323,3  
 - \*(1),18.3-3,322,3  
 - \*(1),5.60-4,316,3  
 - \*(1),= ,327,3

----- 2-1  
 CMASS2,1211,21.0-4,111,2

- \*(1),= ,113,2  
 - \*(1),= ,130,2  
 - \*(1),= ,132,2  
 - \*(1),22.0-4,112,2  
 - \*(1),= ,131,2  
 - \*(1),16.8-4,114,2  
 - \*(1),= ,118,2  
 - \*(1),= ,125,2  
 - \*(1),= ,129,2  
 - \*(1),27.6-4,115,2  
 - \*(1),= ,117,2  
 - \*(1),= ,126,2  
 - \*(1),= ,128,2  
 - \*(1),18.2-4,119,2  
 - \*(1),= ,124,2  
 - \*(1),5.94-4,120,2  
 - \*(1),= ,123,2  
 - \*(1),18.3-3,122,2  
 - \*(1),5.60-4,116,2  
 - \*(1),= ,127,2

----- 2 ND  
 CMASS2,2211,21.0-4,211,2

- \*(1),= ,213,2  
 - \*(1),= ,230,2  
 - \*(1),= ,232,2  
 - \*(1),22.0-4,212,2  
 - \*(1),= ,231,2  
 - \*(1),16.8-4,214,2  
 - \*(1),= ,218,2  
 - \*(1),= ,225,2  
 - \*(1),= ,229,2  
 - \*(1),27.6-4,215,2  
 - \*(1),= ,217,2  
 - \*(1),= ,226,2  
 - \*(1),= ,228,2  
 - \*(1),18.2-4,219,2  
 - \*(1),= ,224,2  
 - \*(1),5.94-4,220,2  
 - \*(1),= ,223,2  
 - \*(1),18.3-3,222,2  
 - \*(1),5.60-4,216,2  
 - \*(1),= ,227,2

----- 3 RD  
 CMASS2,3211,21.0-4,311,2

- \*(1),= ,313,2

- \*(1),= ,330,2  
 - \*(1),= ,332,2  
 - \*(1),22.0-4,312,2  
 - \*(1),= ,331,2  
 - \*(1),16.8-4,314,2  
 - \*(1),= ,318,2  
 - \*(1),= ,325,2  
 - \*(1),= ,329,2  
 - \*(1),27.6-4,315,2  
 - \*(1),= ,317,2  
 - \*(1),= ,326,2  
 - \*(1),= ,328,2  
 - \*(1),18.2-4,319,2  
 - \*(1),= ,324,2  
 - \*(1),5.94-4,320,2  
 - \*(1),= ,323,2  
 - \*(1),18.3-3,322,2  
 - \*(1),5.60-4,316,2  
 - \*(1),= ,327,2

----- 3-1  
 CMASS2,1311,21.0-4,111,1

- \*(1),= ,113,1  
 - \*(1),= ,130,1  
 - \*(1),= ,132,1  
 - \*(1),22.0-4,112,1  
 - \*(1),= ,131,1  
 - \*(1),16.8-4,114,1  
 - \*(1),= ,118,1  
 - \*(1),= ,125,1  
 - \*(1),= ,129,1  
 - \*(1),27.6-4,115,1  
 - \*(1),= ,117,1  
 - \*(1),= ,126,1  
 - \*(1),= ,128,1  
 - \*(1),18.2-4,119,1  
 - \*(1),= ,124,1  
 - \*(1),5.94-4,120,1  
 - \*(1),= ,123,1  
 - \*(1),18.3-3,122,1  
 - \*(1),5.60-4,116,1  
 - \*(1),= ,127,1

----- 2 ND  
 CMASS2,2311,21.0-4,211,1

- \*(1),= ,213,1  
 - \*(1),= ,230,1  
 - \*(1),= ,232,1  
 - \*(1),22.0-4,212,1  
 - \*(1),= ,231,1  
 - \*(1),16.8-4,214,1  
 - \*(1),= ,218,1  
 - \*(1),= ,225,1  
 - \*(1),= ,229,1

```

-      *(1),27.6-4,215,1
-      *(1),=      ,217,1
-      *(1),=      ,226,1
-      *(1),=      ,228,1
-      *(1),18.2-4,219,1
-      *(1),=      ,224,1
-      *(1),5.94-4,220,1
-      *(1),=      ,223,1
-      *(1),18.3-3,222,1
-      *(1),5.60-4,216,1
-      *(1),=      ,227,1

```

```

----- 3 RD
CMASS2,3311,21.0-4,311,1

```

```

-      *(1),=      ,313,1
-      *(1),=      ,330,1
-      *(1),=      ,332,1
-      *(1),22.0-4,312,1
-      *(1),=      ,331,1
-      *(1),16.8-4,314,1
-      *(1),=      ,318,1
-      *(1),=      ,325,1
-      *(1),=      ,329,1
-      *(1),27.6-4,315,1
-      *(1),=      ,317,1
-      *(1),=      ,326,1
-      *(1),=      ,328,1
-      *(1),18.2-4,319,1
-      *(1),=      ,324,1
-      *(1),5.94-4,320,1
-      *(1),=      ,323,1
-      *(1),18.3-3,322,1
-      *(1),5.60-4,316,1
-      *(1),=      ,327,1

```

```

PARAM,AUTOSPC,YES

```

```

RBAR, 112,120,122,123456,,,123456
RBAR, 114,122,123,123456,,,123456
RBAR, 212,220,222,123456,,,123456
RBAR, 214,222,223,123456,,,123456
RBAR, 312,320,322,123456,,,123456
RBAR, 314,322,323,123456,,,123456
RBAR, 101,500,121,123456,,,123456
RBAR, 102,500,221,123456,,,123456
RBAR, 103,500,321,123456,,,123456

```

```

PLOTTEL,5001,500,121
PLOTTEL,5002,500,221
PLOTTEL,5003,500,321

```

```

----- 1ST
CBEAM , 111,6,111,112,501

```

```

-      *(1),6,112,113,=
-      *(1),2,111,115,=
-      *(1),3,192,116,=

```

```

-      *(1),2,113,117,=
-      *(1),1,114,115,=
-      *(1),=,115,117,=
-      *(1),=,117,118,=
-      *(1),=,114,119,=
-      *(1),=,119,125,=
-      *(1),7,119,120,131
-      , 123,9,121,122,501
-      , 125,7,123,124,131
-      , 127,1,118,124,501
-      *(1),=,124,129,=
-      *(1),=,125,126,=
-      *(1),=,126,128,=
-      *(1),=,128,129,=
-      *(1),2,126,130,=
-      *(1),3,127,193,=
-      *(1),2,128,132,=
-      *(1),6,131,130,112
-      *(1),6,132,131,112

```

```

----- 2 ND
CBEAM , 211,6,211,212,501

```

```

-      *(1),6,212,213,=
-      *(1),2,211,215,=
-      *(1),3,292,216,=
-      *(1),2,213,217,=
-      *(1),1,214,215,=
-      *(1),=,215,217,=
-      *(1),=,217,218,=
-      *(1),=,214,219,=
-      *(1),=,219,225,=
-      *(1),7,219,220,231
-      , 223,9,221,222,501
-      , 225,7,223,224,231
-      , 227,1,218,224,501
-      *(1),=,224,229,=
-      *(1),=,225,226,=
-      *(1),=,226,228,=
-      *(1),=,228,229,=
-      *(1),2,226,230,=
-      *(1),3,227,293,=
-      *(1),2,228,232,=
-      *(1),6,231,230,212
-      *(1),6,232,231,212

```

```

----- 3 RD
CBEAM , 311,6,311,312,501

```

```

-      *(1),6,312,313,=
-      *(1),2,311,315,=
-      *(1),3,392,316,=
-      *(1),2,313,317,=
-      *(1),1,314,315,=
-      *(1),=,315,317,=
-      *(1),=,317,318,=

```

```

-   ,(1),-,314,319,-
-   ,(1),-,319,325,-
-   ,(1),7,319,320,331
-   , 323,9,321,322,501
-   , 325,7,323,324,331
-   , 327,1,318,324,501
-   ,(1),-,324,329,-
-   ,(1),-,325,326,-
-   ,(1),-,326,328,-
-   ,(1),-,328,329,-
-   ,(1),2,326,330,-
-   ,(1),3,327,393,-
-   ,(1),2,328,332,-
-   ,(1),6,331,330,312
-   ,(1),6,332,331,312
CBEAM , 101,6,101,111,501
-   ,(1),-,113,102,-
-   ,(1),-,130,103,-
-   ,(1),-,104,132,-
CBEAM , 201,6,201,211,501
-   ,(1),-,213,202,-
-   ,(1),-,230,203,-
-   ,(1),-,204,232,-
CBEAM , 301,6,301,311,501
-   ,(1),-,313,302,-
-   ,(1),-,330,303,-
-   ,(1),-,304,332,-

```

GRID, 101,0,-8.75 , 2.88 ,0.0

```

-   ,(1),-, -, -2.88 , -
-   ,(1),-, 8.75 , 2.88 , -
-   ,(1),-, -, -2.88 , -

```

GRID, 201,1,-8.75 , 2.88 ,0.0

```

-   ,(1),-, -, -2.88 , -
-   ,(1),-, 8.75 , 2.88 , -
-   ,(1),-, -, -2.88 , -

```

GRID, 301,2,-8.75 , 2.88 ,0.0

```

-   ,(1),-, -, -2.88 , -
-   ,(1),-, 8.75 , 2.88 , -
-   ,(1),-, -, -2.88 , -

```

GRID, 500,0, 0.0 ,13.0 ,3.0

GRID, 501,0, 0.0 ,13.0 ,0.0

----- 1 ST

GRID, 111,0,-8.75 , 1.44 ,0.0

```

-   ,(1),-, -, 0.0 , -
-   ,(1),-, -, -1.44 , -
-   , 130,-, 8.75 , 1.44 , -
-   ,(1),-, -, 0.0 , -
-   ,(1),-, -, -1.44 , -
-   , 114,-, -1.75 , 4.5 ,0.0
-   ,(1),-, -, 1.44 , -
-   ,(1),-, -2.75 , 0.0 , -

```

```

-   ,(1),-, -1.75 , -1.44 , -
-   ,(1),-, -, -4.5 , -
-   , 125,-, 1.75 , 4.5 , -
-   ,(1),-, -, 1.44 , -
-   ,(1),-, 2.75 , 0.0 , -
-   ,(1),-, 1.75 , -1.44 , -
-   ,(1),-, -, -4.5 , -
-   , 119,-, 0.0 , 4.5 , -
-   ,(1),-, -, 1.5 , -
-   ,(1),-, -, 0.0 ,3.0
-   ,(1),-, -, 0.0 ,0.0
-   ,(1),-, -, -1.5 , -
-   ,(1),-, -, -4.5 , -

```

----- 2 ND

GRID, 211,1,-8.75 , 1.44 ,0.0

```

-   ,(1),-, -, 0.0 , -
-   ,(1),-, -, -1.44 , -
-   , 230,-, 8.75 , 1.44 , -
-   ,(1),-, -, 0.0 , -
-   ,(1),-, -, -1.44 , -
-   , 214,-, -1.75 , 4.5 ,0.0
-   ,(1),-, -, 1.44 , -
-   ,(1),-, -2.75 , 0.0 , -
-   ,(1),-, -1.75 , -1.44 , -
-   ,(1),-, -, -4.5 , -
-   , 225,-, 1.75 , 4.5 , -
-   ,(1),-, -, 1.44 , -
-   ,(1),-, 2.75 , 0.0 , -
-   ,(1),-, 1.75 , -1.44 , -
-   ,(1),-, -, -4.5 , -
-   , 219,-, 0.0 , 4.5 , -
-   ,(1),-, -, 1.5 , -
-   ,(1),-, -, 0.0 ,3.0
-   ,(1),-, -, 0.0 ,0.0
-   ,(1),-, -, -1.5 , -
-   ,(1),-, -, -4.5 , -

```

----- 3 RD

GRID, 311,2,-8.75 , 1.44 ,0.0

```

-   ,(1),-, -, 0.0 , -
-   ,(1),-, -, -1.44 , -
-   , 330,-, 8.75 , 1.44 , -
-   ,(1),-, -, 0.0 , -
-   ,(1),-, -, -1.44 , -
-   , 314,-, -1.75 , 4.5 ,0.0
-   ,(1),-, -, 1.44 , -
-   ,(1),-, -2.75 , 0.0 , -
-   ,(1),-, -1.75 , -1.44 , -
-   ,(1),-, -, -4.5 , -
-   , 325,-, 1.75 , 4.5 , -
-   ,(1),-, -, 1.44 , -
-   ,(1),-, 2.75 , 0.0 , -
-   ,(1),-, 1.75 , -1.44 , -

```



```

- ,*(1),-,- , -4.5 ,=-
- , 319,-, 0.0 , 4.5 ,=-
- ,*(1),-,- , 1.5 ,=-
- ,*(1),-,- , 0.0 ,3.0
- ,*(1),-,- , 0.0 ,0.0
- ,*(1),-,- , -1.5 ,=-
- ,*(1),-,- , -4.5 ,=-
ENDDATA

```

# APPENDIX V

## NASTRAN INPUT FILE - - SOLUTION TYPE 5, BUCKLING

```

ID SIRTF,RANDOM
SOL 5
TIME 4
ALTER 24,25
TA1,,ECT,EPT,BGPD,T,SIL,GPTT,CSTM,/EST,,GEI,GPECT,/
      S,N,LUSET/C,N,123/S,N,NOSIMP/1/S,N,NOGENL/
      S,N,GENEL
CHKPNT EST,GEI,GPECT
SETVAL // V,N,NOKGGX / 1
SETVAL // V,N,NOMGG / 1
ALTER 27,34
EMG EST,CSTM,MPT,DIT,GEOM2.../
      KELM,KDICT,MELM,MDICT,,/S,N,NOKGGX/S,N,NOMGG/
      0///C,Y,COUPMASS/////////V,Y,K6ROT=0.0
CHKPNT KELM,KDICT,MELM,MDICT
EMA GPECT,KDICT,KELM,BGPD,T,SIL,CSTM/KGGX,GPST
CHKPNT KGGX,GPST
COND LBL1,SKPMGG
COND JPMGG,NOMGG
EMA GPECT,MDICT,MELM,BGPD,T,SIL,CSTM/MGG,/C,N,-1/
      V,Y,WTMASS = 1.0
CHKPNT MGG
LABEL JPMGG
ALTER 48,49
GP4 CASECC,GEOM4,EQEXIN,SIL,GPDT,BGPD,T,CSTM/
      RG,YSB,USBTB,ASET/LUSET/S,N,MPCF1/S,N,MPCF2/
      S,N,SINGLE/S,N,OMIT/S,N,REACT/S,N,NSKIP/
      S,N,REPEAT/S,N,NOSET/S,N,NOL/S,N,NOA/C,Y,SUBID
GPSP1 KGG,RG,USBTB,SIL,GPL,YSB/USBT,YS/S,N,SINGLE/
      C,Y,AUTOSPC=NO/C,Y,PRGPST=YES/C,Y,SPCGEN=0/
      C,Y,EPZERO=1.E-8/0/S,N,SING/C,Y,EPPRT=1.E-8
PARAML USBT//USBT/////
      C,N,A/V,N,NOASET/
      C,N,G/V,N,NOGSET/
      C,N,L/V,N,NOLSET/
      C,N,O/V,N,OMIT/
      C,N,S/V,N,SINGLE/
      C,N,R/V,N,REACT
PARAM //C,N,EQ/NOA/NOGSET/NOASET
PARAM //C,N,AND/NOSET/NOA/REACT
COND NOPRUST,USBTPT
TABPRT USBT,EQEXIN//USBT/V,Y,USBTPT--1/V,Y,USBTSEL
LABEL NOPRUST
ALTER 59,61
ALTER 102
GPFDR CASECC,UGV,KELM,KDICT,ECT,EQEXIN,GPECT,PG .

```

```

      QG,BGPDT,SIL,CSTM,/ONRGY1,OGPFB1/BKL0/C,Y,TINY
OFF   ONRGY1,OGPFB1//S,N,CARDNO
ALTER 103,107
COND  P2,JUMPPLOT
PLOT  PLTPAR,GPSETS,ELSETS,CASECC,BGPDT,EQEXIN,SIL,
      PUGV1,,GPECT,OES1/PLOTX2/V,N,NSIL/V,N,LUSET/
      V,N,JUMPPLOT/V,N,PLTFLG/S,N,PFILE
PRTMSG PLOTX2 //
LABEL P2
ALTER 108,109
PARAML CASECC//DTI/1/7//V,N,TSET
PARAML CASECC//DTI/1/6//V,N,DEFSET
EMG   EST,CSTM,MPT,DIT,,UGV,GPTT,EDT/KDELM,KDDICT,..../
      1/0/0///V,N,TSET/V,N,DEFSET/////////K6ROT
CHKPNT KDELM,KDDICT
EMA   GPECT,KDDICT,KDELM,BGPDT,SIL,CSTM/KDGG,-1
CHKPNT KDGG
ALTER 145,149
COND  P3,JUMPPLOT
PLOT  PLTPAR,GPSETS,ELSETS,CASECC,BGPDT,EQEXIN,SIL,,
      PPHIG ,GPECT,OBES1/PLOTX3/V,N,NSIL/V,N,LUSET/
      V,N,JUMPPLOT/V,N,PLTFLG/S,N,PFILE
PRTMSG PLOTX3 //
LABEL P3
      END OF RF ALTER 5$33
CEND
TITLE- SIRTF ONE METER GIMBAL ASSEMBLY
SPC-23
SPCFORCE - ALL
SUBCASE 1
SUBTITLE - STATIC SOLUTION (X-DIRECTION)
LOAD-1
DISPLACEMENT - ALL
SUBCASE 2
SUBTITLE - EIGENSOLUTION (X-DIRECTION)
METHOD-1
DISPLACEMENT - ALL
OUTPUT(PLOT)
PLOTTER NAST
SET 1 - ALL
FIND SCALE, ORIGIN 1, SET 1
UNDEFORMED MESH
PLOT,SET 1,ORIGIN 1
DEFORMED MESH
MAXIMUM DEFORMATION .5
DEFORMED BUCKLED MESH
PLOT MODAL DEFORMATION 0,2,4,6,SET 1,ORIGIN 1
AXES Y,Z,X
VIEW 0.,0.,0.
FIND SCALE,ORIGIN 2,SET 1
PLOT SET 1, ORIGIN 2
PLOT MODAL DEFORMATION 0,2,4,6,SET 1,ORIGIN 2

```

```

AXES Z,X,Y
VIEW 0.,0.,0.
FIND SCALE,ORIGIN 3,SET 1
PLOT SET 1, ORIGIN 3
PLOT MODAL DEFORMATION 0,2,4,6,SET 1,ORIGIN 3
AXES X,Y,Z
VIEW 0.,0.,0.
FIND SCALE,ORIGIN 4,SET 1
PLOT SET 1, ORIGIN 4
PLOT MODAL DEFORMATION 0,2,4,6,SET 1,ORIGIN 4
BEGIN BULK

```

*Program listing begins double column here*

```

PBEAM ,1,1,10.0 ,4.0 ,4.0 ,0.0,10.0
- ,2,1, 1.75,0.25,0.07031,0.0, 0.2813
- ,3,1, 7.06,3.97,3.97 ,0.0, 7.95
PSHELL,1,1,0.13,1
- ,2,-,0.19,-
- ,3,-,0.75,-
- ,4,-,1.50,-
MAT1,1,18.0+6...3
SPC1,23 ,123456,126,135
SPC1,23 ,456 ,216

```

```

FORCE,1,216,0,1.0,1.0,0.0,0.0

```

```

EIGB,1,INV,0.,10000.,3,3,0.,+EIGB1
+EIGB1,MAX
PARAM,AUTOSPC,YES

```

```

GRID, 1 ,0,-8.75, 2.88, 1.5
- , *(3),-,- ,*(-1.44),==
-(3)
GRID, 2 ,0,-8.75, 2.88, 0.75
- , *(3),-,- ,*(-1.44),==
-(3)
GRID, 3 ,0,-8.75, 2.88, 0.0
- , *(3),-,- ,*(-1.44),==
-(3)
GRID, 16 ,0, 8.75, 2.88, 1.5
- , *(3),-,- ,*(-1.44),==
-(3)
GRID, 17 ,0, 8.75, 2.88, 0.75
- , *(3),-,- ,*(-1.44),==
-(3)
GRID, 18 ,0, 8.75, 2.88, 0.0
- , *(3),-,- ,*(-1.44),==
-(3)
GRID, 31 ,0, -7.75, 1.44, 1.5
- , *(18),-,- ,*(1.0),==
-(5)
GRID, 32 ,0, -7.75, 1.44, 0.75

```

```

- , *(18),-,- ,*(1.0),==
-(5)
GRID, 33 ,0, -7.75, 1.44, 0.0
- , *(18),-,- ,*(1.0),==
-(5)
GRID, 37 ,0, -7.75, -1.44, 1.5
- , *(18),-,- ,*(1.0),==
-(4)
GRID, 38 ,0, -7.75, -1.44, 0.75
- , *(18),-,- ,*(1.0),==
-(4)
GRID, 39 ,0, -7.75, -1.44, 0.0
- , *(18),-,- ,*(1.0),==
-(4)
GRID, 40 ,0, 7.75, 1.44, 1.5
- , *(18),-,- ,*(-1.0),==
-(4)
GRID, 41 ,0, 7.75, 1.44, 0.75
- , *(18),-,- ,*(-1.0),==
-(4)
GRID, 42 ,0, 7.75, 1.44, 0.0
- , *(18),-,- ,*(-1.0),==
-(4)
GRID, 46 ,0, 7.75, -1.44, 1.5
- , *(18),-,- ,*(-1.0),==
-(4)
GRID, 47 ,0, 7.75, -1.44, 0.75
- , *(18),-,- ,*(-1.0),==
-(4)
GRID, 48 ,0, 7.75, -1.44, 0.0
- , *(18),-,- ,*(-1.0),==
-(4)
GRID, 34 ,0, -7.75 , 0.00, 1.5
- , *(18),-,- ,*(1.0),==
-(4)
GRID, 35 ,0, -7.75, 0.00, 0.75
- , *(18),-,- ,*(1.0),==
-(4)
GRID, 36 ,0, -7.75, 0.00, 0.0

```

```

- , *(18),-, *(1.0),=-
-(4)
GRID, 43 ,0, 7.75, 0.00, 1.5
- , *(18),-,*(-1.0),=-
-(4)
GRID, 44 ,0, 7.75, 0.00, 0.75
- , *(18),-,*(-1.0),=-
-(4)
GRID, 45 ,0, 7.75, 0.00, 0.0
- , *(18),-,*(-1.0),=-
-(4)
GRID, 142 ,0, -1.75, -1.44, 1.5
- , *(1) ,-,= , 0.75
- , *(1) ,-,= , 0.0
GRID, 145 ,0, 1.75, 1.44, 1.5
- , *(1) ,-,= , 0.75
- , *(1) ,-,= , 0.0
GRID, 148 ,0, 1.75, -1.44, 1.5
- , *(1) ,-,= , 0.75
- , *(1) ,-,= , 0.0
GRID, 151 ,0, -1.75, 3.0 , 1.5
- , *(1) ,-,= , 0.75
- , *(1) ,-,= , 0.00
GRID, 154 ,0, -1.75, -3.0 , 1.5
- , *(1) ,-,= , 0.75
- , *(1) ,-,= , 0.00
GRID, 157 ,0, 1.75, 3.0 , 1.5
- , *(1) ,-,= , 0.75
- , *(1) ,-,= , 0.00
GRID, 160 ,0, 1.75, -3.0 , 1.5
- , *(1) ,-,= , 0.75
- , *(1) ,-,= , 0.00
GRID, 163 ,0, -1.75, 4.5 , 1.5
- , *(1) ,-,= , 0.75
- , *(1) ,-,= , 0.00
GRID, 166 ,0, -1.75, -4.5 , 1.5
- , *(1) ,-,= , 0.75
- , *(1) ,-,= , 0.00
GRID, 169 ,0, 1.75, 4.5 , 1.5
- , *(1) ,-,= , 0.75
- , *(1) ,-,= , 0.00
GRID, 172 ,0, 1.75, -4.5 , 1.5
- , *(1) ,-,= , 0.75
- , *(1) ,-,= , 0.00
GRID, 175 ,0, -1.5 , 4.5 , 1.5
- , *(1) ,-,= , 0.75
- , *(1) ,-,= , 0.00
GRID, 178 ,0, -1.5 , -4.5 , 1.5
- , *(1) ,-,= , 0.75
- , *(1) ,-,= , 0.00
GRID, 181 ,0, 1.5 , 4.5 , 1.5
- , *(1) ,-,= , 0.75

```

```

- , *(1) ,-,= , 0.00
GRID, 184 ,0, 1.5 , -4.5 , 1.5
- , *(1) ,-,= , 0.75
- , *(1) ,-,= , 0.00
GRID, 187 ,0, 0.0 , 4.5 , 1.5
- , *(1) ,-,= , 0.75
- , *(1) ,-,= , 0.00
GRID, 190 ,0, 0.0 , -4.5 , 1.5
- , *(1) ,-,= , 0.75
- , *(1) ,-,= , 0.00
- , *(1) ,-,= , 3.0 , 1.5
- , *(1) ,-,= , 0.75
- , *(1) ,-,= , 0.00
- , *(1) ,-,= , -3.0 , 1.5
- , *(1) ,-,= , 0.75
- , *(1) ,-,= , 0.00
- , *(1) ,-,= , 1.5 , 1.5
- , *(1) ,-,= , 0.75
- , *(1) ,-,= , 0.00
- , *(1) ,-,= , -1.5 , 1.5
- , *(1) ,-,= , 0.75
- , *(1) ,-,= , 0.00
GRID, 205 ,0, -1.5 , 3.0 , 0.75
- , *(1) ,-,= 1.5 , 3.0 , =
- , *(1) ,-,= -1.5 , 1.5 , =
- , *(1) ,-,= 1.5 , 1.5 , =
- , 209 ,-, -1.5 , -3.0 , =
- , *(1) ,-,= 1.5 , -3.0 , =
- , *(1) ,-,= -1.5 , -1.5 , =
- , *(1) ,-,= 1.5 , -1.5 , =
GRID, 213 ,0, -1.5 , 0.0 , =
- , *(1) ,-,= 0.0 , =
- , *(1) ,-,= 1.5 , =
- , *(1) ,-,= 0.0 , = 3.75

```

#### ELELENT DATA

```

CQUAD4, 1 ,3, 1 , 2 , 5 , 4
- , *(1),-,*(3),*(3),*(3),*(3)
-(2)
CQUAD4, 5 ,3, 2 , 3 , 6 , 5
- , *(1),-,*(3),*(3),*(3),*(3)
-(2)
CQUAD4, 89 ,3, 16 , 17 , 20 , 19
- , *(1),-,*(3),*(3),*(3),*(3)
-(2)
CQUAD4, 93 ,3, 17 , 18 , 21 , 20
- , *(1),-,*(3),*(3),*(3),*(3)
-(2)
CQUAD4, 9 ,1, 4 , 5 , 32 , 31
- , 16 ,-, 5 , 6 , 33 , 32
- , 23 ,-, 7 , 8 , 35 , 34

```

```

-      , 29 ,=, 8 , 9 , 36 , 35
-      , 35 ,=, 10 , 11 , 38 , 37
-      , 42 ,=, 11 , 12 , 39 , 38
-      , 55 ,=, 40 , 41 , 20 , 19
-      , 62 ,=, 41 , 42 , 21 , 20
-      , 68 ,=, 43 , 44 , 23 , 22
-      , 74 ,=, 44 , 45 , 24 , 23
-      , 81 ,=, 46 , 47 , 26 , 25
-      , 88 ,=, 47 , 48 , 27 , 26
CQUAD4, 10 ,1, 31 , 32 , 50 , 49
-      ,*(1),=,*(18),*(18),*(18),*(18)
=(4)
CQUAD4, 17 ,1, 32 , 33 , 51 , 50
-      ,*(1),=,*(18),*(18),*(18),*(18)
=(4)
CQUAD4, 24 ,1, 34 , 35 , 53 , 52
-      ,*(1),=,*(18),*(18),*(18),*(18)
=(3)
CQUAD4, 30 ,1, 35 , 36 , 54 , 53
-      ,*(1),=,*(18),*(18),*(18),*(18)
=(3)
CQUAD4, 36 ,1, 37 , 38 , 56 , 55
-      ,*(1),=,*(18),*(18),*(18),*(18)
=(3)
CQUAD4, 43 ,1, 38 , 39 , 57 , 56
-      ,*(1),=,*(18),*(18),*(18),*(18)
=(3)
CQUAD4, 41 ,1, 127 , 128 , 143 ,
142
CQUAD4, 48 ,1, 128 , 129 , 144 ,
143
CQUAD4, 49 ,1, 145 , 146 , 131 ,
130
CQUAD4, 56 ,1, 146 , 147 , 132 ,
131
CQUAD4, 50 ,1, 130 , 131 , 113 ,
112
-      ,*(1),=,*(18),*(18),*(18),*(18)
=(3)
CQUAD4, 57 ,1, 131 , 132 , 114 ,
113
-      ,*(1),=,*(18),*(18),*(18),*(18)
=(3)
CQUAD4, 63 ,1, 133 , 134 , 116 ,
115
-      ,*(1),=,*(18),*(18),*(18),*(18)
=(3)
CQUAD4, 69 ,1, 134 , 135 , 117 ,
116
-      ,*(1),=,*(18),*(18),*(18),*(18)
=(3)
CQUAD4, 75 ,1, 148 , 149 , 137 ,

```

```

136
CQUAD4, 82 ,1, 149 , 150 , 138 ,
137
CQUAD4, 76 ,1, 136 , 137 , 119 ,
118
-      ,*(1),=,*(18),*(18),*(18),*(18)
=(3)
CQUAD4, 83 ,1, 137 , 138 , 120 ,
119
-      ,*(1),=,*(18),*(18),*(18),*(18)
=(3)
CQUAD4, 97,3, 163 , 164 , 152 , 151
-      ,*(1),=, 151 , 152 , 140 , 139
-      ,*(1),=, 139 , 140 , 143 , 142
-      ,*(1),=, 142 , 143 , 155 , 154
-      ,*(1),=, 154 , 155 , 167 , 166
-      ,*(1),=, 164 , 165 , 153 , 152
-      ,*(1),=, 152 , 153 , 141 , 140
-      ,*(1),=, 140 , 141 , 144 , 143
-      ,*(1),=, 143 , 144 , 156 , 155
-      ,*(1),=, 155 , 156 , 168 , 167
-      ,*(1),=, 169 , 170 , 158 , 157
-      ,*(1),=, 157 , 158 , 146 , 145
-      ,*(1),=, 145 , 146 , 149 , 148
-      ,*(1),=, 148 , 149 , 161 , 160
-      ,*(1),=, 160 , 161 , 173 , 172
-      ,*(1),=, 170 , 171 , 159 , 158
-      ,*(1),=, 158 , 159 , 147 , 146
-      ,*(1),=, 146 , 147 , 150 , 149
-      ,*(1),=, 149 , 150 , 162 , 161
-      ,*(1),=, 161 , 162 , 174 , 173
-      ,*(1),=, 163 , 164 , 176 , 175
-      ,*(1),=, 175 , 176 , 188 , 187
-      ,*(1),=, 187 , 188 , 182 , 181
-      ,*(1),=, 181 , 182 , 170 , 169
-      ,*(1),=, 164 , 165 , 177 , 176
-      ,*(1),=, 176 , 177 , 189 , 188
-      ,*(1),=, 188 , 189 , 183 , 182
-      ,*(1),=, 182 , 183 , 171 , 170
-      ,*(1),=, 166 , 167 , 179 , 178
-      ,*(1),=, 178 , 179 , 191 , 190
-      ,*(1),=, 190 , 191 , 185 , 184
-      ,*(1),=, 184 , 185 , 173 , 172
-      ,*(1),=, 167 , 168 , 180 , 179
-      ,*(1),=, 179 , 180 , 192 , 191
-      ,*(1),=, 191 , 192 , 186 , 185
-      ,*(1),=, 185 , 186 , 174 , 173
CQUAD4, 133 ,1, 187 , 188 , 194 ,
193
-      ,*(1),=, 193 , 194 , 200 , 199
-      ,*(1),=, 188 , 189 , 195 , 194
-      ,*(1),=, 194 , 195 , 201 , 200

```

```

-      ,(1),2, 176 , 205 , 194 , 188
-      ,(1),=, 188 , 194 , 206 , 182
-      ,(1),=, 205 , 207 , 200 , 194
-      ,(1),=, 194 , 200 , 208 , 206
-      ,(1),4, 207 , 213 , 214 , 200
-      ,(1),=, 200 , 214 , 215 , 208
-      ,(1),=, 213 , 211 , 203 , 214
-      ,(1),=, 214 , 203 , 212 , 215
-      ,(1),2, 211 , 209 , 197 , 203
-      ,(1),=, 203 , 197 , 210 , 212
-      ,(1),=, 209 , 179 , 191 , 197
-      ,(1),=, 197 , 191 , 185 , 210
-      ,(1),1, 202 , 203 , 197 , 196
-      ,(1),=, 196 , 197 , 191 , 190
-      ,(1),=, 203 , 204 , 198 , 197
-      ,(1),=, 197 , 198 , 192 , 191
CBEAM , 201 ,1, 199 , 200 , 214
-      ,(1),=, 200 , 201 ,==
-      ,(1),=, 202 , 203 ,==
-      ,(1),=, 203 , 204 ,==
-      ,(1),2, 124 , 125 ,==
-      ,(1),=, 125 , 126 ,==
-      ,(1),=, 133 , 134 ,==
-      ,(1),=, 134 , 135 ,==
-      , 209 ,3, 216 , 214 , 200
ENDDATA

```

# Report Documentation Page

1. Report No. <b>NASA CR-177495</b>		2. Government Accession No.		3. Recipient's Catalog No.	
4. Title and Subtitle <b>Design of a Flexure Mount for Optics in Dynamic and Cryogenic Environments</b>				5. Report Date <b>February 1989</b>	
				6. Performing Organization Code	
7. Author(s) <b>Lloyd Wayne Pollard</b>				8. Performing Organization Report No.	
				10. Work Unit No. <b>159-41-06</b>	
9. Performing Organization Name and Address <b>Ames Research Center Moffett Field, CA 94035</b>				11. Contract or Grant No. <b>NCC2-426</b>	
				13. Type of Report and Period Covered <b>Contractor Report</b>	
12. Sponsoring Agency Name and Address <b>National Aeronautics and Space Administration Washington, DC 20546-0001</b>				14. Sponsoring Agency Code	
15. Supplementary Notes <b>Point of Contact: Ramsey Melugin, Ames Research Center, MS 244-10, Moffett Field, CA 94035 (415) 694-3193 or FTS 464-3193</b>					
16. Abstract <p>The design of a flexure mount for a mirror operating in a cryogenic environment is presented. This structure represents a design effort recently submitted to NASA Ames for the support of the primary mirror of the Space Infrared Telescope Facility (SIRTF). The support structure must passively accommodate the differential thermal contraction between the glass mirror and the aluminum structure of the telescope during cryogenic cooldown. Further, it must support the one meter diameter, 116 kilogram (258 pound) primary mirror during a severe launch to orbit without exceeding the micro-yield of the material anywhere in the flexure mount. Procedures used to establish the maximum allowable radial stiffness of the flexural mount, based on the finite element program NASTRAN and the optical program FRINGE, are discussed. Early design concepts were evaluated using a parametric design program, and the development of that program is presented. Dynamic loading analyses performed with NASTRAN are discussed. Methods of combining modal responses resulting from a displacement response spectrum analysis are discussed, and a combination scheme called MRSS, Modified Root of Sum of Squares, is presented. Model combination schemes using MRSS, SRSS, and ABS are compared to the results of the Modal Frequency Response analysis performed with NASTRAN.</p>					
17. Key Words (Suggested by Author(s)) <b>Dynamic and thermal loading Glass fracture statistics and fracture mechanics Displacement response spectrum</b>				18. Distribution Statement <b>Unclassified-Unlimited</b>  <b>Subject Category - 14</b>	
19. Security Classif. (of this report) <b>Unclassified</b>		20. Security Classif. (of this page) <b>Unclassified</b>		21. No. of pages <b>137</b>	
				22. Price <b>A07</b>	